Hadi Jahanshahi · Naeimeh Najafizadeh Sari

Robot Path Planning Algorithms: A Review of Theory and Experiment

Hadi Jahanshahi
University of Tehran
hadi_jahanshahi@ut.ac.ir
Iran

Naeimeh Najafizadeh Sari
University of Tehran
naeimeh.najafi@ut.ac.ir
Iran

Preface

The scope of robotic science and its applications are developing step by step through increased safety and efficiency. In general, research on various robots can be divided into three categories of design and manufacture, navigation and guidance, and their application. So, to speak, the robot should first be designed and developed, at that point navigated and guided, lastly utilized as a part of various situations for various purposes. Whatever the mission of the robot, it doesn't have any impact on the role of navigation and the guidance of the robot. Given the wide extent of research in the field of navigating and guidance the robot, it breaks into four general areas of positioning, path planning (routing), motion planning (control), and mapping.

Each robot needs a set of commands and rules known as robot path planning and navigation to perform a mission properly and completely. Path planning has a long history in robotics. Even before the development of robots, two well-known issues such as the "Travelling Salesman Problem" and "Piano Mover's Problem" have been around for many years and have been solved in various ways. According to the available information from the environment, robotic path planning can be divided into three general categories of path planning in a known environment, path planning in a semi-known environment, and path planning in an unknown environment. The dominant theme of this book is to introduce different path planning methods and suggest some of the most appropriate ones for robotic path planning; methods that are capable of running on a variety of robots and are resistant to disturbances; being real-time, being autonomous, and the ability to identify high risk areas and risk management are the other features that will be mentioned in the introduction of the methods.

The first chapter of the book provides an introduction on the importance of robots and describes the subject of navigation and path planning. The second chapter deals with the topic of path planning in unknown environments. In the first part of this chapter, the family of bug algorithms including Bug1, Bug2, ALG1 and ALG2, DistBug, Tangent Bug and some others are introduced. In the following, other common methods include D^*, Com, Class, and Rev algorithms are presented. The final part of this chapter is devoted to the introduction of two new path planning methods; “Histograms of Vector Fields" and "multi-strategy approach".

In Chapter 3, path planning is considered in the known environment. In a known environment, the robot either uses maps provided by external sources (such as the GPS) or uses the sensor to provide the maps from the surrounding environment. There are three general strategies for guiding the robot towards the target, including feature-based guidance, guidance with potential field and histograms of vector fields, which the third approach is described in the second chapter. In Chapter 3, the two first approaches are introduced.

The fourth chapter focuses on robot path planning based on the robot vision sensors and computing hardware. The first part of this chapter deals with path planning methods based on mapping capabilities. In this section, three mapping methods, including polygonal, gridding and hierarchical maps, are described and the advantages and disadvantages of each one is examined. The second part deals with the path planning based on vision sensors, which are usually the best sensors in the path planning subject. This part first describes the nature of the light, and then defines the light recording, storage, and detection with vision sensors. In the third part of this chapter, the displacement of two-dimensional robots with two or three degrees of freedom is investigated. Two methods of configuration space and potential field, which are more general, are briefly explained and based on them, a combination algorithm with high speed and high reliability is presented and its implementation results are presented in different circumstances.

In Chapter 5, the performance of some of the most important path planning methods introduced in the second to fourth chapters are presented in terms of implementation in various environments. The first part of this chapter is devoted to the implementation of the algorithms Bug1, Bug2 and Distbug on the pioneer robot. In the second part, an analytical method is proposed to enhance the robot's performance in avoiding collisions with obstacles This method, based on the tangential escape, attempts to cross the robot with a variety of obstacles with curved corners (obstacles U, V, Z, and zigzag shapes). In the third and fourth parts of this chapter, path planning is introduced in environments with in absence and in the presence of danger space. Four approaches of artificial fuzzy potential field, linguistic method, Markov decision making, and fuzzy Markov decision making have been introduced in these two parts and implemented on the Nao humanoid robot. The results of these methods are presented.

Hadi Jahanshahi

Naeimeh Najafizadeh Sari

Contents

Chapter 1- **Introduction**

1-1- Robot and its variants

There have been always disagreements and controversies about the definition of a robot, between academia and industry in the field of robotics among experts and activists. Sometimes there was a technological definition of a robot and sometimes a trading company, offered an industrial definition, based on the manufactured robots. For example, Robotic Industrial Association, a well-established company in the field of industrial robot arms, defined robot as follows:

"A robot is a reprogrammable, multifunctional manipulator designed to move material, parts, tools or specialized devices through variable programmed motions for the performance of a variety of tasks."

According to the International Standard Organization (ISO), Document 8373 (ratified 2012), Robot is defined as follows:

"An actuated mechanism programmable in two or more axes with a degree of autonomy manipulator within its environment, to perform intended tasks."

Also, the document defines autonomy as follows:

"The ability to perform intended tasks based on current state and sensing, without human intervention." According to this definition, a block diagram for a robot can be drawn as Fig. 1.1.

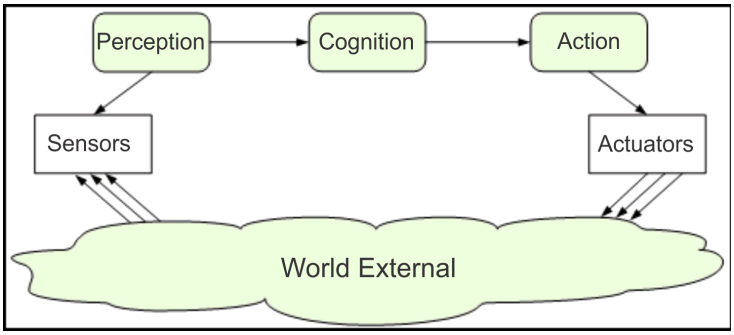

Fig. 1.1. Block diagram of a robot based on the definition of 'autonomy'.

One of the first robots to be built, called Hidden Mafia, was made in 1950s and 1960s by George de Waal and Joseph Engelberger. Engelberger founded the first robot-making company named Roboband, and that's why the title "father of robotics" was dedicated to him.

There are various ways of categorizing robots, among which two common methods are based on the robot's body-style and performance. This categorization is shown in table 1.1. Among them, humanoid robots, are considered as the most specific types and nowadays, they are in the spotlight of robotics researchers. Of the main reasons for this popularity, one could mention matching and adaptation capabilities of humanoid robots with man's living conditions. This kind of robot has the ability to cross the obstacles in human lives, due to its better maneuverability compared to the other types. Many studies are also being carried out on robots, aiming to make artificial limbs for humans. Despite these attractions, due to their high complexity, there exists a far distance to make servant humanoid robots marketable.

In Table 1.1, BEAM robots, are robots which are controlled taking advantage of biological characteristics and behaviors of organisms. BioRobots are often modeled based on nature and since making insects in mechanical form is simple, a lot of them are like insects. Building these robots are very popular, as they have simple mechanical movements, require low power and complicated calculations. Electronic robots have electronic circuits, just like all other robots. Aesthetics robots have traditional and elegant appearance and have no need for multi-stage printed circuits.

Table 1.1. Two common classifications of robots based on configuration and performance

Categorization based on configuration	Categorization based on Performance
flying robot	Mobile robot
reptile robot	- Rolling Robot
robot fish	- walking robot
warrior robot	Static robot
soccer robot	Autonomous robot
humanoid robot	Control robot
robot minesweeper	BEAM (Bio, Electronic, Aesthetics, Mechanic)
Service robot	Virtual Robot

Since that humans are considered as one of the most complicated creatures in nature, humanoid robots are also the most complicated human made ones. However, from the advances made in this field, was utilized for driving other technologies forward. Among these technologies we can point to artificial prostheses. From among the most famous humanoid robots we can mention Mahro, Atlas, Kobian-R and HRP4 which are produced by Korean Institute of Science and Technology, Boston Dynamics Company, Waseda University and Kavada industries, respectively. These robots are shown in Fig. 1.2.

In addition to industrial robots, small humanoid robots are also manufactured for laboratory purposes, which among the most important ones are; Nao, Zeno and Darvin-OP (products of Aldebaran Robotics (France), Hanson Robokind and Robotis, respectively). They are shown in Fig. 1.3.

The importance of robots should be sought in their application and role in the present and future. Specifically, humanoid robots will be the most used ones in the future and will play an extensive role in manufacturing, military, aerospace, medical and other similar industries. Nowadays, the large companies of the world are seeking to replace traditional arms with humanoid robots. For example, a German company, DLR, introduced the first humanoid robot named Rollin Justin for work on production lines. Since 2013, America's military industries have brought humanoid robots for future wars into exploitation and operation stage. Atlas Robot (Fig. 1.4) is the first robot designed and produced by Boston Dynamics in order to serve

the military, ordered by Defense Advanced Research Projects Agency (DARPA). According to evolutions in possible wars in the future, the importance of robots, particularly humanoid robots is apparent more than ever before. In addition to the military contexts, humanoid robots have entered space industry. Costs and risks of sending humans into space is very high and National Aeronautics and Space Administration (NASA) has revised its plans and announced that in order to reduce its workforce, from now on, several humanoid robots will also join men on their trip to the moon. So far, this administration has sent humanoid robot Robonaut II (Fig. 1.5) to the International Space Station and plans to send it to a thousand-day journey to moon.

1-2- Routing, an ongoing challenge in robot guidance

As a general rule, researches in the field of various robots, in particular, humanoid robots, can be divided into three categories:

- Design and manufacture,
- Navigation and guidance,
- Application.

In other words, the robot must be designed and manufactured. Then, must have a navigation and guidance system and eventually be used in different environments with different purposes. Whether it works at home or on agricultural fields, does not have an effect on its role of navigation and guidance. It means that employed in any situation, the robot requires navigation and guidance. Regarding wide scope of researches in the field of robot's navigation and guidance, it can be divided into four major areas:

- Positioning,
- Path planning (Routing),

- Motion planning (Control), and
- Mapping.

Atlas from Boston Dynamics

Mahru from Korean Institute of Science and Technology

HRP-4 from Kavada industries

Kobian-R from Waseda University

Fig 1.2. Examples of human-size humanoid robots

Zeno from Hanson Robokind

Nano from Aldebaran Robotics

Darvin-OP from Robotis

Fig. 1.3. Examples of small-size humanoids

Fig. 1.4. Rollin' Justin from DLR

Fig. 1.5. robonaut2 from NASA.

Generally, a robot must proceed to calculate positions for conducting navigation and guidance. These positions could be quantitative (namely, coordinates in terms of unit length) or symbolic (such as color signs, etc.). After this step, the robot should identify a rout or path based on their current position, destination position (target) and the perception from the environment (whether with or without a map). How to specify the path is called "path planning". After identifying path, the robot must be controlled such that it moves along this path. Robot motion control, is referred as motion planning. Some of the robots, including humanoid robots map their environment so they can use the map for their next routing purpose. Regarding the robot's information from its environment, routing falls into 3 general categories;

- Routing in a known environment,
- Routing in a pseudo-known environment,
- Routing in an unknown environment.

In the case of known environment, a complete map is given to the robot, or complete information of the rout is available with the help of broad vision from a camera or a network of cameras. Having available complete maps or broad vision, is not possible in most cases, except in special situations. Extensive researches have been done in this area and today, routing dimensions in known environments are fully identified and solved.

In pseudo -known environment, firstly, the robot will be given a map of the environment. Although there may be minor changes in the plan or few dynamic obstacles (such as a human or an animal), due to lack of the ability to save, this information does not exist in the map, but in this environment also one can act as in a known environment and when faced with changes, the map gets updated.

In an unknown environment, the robot doesn't have any maps initially and receives its information from sensors. In this case, according to the type of robot hardware, routing can be conducted regarding Table 1.2.

Table 1.2. Robot routing methods in unknown environment

Classification method	Classification			
Based on sensors	Visual sensor	Distance sensors	Attendance sensors	data fusion
	Single vision Dual vision multiple vision	ultrasonic sensor Lasor sensor		-
Based on drawing ability	Without map (without memory)	mapping the travelled path	mapping the environment	

The ability to draw the complete map, where the robot is supposed to travel a short distance could be justified, but it is not feasible practically over long distances due to the need for large memory as well as increased processing workload for finding the optimal route. For medium distances, the method of mapping the traveled path looks reasonable.

Attendance sensors make the route longer and provide the least information to the robot. For this reason, the methods that rely solely on the attendance sensors are outdated. Distance sensors provide appropriate information for routing. However, the data obtained from these sensors cannot provide robots with the information of the danger zones. Also, the use of these sensors during war (because of being active and rapidly identified by the enemy) is not wise. Visual sensors (cameras) are the best sensors in the context of routing, based on the information they provide. All the humanoid robots have at least one sensor for vision. To obtain the accurate distance, having double or multiple vision is required.

The main topic of this book, is introducing different methods of routing and proposing some of the most suitable ones for robot navigation, the ways that often have the following conditions:

- Ability to run on a variety of robots;
- Resistance to natural turbulences(noises);

- Being real-time;
- Self-regulation (autonomy);
- Ability to identify high risk areas and risk management.

Chapter 2- **Path Planning in Unknown Environments**

2-1- Introduction

Routing has a long history in robotics science. Even before the emergence of robots, both the main problems known as “Travelling Salesman Problem” and “Piano Mover's Problem” were around for years and has been solved in various ways. Initially, the routing problem was explained for robotic arms and then for wheeled robots and flying robots. With the rise of humanoid robots, to date, there have been several proposed solutions for routing them, each of which has its own advantages and disadvantages. This broadness is at such an extent that routing is still an open issue.

In this chapter, it is firstly essential to know two current terms used in robot navigation:

Guidance: Guidance, in robotics, refers to moving a robot from one place to another on a free-clash route. In guidance, the robot must either reach itself to the target based on a gradual recognition of the environment or follow a predefined path. During a robot’s guidance to its target, to make the best choice, it often relies on sensor data, and updating current position and direction.

Path planning: In fact, path planning involves data collection and calculation of some path that meets one or more conditions (such as avoiding obstacles, having the shortest distance length, imposing minimal rotation of robot, and having the greatest safety). If using a fixed path for guidance, this path is usually predefined.

Robot guidance methods towards a target is dependent on the following two essential questions:

1. Are the initial and final positions of the robot determined in advance?

   If the final position (target) is being specified in advance, this position's coordinates is given to the robot. Otherwise, for the robot to find its target position, it requires a search. The robot moves along the route at any time, or it can recognize its position itself or do this by using external tools such as a GPS receiver.

2. Are the obstacles specified in advance?

   The coordinates of specified obstacles can be given to the robot. Otherwise, the robot must scan the obstacles with the help of its sensors.

For the robot to perform its missions, it must pre-design its path. The planned movement of the robot applies in cases like robot moving in short distances, painting and cleaning up the environment (operations in which the robot should cover the entire environment) and espionage operations which is more related to national security.

In unknown environments where there is no or little information, the robot itself should be able to plan its path and follow it towards the target. In this chapter, routing methods for robots in such environments is discussed and several new methods are proposed, in addition to conventional methods. In the second part of this chapter, Bug algorithms family, including Bug 1, Bug 2, ALG 1 & 2, Distbug, TangBug algorithms and some other ones in this family will be addressed (Ng 2010). Furthermore, other conventional methods including D-star, Com, Class and Rio algorithms are introduced.

The last section of this chapter also introduces two novel ways of routing called "Vector Filed Histogram" (Borenstein and Koren 1991) and "Multi Strategic" (Bianco and Cassinis 1996). Vector Filed Histogram field is a common method for unknown and known environments and

works based on environment gridding and drawing a histogram graph. Multi strategic method also addresses routing in unknown environments using multiple strategies simultaneously.

2-2- Bug Algorithms Family

Two-dimensional robot guidance environment consists of a starting point and a target point. The robot tries to find an obstacle-free path, while moving from the start point to the target point. Figure 2.1 shows an example of two-dimensional environments, in which the robot should start from the box-shaped starting point and reach the circle-shaped target point without confusion and entanglement.

The early works about path design was done by Lumelsky (Lumelsky and Stepanov 1986, 1987, 1984, Lumelsky 1985, 1986a, b, 1987c, 1988, 1991; Lumelsky and Sun 1987; Sun and Lumelsky 1987; Lucas et al. 1988; Lumelsky and Skewis 1988, 1990; Lumelsky and Tiwari 1994; Skewis and Lumelsky 1994). Prior to him, robot guidance in unknown environments was a winding path that was carried out by algorithms such as Pledge (Abelson and DiSessa 1986) and Tarry (Ore and Ore 1962). Unfortunately, the Pledge algorithm lacked the ability to deliver a robot to a specific point. Besides, the route traveled by the robot by using these two algorithms becomes very long. Of course, there exist some innovative ways requiring information from their surrounding environment.

Bug algorithms are the first path planning algorithms that ensure the situation for the robot to reach the target. These algorithms are very appropriate for the robots which have an instantaneous and immediate, so-called real-time performance.

The objective of bug algorithms is to guide the robot from a starting point S towards a target point T, in some environment with limited information. If no path was found to attain the target point, the algorithm reports the result, which is "unattainability of the target point".

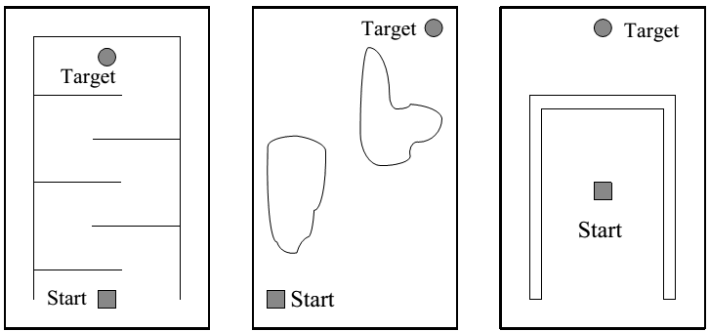

Fig 2.1. Examples of 2D environments for robot guidance.

Bug algorithms can be implemented in any robots equipped with tactile sensors or range-estimation sensors, which are equipped with a method of determining the local position (such as a length-calculator or a GPS system). By utilizing this algorithm, the robot can automatically find its path to the target point. Lumelsky has applied this algorithm on robot arms, which are determined to reach to a certain point (Lumelsky 1986a, 1987b, c). The movement of robot arms are very similar to the movement of mobile robots in an unknown environment and the only difference is that the base of robot arms is constant.

Another application of this algorithm is in inspection and searching in an environment up to a specified range and achieving the target (Miskon and Russell 2009). After finding the target, the robot gets closer to the target in order to examine it in more details. A model of these robots is used in nuclear reactors for finding radioactive materials. If the robot senses a suspicious object, remotely, it should get close to it and do a closer inspection from a closer distance. It requires defining a strategy for the robot to approach the suspicious object in environments containing a large number of objects.

For the first time, Lumelsky and Skewis used sensors in Bug algorithms (Lumelsky and Skewis 1990). Using sensors led to development of the Bug 2 algorithm, which by creating shortcuts, resulted in shortened length of the path. Afterwards, the debate over the best point to get around obstacles by robots was raised, and Kamon developed "DistBug" Algorithm for this purpose.

"TangentBug" is the next algorithm in which the robot uses some sensors to observe the surroundings (Kamon et al. 1998).

The main similarities and differences between the Bug algorithms is in the methods used to ensure they complete their missions. SenseBug is a new algorithm for use with sensors. In this algorithm, three performance criteria are considered: frequency of data collection, amount of efforts to search and path lengths. Reduction in frequency of collecting the accessible information in environment and search effort amounts in any time to collect information are the tricks of this algorithm. Using these tricks will not prevent completing and accomplishing the mission.

Since the environment may change all the time, and at every moment there may be brief information from it, the strategy to guide the robot must be formulated somehow that with a minimum amount of information from environment (preferably containing target position and robot position at any moment) it can guide the robot to its target. Some well-known path design tricks such as A^* (Nilsson 1969; Pearl 1984; Ko et al. 1993), Dijkstra (Foux et al. 1993), Distance Conversion (Jarvis 1985; Choset 2005; LaValle 2006), Potential Field (Khatib 1986; Masoud and Masoud 2002; Trevisan et al. 2006; Bräunl 2008; Latombe 2012), Sampling-based (Kavraki et al. 1996; Geraerts and Overmars 2004), and piano stimulation problem (Lozano-Perez 1983; Schwartz and Sharir 1983; Yap 1987) need more information than those two tricks mentioned above, and sometimes they require a full map. These weaknesses show that in unknown environments, point-to-point guidance is necessary.

This algorithm has been used also in designing path to guide a robot on the grass (Huang et al. 1986), to harvest crops (Ollis and Stentz 1996), and to work in mines (Land and Choset 1998). Laubakh and Burdick implemented an algorithm called "WedgeBug" on mobile robots to explore the surface of Mars, the planet.

Langer, Coelho & Oliveira (Langer et al. 2007) felt the increasing demands to use path planning in unknown environments for use in the construction industry, transportation, medicine (such as operating rooms with remote control capability), military industries, video games and space exploration, and continued path planning in these applications (Lozano-Perez 1983; Schwartz and Sharir 1983; Huang et al. 1986; Ollis and Stentz 1996; Land and Choset 1998; Langer et al. 2007; Sciavicco and Siciliano 2012). "K-Bug" Algorithm was tested in an office room similar to a real environment and showed that the algorithm designs the paths that can compete with paths created by the A^* algorithm.

In total, among the advantages of Bug algorithms, one could mention its simplicity and its ability to understand and implement. These algorithms also, at least in theory, guarantee to attain their target.

2-2-1- *Symbols and terminology of algorithms Bug*

Before entering the descriptions about Bug family algorithms, it is required to introduce the symbols and terminology of these algorithms. Some of the most important ones are:

S : Starting point

T : Target point, also called end point.

x : Current position of the robot.

H_i : The i^{th} collision point (from all the time collision points) which in fact represents the i^{th} time from all the times that the robot encounters an obstacle boundary.

L_i : The i^{th} separation point, which in fact determines the i^{th} time that the robot separates from obstacle boundary and moves to the target.

$d(a,b)$: Geometric distance between arbitrary points of *b* and a.

$d_{path}(a,b)$: The length of the path traveled by the robot between two arbitrary points of b and a.

r : Maximal range of position sensors.

$r(\theta)$: Free space along θ distance between the robot and the first observable obstacle in that direction.

F : Free space along the target. If θ is along the target, then F and *r* will be the same.

Besides, in order to show the difference among various routing algorithms, the performance of each one has been tested in the same hypothetical environment, which is Fig. 2.2. In this figure, the starting point and the target point have been labeled with S and T letters, respectively. As we shall see furtherly, different algorithms, propose dissimilar and sometimes suboptimum paths to convey the robot from the starting point to the target point.

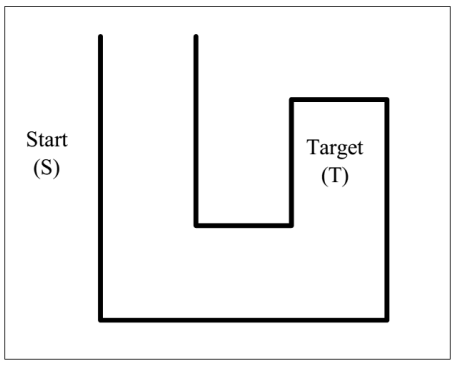

Fig 2.2. The Hypothetical environment for comparing the performance of different Bug algorithms.

2-2-2- *Bug 1 Algorithm*

Bug 1 algorithm is the first algorithm from Bug algorithms family (Lumelsky and Stepanov 1984, 1986, 1987) that has was developed by Lumelsky and Stepanov. Based on this algorithm strategy, the robot will continue its movement towards the target point, until it encounters an obstacle, then gets around the obstacle and finds the nearest point towards the target. In this algorithm, it is assumed that the robot knows the target position but cannot see it.

Performance principle of Bug 1 algorithm is as follows and in accordance with the mission demonstrated in Fig. 2.3.

Step 0. Set i=0 as an initial value.

Step 1. Add one unit to i and the robot goes towards the target, until one the following scenarios occurs:

Step 1.1. Reach the target; a successful exit from the algorithm.

Step 1.2. Encounter with an obstacle, in this case, the point of encounter with the barrier will be labeled "H_i "and then run step 2.

Step 2. Get around the obstacle from left side to reach the point H_i, and search for point (or points) L_i with two conditions of "the shortest distance to target" and "the possibility to move towards the target".

Step 3. Examine travel to target point

Step 3.1. If there exist a point L_i go to point L_i and run step 1.

Step 3.2. If there exist no point L_i, the target is not "attainable", stop the algorithm.

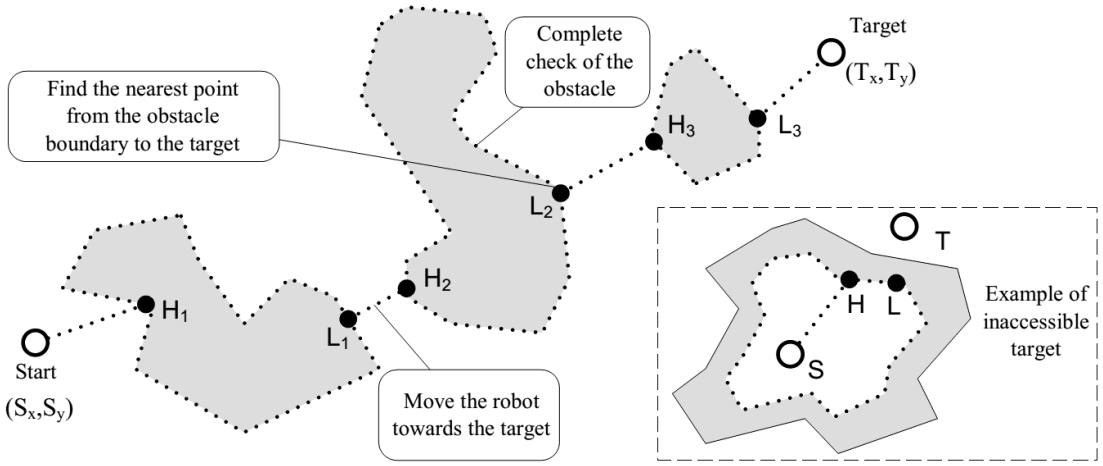

Fig. 2.3. The general principle of Bug 1 routing method, for the two kinds of target; accessible and inaccessible.

The robot on the move, records the length of path between the two points H_i and x as $d_{path}(x, H_i)$. It occurs from the points where d, is minimum and from which the robot is able to move towards the target. Then, the robot labels one of the minimum points (L_i), and until it comes back again to H_i, it checks whether the target is achievable if the robot moves from point. If the robot is not able to achieve the target, the mission fails and it will be reported that the target is not "attainable". But, if possible, the direction to navigate the wall is selected somehow that $d_{path}(x, H_i)$ becomes minimized. Consequently, the maneuver towards attaining L_i is accomplished and Step 1 becomes completed.

The proposed pseud-code for this algorithm is as follows:

```
While  (TRUE)
  LET Len = line from S to T
  REPEAT
    Move from S towards T
     x = robot’s current location
  UNTIL  ((x == T)  OR  (obstacleIsEncountered))
    IF  (x == T)  THEN  quit    // target reached
    LET H = x                   // contact location
  REPEAT
  Follow obstacle boundary
  x = robot’s current location
  LET L = intersection of x and Len
  UNTIL  (((L is not null)  AND  (dist (L,T) ,dist (H,T)  OR  (x==T)
            OR  (x==H))
    IF  (x == T)  THEN quit    // target reached
    Move to L along obstacle boundary
    IF  (obstacleIsEncountered at L in direction of T)
    THEN quit                 // target not reachable
ENDWHILE
```

In Bug 1 algorithm, the maximum traversed path by the robot is calculated using the following equation:

$$\left|\overline{ST}\right| = 1.5\left[\text{perimeter}(obj_1) + \text{perimeter}(obj_2) + \cdots + \text{perimeter}(obj_n)\right] \qquad (2.1)$$

where S is the starting point and T refers to the end point. A coefficient of 1.5 is because the robot gets around the obstacle with a complete round, in order to find the best possible position to leave the obstacle border, and the remaining half round is used to return to the best place.

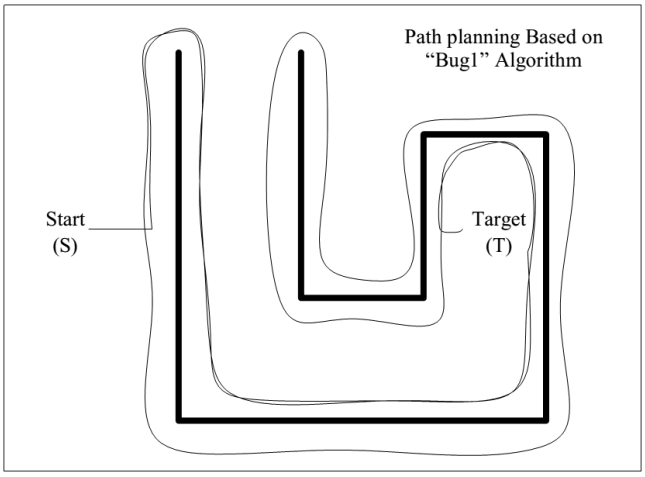

Fig. 2.4. An example of the application of Bug 1 algorithm in a hypothetical environment.

In the Bug 1 algorithm, the robot always finds the target, if it is attainable. Also, the robot searches for the best place to leave the obstacle and move towards the target. Fig. 2.4 is an example of the application of this algorithm in a hypothetical environment.

2-2-3- *Bug 2 algorithm*

Bug 2 algorithm was also introduced by Lumelsky and Stepanov (Lumelsky and Stepanov 1984, 1986, 1987). Bug 2 algorithm demonstrates less conservativeness than Bug 1 algorithm and leaves the obstacle encountering it more easily. In Bug 1 algorithm, the robot searches for all the points of an obstacle to find the nearest point to the target, while in the Bug 2 algorithm, the complete obstacle bypass is prevented. The strategy is that the robot, before hitting an

obstacle, moves along a straight line which is connected from the start point to the target point, and if it encounters any obstacles, it gets around from the left side.

How to operate the Bug 2 algorithm is as follows in accordance to the hypothetical mission shown in Fig. 2.5:

Step 0- First, draw a hypothetical line from the starting point to the end point and give i an initial value of zero.

Step 1. Add a unit to i and at the same time, move along the line M towards the target until one of the following scenarios occurs:

Step 1.1. Reach the target; a successful exit from the algorithm.

Step 1.2. Encounter with an obstacle; in this case, the collision point will be labeled "H_i" and step 2 will be run.

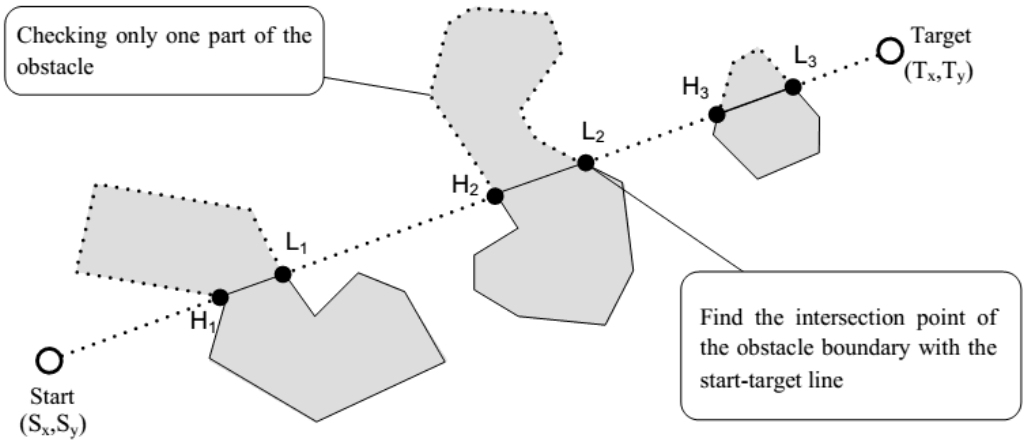

Fig. 2.5. An example of Bug2 algorithm's operation in a hypothetical environment.

Step 2. Bypass the obstacle border on the left side until one of the following scenarios occurs:

Step 2.1. The target is found, successful exit from the algorithm.

Step 2.2. Some point along the line M will be found such that $d(x,t) < d(H_i,T)$. If you are able to move towards the target, the point is labeled "L_i "and Step 1 will be run.

Step 2.3. You get back to the point H_i; if so, the target is unattainable, and the algorithm will stop.

The proposed pseudo-code for the algorithm is as follows:

```
While  (TRUE)
  LET Len = line from S to T
  REPEAT
    Move from S towards T
     x = robot's current location
  UNTIL  ((x == T)  OR  (obstacleIsEncountered))
   IF  (x == T)  THEN quit       // target reached
   LET H = x        // contact location
   REPEAT
     Follow obstacle boundary
     x = robot's current location
     LET L = intersection of x and Len
   UNTIL  (((L is not null)  AND  (dist (L,T) ,dist (H,T)  OR  (r==T)  OR  (x==H))
   IF  (x == T)  THEN quit     // target reached
ENDWHILE
```

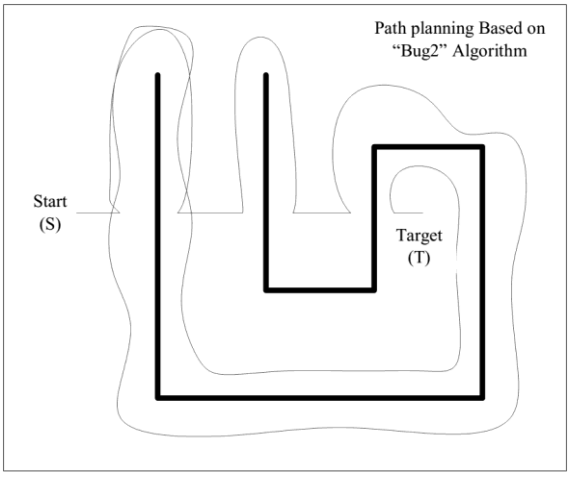

Fig. 2.6. An example of Bug 2 algorithm's implementation in a hypothetical environment.

This algorithm also, scans for the target and certainly achieves it like Bug 1 algorithm, if the target is attainable. The robot in order to find the best point to leave the barrier, proceeds to

search ubiquitously and in full scale. An example of the implementation of this algorithm at the desired sample environment, is shown in Fig. 2.6.

The maximal mileage (distance traveled) by the robot in Bug 2 algorithm is obtained from the following equation:

$$\left|\overline{ST}\right| = O(\text{perimeter}(obj_1)) + O(\text{perimeter}(obj_2)) + \cdots + O(\text{perimeter}(obj_n)) \qquad (2.2)$$

Since obstacle bypass orientation (from left or right) is predefined and does not change along the way, according to the starting position and end position, the distance traveled by robots can be optimum or suboptimal. The worst case, is a condition such as Fig. 2.7 in which the robot based on its suboptimal selection, travels a path that has a length approximately equal to the maximal possible distance. Fig. 2.8 also is another example of suboptimal selected path. While the robot travels a relatively long path, by choosing a bypass from the left to reach the target, it could have bypassed from the right, and it would have traveled a significantly shorter path.

Clearly, we can see that Bug 2 algorithm is faster than Bug 1. It should be noted that in both of these algorithms, it is assumed that the robot in its vicinity is only able to detect the presence of just one obstacle. Equipped with obstacle-detecting sensors in 360 Degrees angular range, the robot can use improved Bug 1 and Bug 2 algorithms.

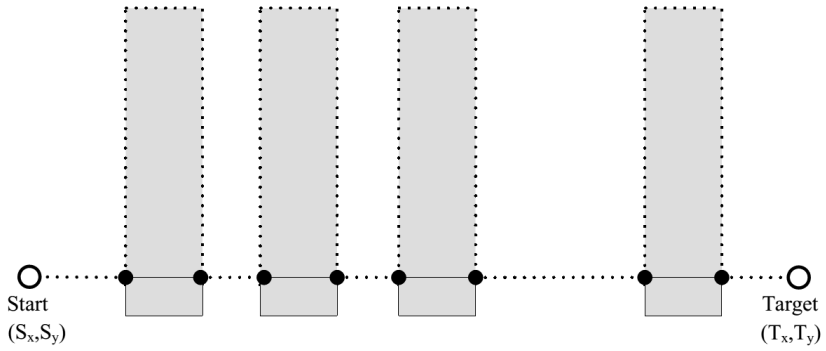

Fig. 2.7. Traveling an approximate maximum distance due to suboptimal path choice by Bug2 algorithm.

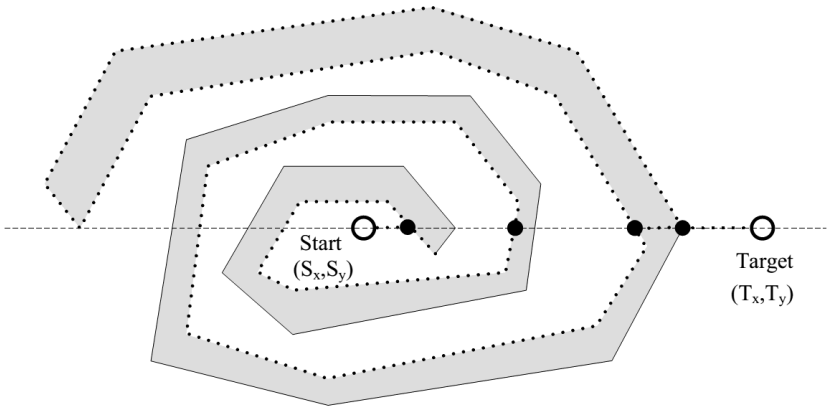

Fig. 2.8. Turning left to get around the obstacle, another suboptimal choice by Bug 2.

2-2-4- ALG1 algorithm

This algorithm is an extended version of Bug 2 algorithm, developed by Sankaranarayanan and Vidyasagar (Sankaranarayanan and Vidyasagar 1990). A weakness in Bug 2 algorithm, is the possibility of traveling the path one or more times by robot, resulting longer generated paths. To improve this weakness, algorithm ALG1 remembers the robot's collision and leaving points to obstacles in its memory and uses them for creating next shorter paths.

Working principle of ALG1 algorithms is as follows:

Step 0. First, draw an imaginary line from the starting point to target point , i be given 0 as an initial value.

Step 1. Add one unit to i , while the robot is moving along the line M towards the target until one of the following scenarios occurs:

Step 1.1. Reach the target; successfully quitting the algorithm.

Step 1.2. Encounter with an obstacle; in this case, the collision point is labelled "H_i", then step 2 will be run.

Step 2. Bypass the obstacle border on the left side, such that one of the following scenarios occurs:

Step 2.1. The target is found; exit successfully from the algorithm.

Step 2.2. Some point y with the following characteristics will be found:

- The point is located on the line M .
- For all the *x*'s: $d(y,T) < d(x,T)$
- The robot in point y can move towards the target.

Step 2.2.1. The point found is labelled " L_i ", and step 1 is repeated.

Step 2.3. Turn around the vicinity of point H_i and then return to it. Once you reach H_i, follow the obstacle border and bypass the wall from the left side.

Step 2.4. Return to the point. In this case, the target is unattainable; stop.

An example of the application of this algorithm in a hypothetical environment, is shown in Fig. 2.9.

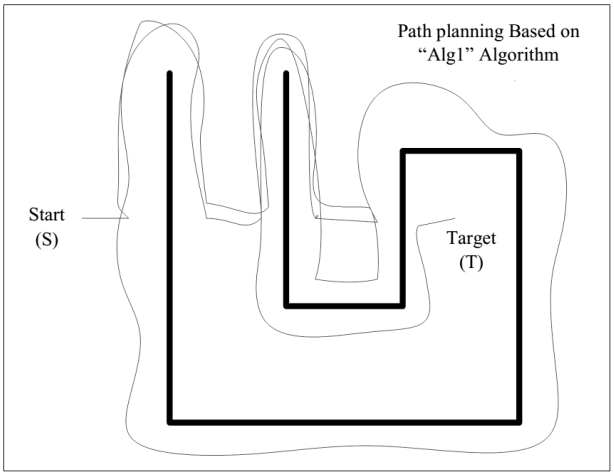

Fig. 2.9. An example of the application of ALG1 algorithm in a hypothetical environment.

2-2-5- *ALG2 algorithm*

This algorithm is an improved version of ALG1 algorithm which has been proposed by Sinkaranarayanan and Vidyasagar (Sankaranarayanan and Vidyasagar 1990). The concept of

line M (the line connecting the starting point and the target point) is no longer used in this algorithm and new conditions are defined to leave barrier by the robot. Working principle of Algorithms ALG2 is as follows:

Step 0. Two initial settings are: and $Q = D(S,T)$.

Step 1. Add one unit to i and advance towards the target. At the same time, the amount of Q will be updated and sets the value of $d(x,T)$ to itself. Updating Q continues as long as the condition $Q < d(x,T)$ holds. Q indicates the nearest robot point to the target. This process continues until one of the following scenarios occurs:

Step 1.1. The target point is found; successful exit from the algorithm.

Step 1.2. An obstacle is found, the point will be labelled "H_i" and step 2 will be run.

Step 2 Always keep the obstacle on its right (namely, bypass the obstacle from left side) and at the same time, continually update Q with $d(x,T)$ until the condition $Q < d(x,T)$ holds, this process continues until one of the following scenarios occurs:

Step 2.1. The target is found; successful exit from the algorithm.

Step 2.2. The point y is found with the two following conditions:

- $d(y,T) < d(Q,T)$
- At this point, the robot can move towards the target.

Step 2.2.1. The found point is labelled" L_i", and step 1 is run.

Step 2.3. Turns around in the vicinity of point H_i and then return to it. When you reach H_i, bypass the obstacle from the left.

Step 2.4. Return to point H_i. The target is unattainable; stop.

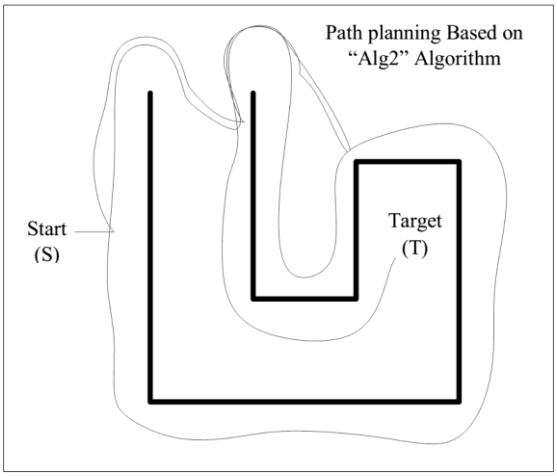

Fig. 2.10. ALG2 algorithm's manner in an arbitrary environment.

An example of the manner in which this algorithm performs in an arbitrary environment is shown in Fig. 2.10.

It is worth noting that the algorithm ALG2 has been much improved compared to the previous algorithms, from a barrier leaving conditions viewpoint, since it has no need for line M in order leave the barrier.

2-2-6- DistBug algorithm

This algorithm has been proposed by Kamon and Rivlin (Kamon and Rivlin 1997). This algorithm makes use of a distance-finder sensor to find free space F and to define the conditions to leave the barrier.

DistBug algorithm's working principle is as follows:

Step 0. Give i an initial value of 0 and traverse a distance equal to the wall thickness (the minimum thickness of a barrier in the environment and must be given by the user to the application and in this regard is considered as a weak point for the algorithm).

Step 1. Add one unit to i and the move towards the target to fulfill one of the following two conditions;

Step 1.1. The target is found, successful exit from the algorithm.

Step 1.2. Encounters an obstacle. This point is labelled "H_i" and step 2 is run.

Step 2. Bypass the barrier from the left and at the same time, update the minimum amount of $d(x,T)$ and records it with name of $d_{min}(t)$. This process continues until one of the following conditions is realized:

Step 2.1. The target is observable, namely, the condition $d(x,T)-F$ holds. This point is labelled "L_i "and step 1 is run.

Step 2.2. If $(x,T)-F \le d_{min}(T)-step$, this point will be labelled "L_i "and step 1 is run.

Step 2.3. Travel in a ring path and return again to H_i which means an unattainable target; stop.

An example of how this algorithm works, in a hypothetical environment, is shown in Fig. 2.11.

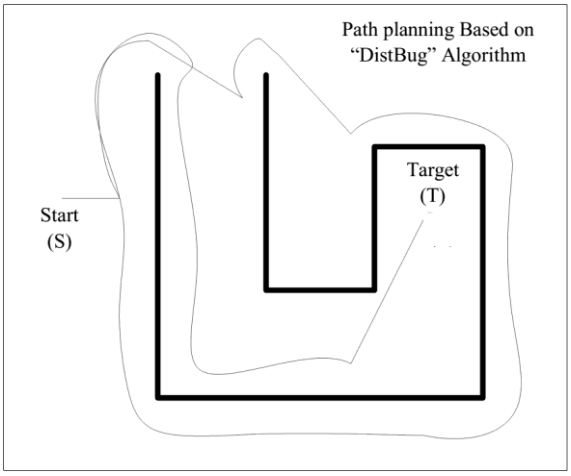

Fig. 2.11. Distbug algorithm's manner in an arbitrary environment.

2-2-7- The TangBug algorithm

TangBug algorithm has been developed by Kamon, Rivlin and Rimon (Kamon et al. 1998). This algorithm incorporates distance-finding sensors to create a map of robot's surrounding environment and tries to minimize the path to the target. Suppose the robot has sensors that can determine the distance of obstacles around itself.

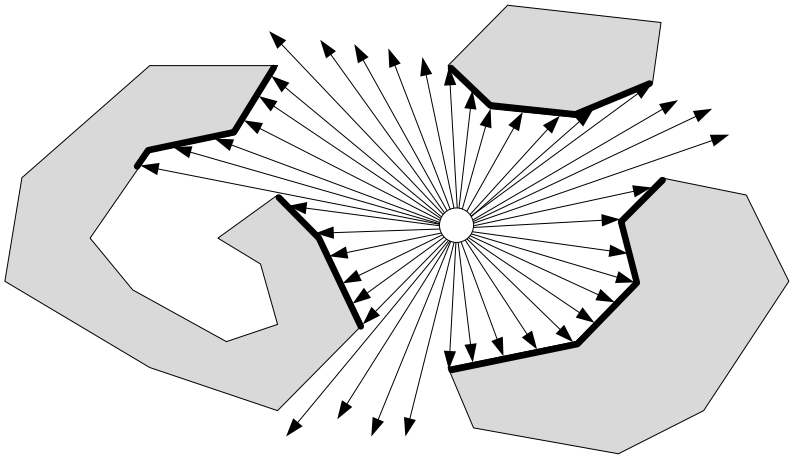

Fig. 2.12. Obstacle recognition with the help of sensors.

However, in practice, the robot's sensors don't scan all the angles to determine its distance to barriers continuously and perform it discretely. For example, the distance from the robot to a barrier is determined after each rotation by 5 degrees. However, in between these angle intervals, there may be t some obstacles that remain hidden from the robot's vision with this strategy. On one hand, these sensors may only cover a certain range, and if there be an obstacle outside this range, the robot will not be able to recognize them.

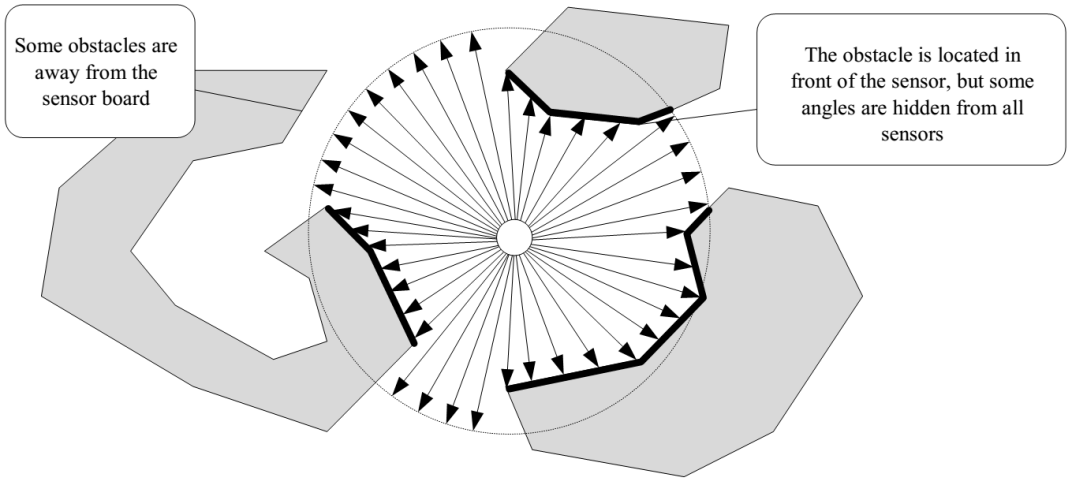

Fig. 2.13. Obstacle recognition with the help of limited-range sensors.

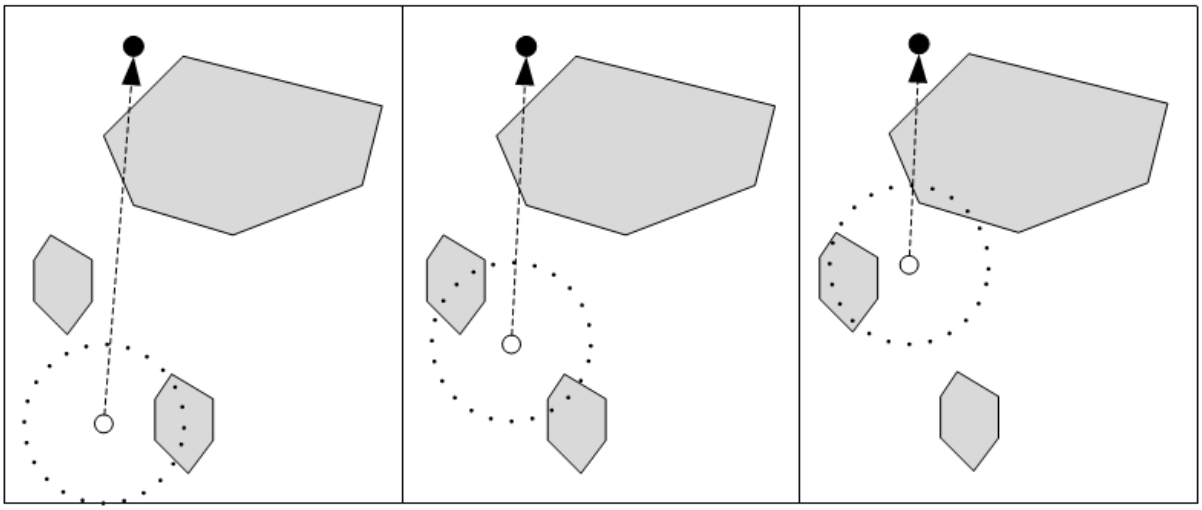

Fig. 2.14. Robot's straight movement towards the target before sensing the obstacle.

TangBug works similar to Bug 2 algorithm:

Step 0. Move towards the target until sensors sense an object between itself and the target directly.

Step 1. After that, move towards discontinuity points of e_1 or e_2. The principle that robot meets to choose one of these two points, is shortening the path to the target. For example, in Fig. 2-15 the robot chooses its path based on this algorithm so that the amount $Min\left(\left|S\overline{c_1}\right|+\left|\overline{e_1T}\right|,\left|\overline{Se_2}\right|+\left|\overline{e_2T}\right|\right)$ is achieved.

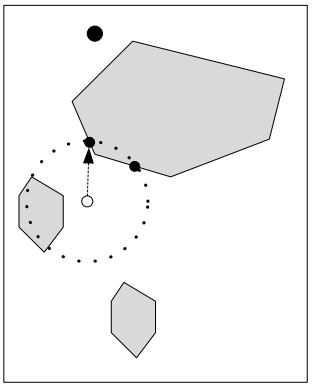

Fig. 2.15. Robot's movement towards discontinuity points.

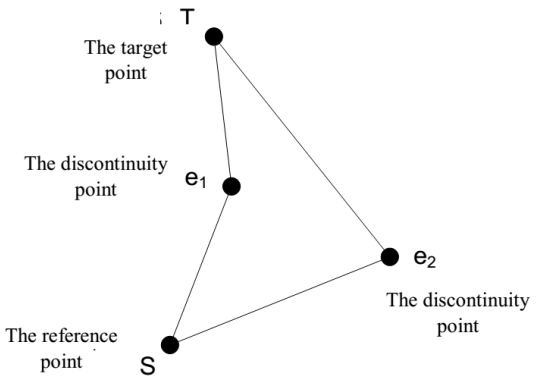

Fig. 2.16. The start point, target point and two discontinuity points.

2-2-7-1- Surround Tangential Chart

In the beginning, consider an environment, such as Fig. 2.17a, which includes obstacles, a starting point, and an end point. At first, according to Fig. 2.17b, convex vertices of all the obstacles are determined. Then, straight lines connect the specified vertices and starting and ending points, mutually; so that the lines do not intersect the barriers. The resulting graph, which is shown in Fig. 2.17.c, is called a surround tangential graph. It can be proved that surround tangential graph always contains the optimal route from the starting point to the end point. This optimal route for understudy environment is shown in Fig. 2.17.d.

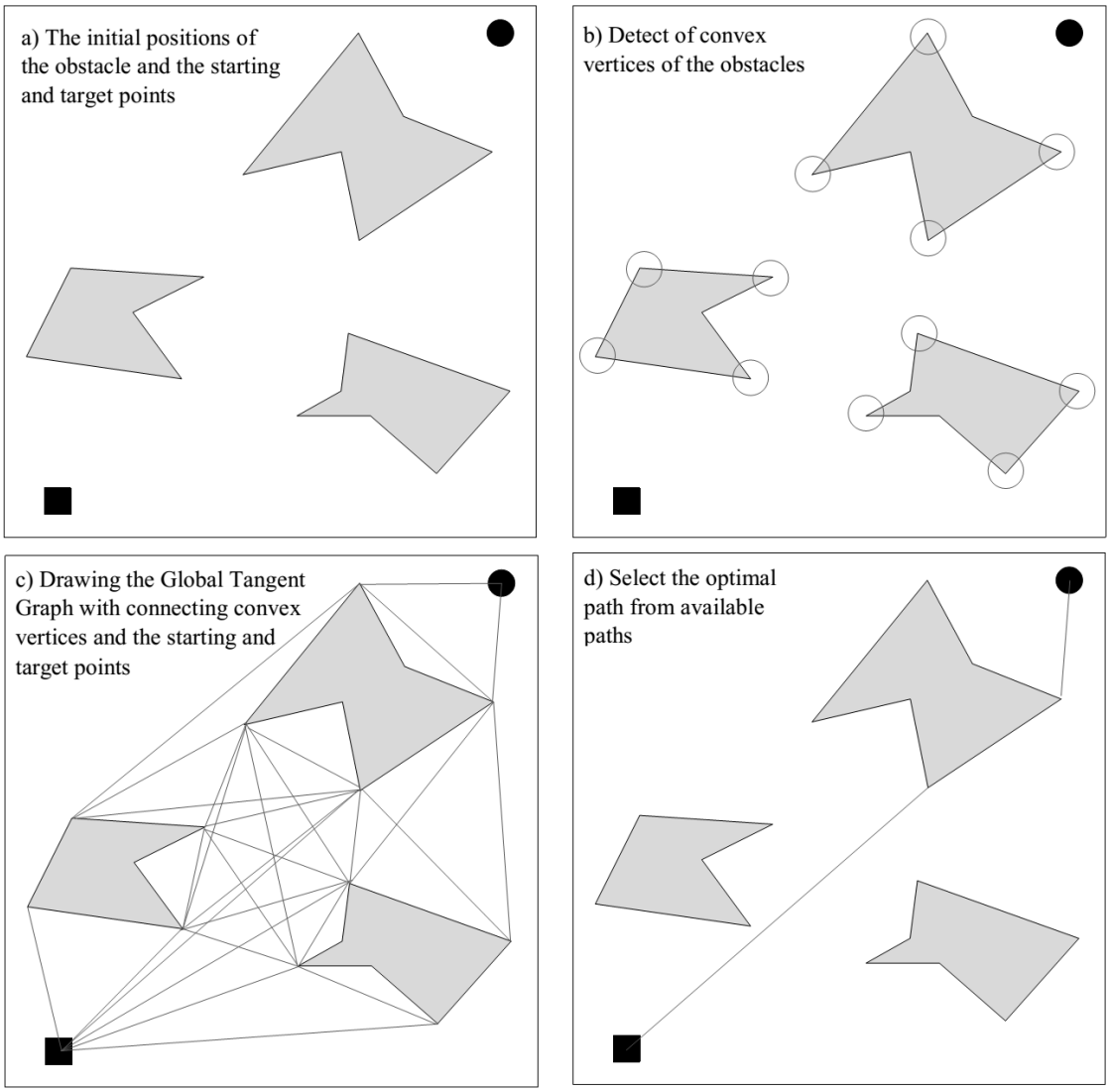

Fig. 2.17. The stages of drawing the tangential diagram and selecting the optimal route in an environment including obstacles and starting points and targets

2-2-7-2- Local Tangent Graph

When the robot lacks the ability to acquire surrounding information from the environment, it tries to generate a local map, known as the local tangent graph (LTG). An example of this graph has been shown in Fig. 2.18. Creating local tangent graph requires collecting information for two functions $r(\theta)$ and F. The function $r(\theta)$ calculates the distance to the first visible barrier along θ and function F shows the free space in front of the robot. With this information, local tangent chart nodes and the optimal route is calculated as follows

A. nodes resulted from examining status F:

- If $d(x,T) \leq F$, the target is visible and a node named T is created on it.
- If $F \geq r$ it means that no obstacle is seen along the target point, and as a result, the node T is created along the target. An examples of these nodes is shown in Fig. 2.18.

B. The nodes resulted from examining state of function $r(\theta)$:

- Once viewing any discontinuity in the function $r(\theta)$, a node along θ is created. An example of these nodes is shown in Fig. 2-18 with numbers 1, 2, 3 and 4.
- If $r(\theta) = r$, (meaning the distance of barrier is equal to the maximal range of sensor) and then, $r(\theta)$ reduces, a node will be added along θ. The node 5 in Fig. 2-18 is an example of such nodes.
- If $r(\theta) \neq r$ and afterwards, (θ) becomes equal to r, then a node is created along θ.

C. Determining the Optimal Path:

- For each node, the distance, $d(N_i, T)$ is calculated, where N_i denotes the i^{th} node.
- Any node that has the lowest value of $d(N_i, T)$, is introduced as the optimal node and is labelled "N^*".

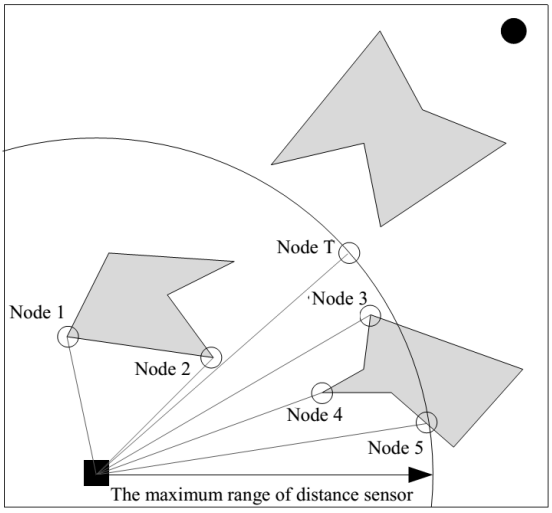

Fig. 2.18. An example of localized tangent diagrams.

2-2-7-3- Local Minimum

Fig. 2.19 clearly shows that sometimes, despite the straight movement of robot towards the target, which makes the distance shorter, existence of a barrier between the robot and the target, makes the robots away the target. In other words, despite the fact that this position of the robot is locally minimum, moving towards the target makes it away from the target. For this reason, to make the robot approach the target, some broader aspects of the environment must be taken into account.

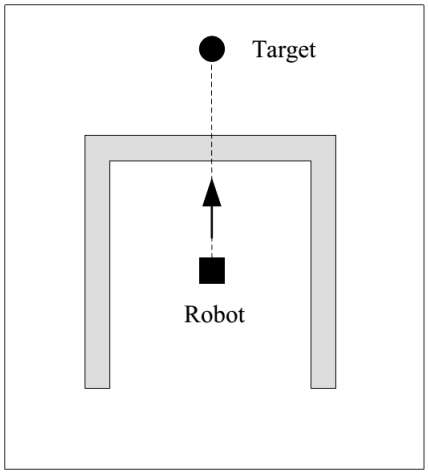

Fig. 2.19. Robot getting away from the target due to local minimum position.

In a case, that robot is in local minimum, TangentBug algorithm adopts the status of following the wall of the barrier. In this case, the robot selects one direction for bypassing the barrier by using a graph of local tangential and continually updates the following two variables:

$d_{followed}(T)$: The minimum distance to the target along some barrier which has the lowest influence;

$d_{reach}(T)$: The minimum distance from point *P* to the target.

TangentBug algorithm scans at any moment the accessible environment for the robot and specifies the point *P* where $d(P,T)$ becomes minimum. Furtherly, the amount of $d(P,T)$ replaces the current value of $d_{reach}(T)$. The act of following the barrier's wall continues until one of the following two conditions occurs:

- If $d_{reach}(T) < d_{followed}(T)$ the target is unattainable
- If the robot completely bypasses the obstacle and repeats it; in this case the target is unattainable as well and the mission stops.

The pseudo-code for TangentBug algorithm in an environment as shown in Fig. 2.20 is as follows:

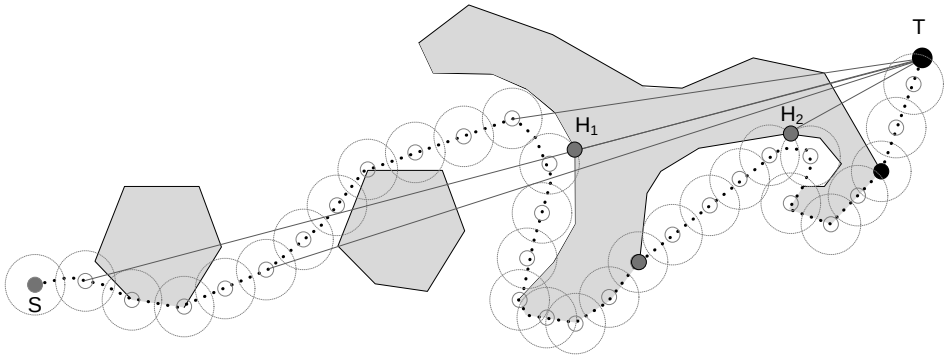

Fig. 2.20. Routing strategy in Tangentbug algorithm in an environment with different barriers.

```
While  (TRUE)
  LET w = T
  REPEAT
  x' = x  // robot's previous location
      update x by moving towards w
      IF  (no obstacle detected in direction w)  THEN w = T
      ELSE
         LET e_L and e_R be discontinuity points
         IF  ((dist (x,e_L) + dist(e_L,T)) < (dist (x, e_R) +dist (e_R,T)))
            THEN w = e_L ELSE w = e_R
  UNTIL  ((x ==T))  OR  (dist  (x' , g)  < dist  (T,g)))
  IF  (x ==g)  THEN quit // target reached
  LET H = L = x // contact location
  LET dir = direction of continuity point  (L or R)
  REPEAT
     LET w = the discontinuity point in direction dir
     IF  (dist  (x,T)  , dist  (L,T) )  THEN L = x
     Update x by moving towards w
  UNTIL  ((dist (x,T)  , dist  (L,T))  OR  (x == T)  OR  (x == H))
  IF  (x == T)  THEN quit   // target reached
  IF  (x == H)  THEN quit   // target not reachable
ENDWHILE
```

In Fig. 2.21, the trace resulted from implementation of TangentBug algorithm in an arbitrary environment is shown.

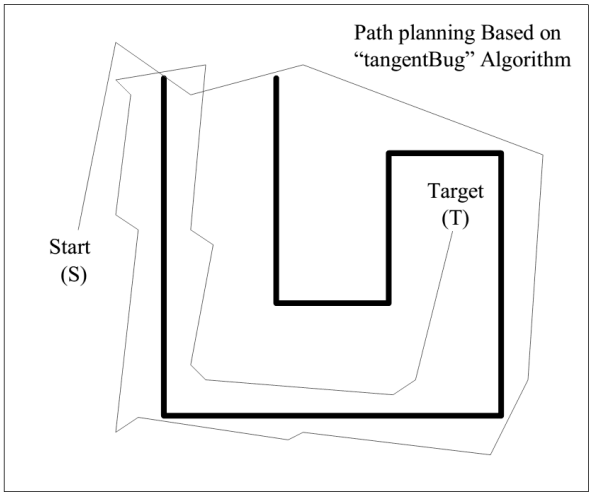

Fig. 2.21. Implementation of TangentBug algorithm in an arbitrary environment.

2-2-8- *Other Bug Algorithms*

In addition to the algorithms already discussed, there exist some other algorithms that operate based on Bug algorithms and each one seeks to optimize it in a specified section and by using assistant tools (sensors, GPS, camera, map, and ...). Of course, these algorithms didn't become much universal, and for this reason, in this section it would be sufficient to mention their name and some brief description about them.

2-2-8-1- HD-I Algorithm

Algorithm "HD-I" is similar to Rio 1 one discussed in section 2-2-4. The difference between these two algorithms is in the orientation of following up the wall. The basis of HD-I algorithm is the distance from the robot to the target, its orientation and the directions that the robot has followed previously. The main advantage of this method is shortening the path to a great extent.

2-2-8-2- Ave Algorithm

Algorithm "Ave", which in fact, is an improved version of HD-I algorithm, proposed by Noboroyo, Nogamy, and Hirao. The most important improved specification of the algorithm, is determining the direction of following up the wall by robots. In the Ave Algorithm, to obtain

the distance to the target, not only current nodes' information, but also the information of other nodes by which the robot has passed, is used.

2-2-8-3- VisBug 21 & 22 Algorithms

Algorithm VisBug 21, developed By Lumelsky and Skouez, allows the robot to follow Bug 2 Algorithm's path using sensors with a specified range. Using sensors are intended to find shortcuts so as to shorten the path. VisBug 22 Algorithm is more risk-taking to find the shortcut compared to Bug 21 algorithm. This algorithm can greatly reduce the robot's path, though there is the possibility to make the route longer if the shortcuts do not work.

2-2-8-4- WedgeBug Algorithm

WedgeBug Algorithm was proposed by Laubakh and Burdick (Laubach and Burdick 1999). This algorithm examines wedges and the first wedge determines the direction that causes the robot to reach the target. If the robot doesn't encounter an obstacle in its way, it moves towards the target, but if there are any obstacles, it proceeds to follow the hypothetical barrier's border. In the meantime, most of the wedges are studied using limited-range sensors of the robot. The main advantage of this algorithm is avoiding the need to create a tangent local or surround graph. It should be noted that local or surround tangent graphs are created in algorithms such as TangBug algorithms. In designing this algorithm, the following conditions should always be taken into account:

- No information already available in advance
- The design should be based on information collected from sensors and cameras;
- The design should be robust, meaning it should predict an appropriate mechanism after changes occur in the environment;

- The design should be complete and correct.

2-2-8-5- CautiousBug Algorithm

CautiousBug algorithm has been developed by Magid and Rivlin (Magid and Rivlin 2004). This algorithm contains spiral motions, which causes the robot's consecutive change of pursuit direction towards the barrier.

2-2-8-6- Three-dimensional Bug (3DBug) Algorithm

3DBug algorithm was proposed by Kamon, aymond and Rivlin (Kamon et al. 1999). The algorithm, is in fact the improved version of TangBug algorithm which works in three dimensions instead of two dimensions. Several major issues arises in this regard, which are not as easy as following barrier's border by the robot, but the robot searches a wider environment, instead.

2-2-8-7- Axis-Angle Algorithm

The concept of Axis-angle algorithm was introduced by Lumelsky and Tiwari (Lumelsky and Tiwari 1994). The main concept of the algorithm is taken from Pledge algorithm (Abelson and DiSessa 1986) and uses two variables for leaving the barrier. First, the angle between the line connecting point x (the current position of the robot) to the target point with the connecting point from the beginning point to the target point; and second, the angle between connecting line from beginning point to the target point with current velocity vector of the robot. One of the advantages of this algorithm compared to other Bug algorithms,is no need for measuring range tools (such as sensors), so that a simple direction indicator can implement and realize this algorithm as well.

2-2-8-8- Opitm-Bug Algorithm

Optim-Bug Algorithm was founded by Kreichbaum (Kriechbaum 2006). Unlike other Bug family algorithms, this algorithm uses an infrared sensor, and when receiving information from surrounding environment, prepares a map from it simultaneously. Optim-Bug algorithm, in case of having full information on the environment, could neglect the step of looking up the border barrier by a robot. Using these sensor as well as a map, makes selecting the shortest path by this algorithm possible, which in return results in minimalism of the time to reach the robot to the target, without encountering obstacles.

2-2-8-9- Unknown Bug algorithm

Unknown Bug algorithm (Kriechbaum 2006) is similar to Optim-Bug algorithm; the only difference is that in the robot path, some sources of uncertainty are developed. This algorithm calculates the optimal route at any stage of the movement and for this purpose, also uses the available information (obtained from GPS, camera, maps, etc.). Another purpose of this algorithm, is reducing the maximum error of final position of the robot regarding the target.

2-2-8-10- SensBug Algorithm

The objective of designing SenseBug algorithm (Kim et al. 2003) is incorporating robots in building environments. In such environments, the obstacles are assumed simple objects with a specific length. Leaving obstacles in this algorithm is similar to leaving obstacles used in COM algorithm, presented in the next section. It is assumed that obstacles can move in building environments. Given this, it is proved that SenseBug is able to guide the robot towards the target, successfully. In this algorithm it is essential to use the wireless network in order to guide the robot in a specified order, in order to shorten the maximal path length during following barriers.

2-2-9- D^* Algorithm

D^* Algorithms was developed by Stentz (Kim et al. 2003) and, it has many differences compared to Bug algorithms, which the most important one is in using maps (mapping is not allowed in Bug algorithms) So D^* algorithms have attractive and unique specifications. This algorithm performs map gridding as shown in Fig. 2.23 and based on scoring them, determines the direction of movement.

2-2-9-1- D^* Algorithm performance without barriers

To understand the algorithm D^* consider this example. Consider a field with 5×5 grid according Fig. 2.23, which in the initial state, the robot is in cell (3, 1) and the target is in cell (3, 5). Suppose that the value of stepping horizontally and vertically are indicated with number 1, and diagonally with number $\sqrt{2}$. With this assumption, D^* algorithm creates table 2-1-a for the cells surrounding the target cell (T). In this table, at first the value of each of cells neighboring the target are determined based on stepping towards the target (in horizontal/vertical or diagonal manner) and then the selected cells with the lowest total value are specified. According to the Table 2.1a and Fig. 2-23-a, the cells (4, 5), (2, 5) and (3, 4) have the lowest total value, and determine the direction towards the target.

In the next phase, the neighbors of the selected cells (4, 5), (2, 5) and (3, 4) are valued with the same pattern. The results of this valuation (i.e. value setting) are shown in table 2-1 (b) and Fig. 2.23 (b). As it can be seen, two cell of (4, 4) and (2, 4) have the lowest total value and are set as chosen cells to continue in the next step and their direction towards the target is specified.

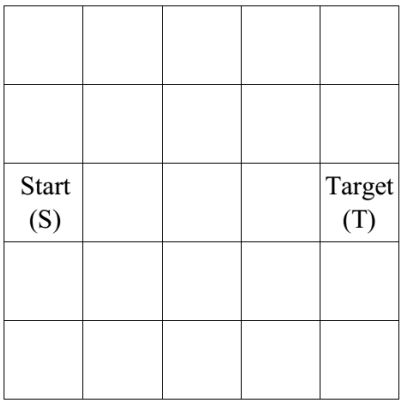

Fig. 2.22. A simple example of gridding the environment using D* method.

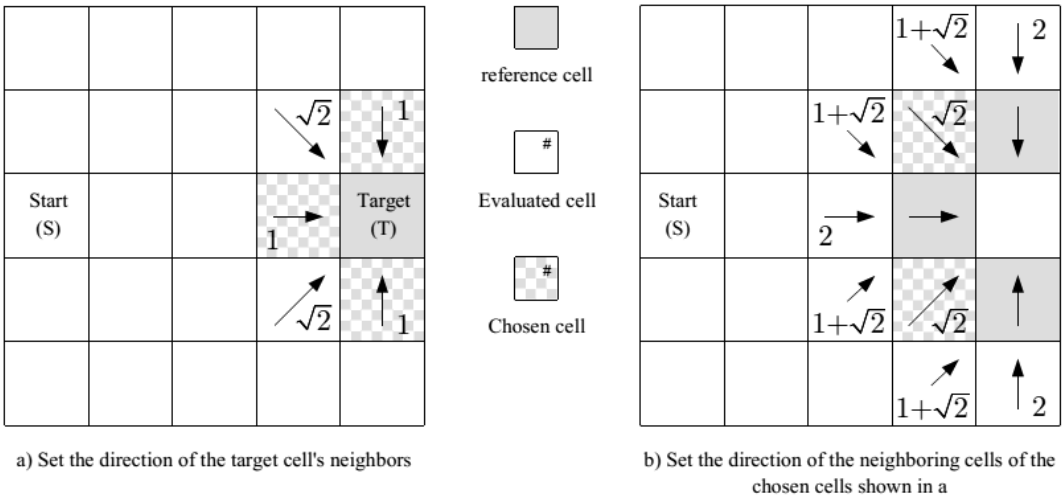

Fig. 2.23. Adjusting the order of the cells with the lowest value to the target cell according to the table 2.1.

Table 2.1. D* algorithm for surrounding cells of target cell.

valued cell	Neighbor cell with at least distance to target*	Step value from (1) to (2)	Step value from (2) to (T)	Total value of cell
Direction determination of neighbor cells of the target cell (Fig. 2.23a)				
(5,4)	T	1	0	1
(5,2)	T	1	0	1
(4,3)	T	1	0	1
(4,2)	T	1.414	0	1.414
(4,4)	T	1.414	0	1.414
Direction determination of neighbors' step 1 selection cells (Fig. 2.23b)				
(5,5)	(5,4)	1	1	2
(4,5)	(5,4)	1.414	1	2.414
(4,4)	T	1.414	0	1.414
(3,4)	(4,3)	1.414	1	2.414
(3,3)	(4,3)	1	1	2
(3,2)	(4,3)	1.414	1	2.414
(4,2)	T	1.414	0	1.414
(4,1)	(4,2)	1.414	1	2.414
(5,1)	(5,2)	1	1	2

* The nearest cell to the target can be the target itself

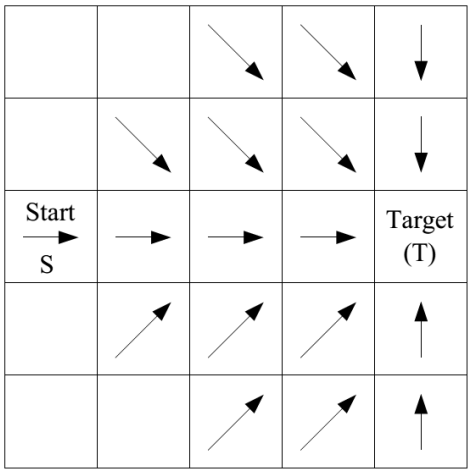

Fig. 2.24. Completing the process of directing the field cells to get to the start cell (robot cell).

This process will continue until the cell hosting the robot also has a pointer. Fig. 2.24 shows the completed process for the example grid. The cells containing a pointer, show the minimum value direction towards the target. Tracing any indicator-containing path, creates a minimum value direction towards the target. Once followed any indicator-containing path, creates a minimum value.

2-2-9-2- Case of taking obstacles in D^* algorithm into account

The method algorithm D^* uses to avoid and move away from the barriers, is increasing stepping value towards the cells containing obstacles. This work of adding value is only done when moving towards barrier-containing cells and are not seen during leaving the cell. For example, if there is an obstacle in cell (3,3) in Fig. 2.25a, the value of movement increases from the neighbors upstream of the barrier (close to the starting point) towards the cell (3,3) (cells (2,2), (3,2), and (4,2)), But lateral cells and the cells downstream it (close to the target) will not change. To clarify the issue, I will continue the previous example in this section, this time with a barrier in the cell (3,3).

Step A: First one must modify the three cells upstream the barrier, namely, cells (2,2), (3,2), and (4,2). As seen in Fig. 2-25-B, despite the fact that among the neighbor cells, cell (3,3) is

the closest one to the target cell, because of the existence of a barrier, it cannot be a standard practice and should be removed from neighboring cells. This way, the suitable neighbors for the cell (2,2) is cell (2,3) and the appropriate cell neighboring cells (3,2) and (4,2) would be cell (4,3). This value-setting process is shown in Table 2.2a, and its result is shown in Fig. 2-25-C. According to the results of this table, both of the cells (2,2) and (4,2) have the least value and will form the basis to continue the process at next step.

Step B: At this step, the cells neighboring both cells (2,2) and (4,2) must be identified and valuated. It has been done in Table 2.2b, base on which, three cells (1,2), (3,2) and (5,2) attain the lowest value, and will form the basis to continue the process at a later step.

Step C: In this step, continuing the process (Table 2.2c) and evaluation the cells neighboring both cells (2,1) and (4,1) have the lowest value and will make the basis of process for the next step.

Step D: At this step, valuation of neighboring cells shows that no cell has a value less than the others (the value of all the cells are the same) and thus, the valuation process ends.

The final grid resulted from this process is shown in Fig. 2.25d.

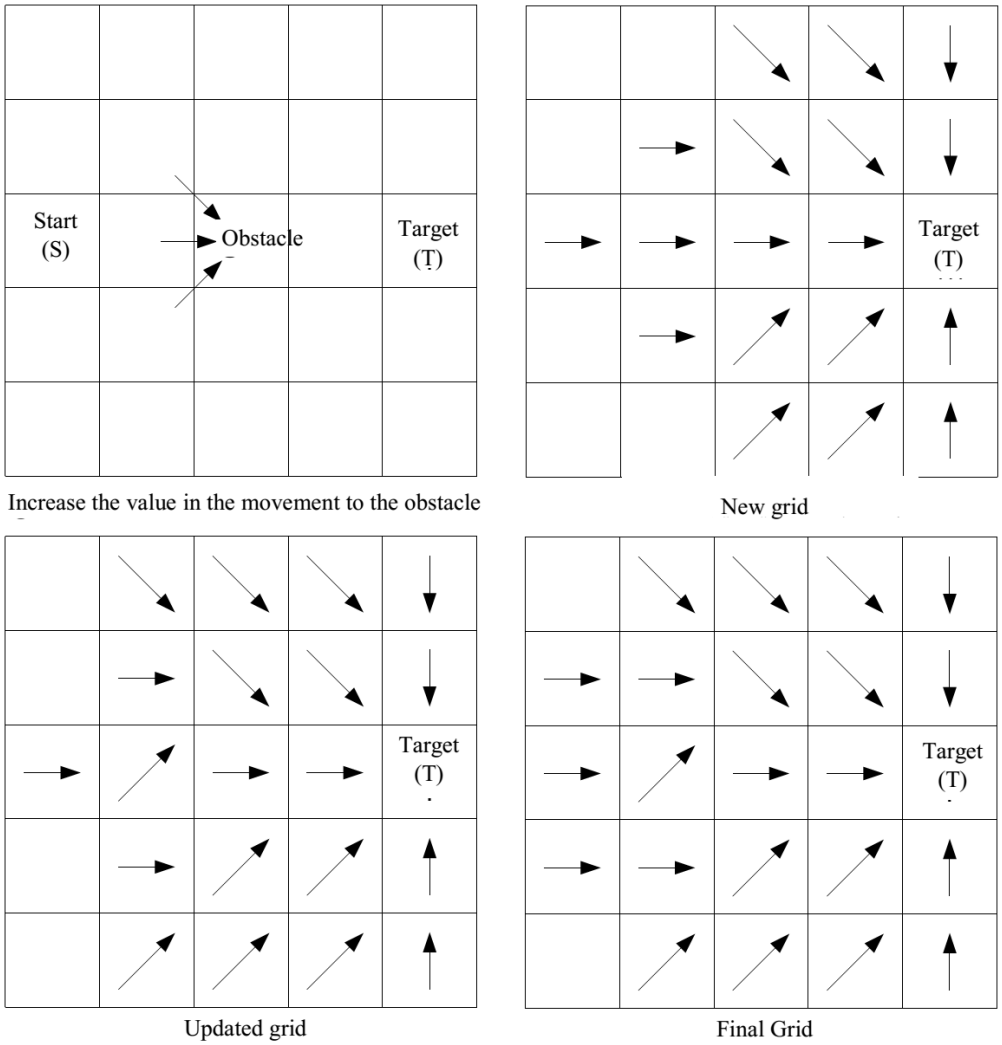

Fig. 2.25. The process of moving vectors to a path in a grid with an obstacle.

It should be noted that the marker located in cell (3,2) will not make the robot return to the its starting point, because D^* algorithm has left behind the optimal path and in another hand will not get trapped in local minima (Choset 2005; LaValle 2006; Latombe 2012). In addition, value correction at each time, will result in dynamically making decisions for the robot, such that when facing with visible obstacles, there will be the possibility to produce optimal paths.

Table 2.2. Evaluation of cells that contain the pointer into cell (3,3).

valued cell	Neighbor cell with at least distance to target	Step value from (1) to (2)	Step value from (2) to (T)	Total value of cell
Evaluation of cells that contain the pointer into cell (3,3) (Fig. 2.23a)				
(2,2)	(3,2)	1	2.414	3.414
(2,3)	(3,4)	1.414	2.414	3.828
(2,4)	(3,4)	1	2.414	3.414
Table of flow frequency for the others cells by the algorithm (Fig. 2.23b)				
(2,3)	(3,4)	1.414	2.414	3.828
(2,1)	(3,2)	1.414	2.414	3.828
(2,5)	(3,4)	1.414	2.414	3.828
(1,4)	(2,4)	1	3.414	4.414
(1,2)	(2,2)	1	3.414	4.414
(1,3)(S)	(2,2)	1.414	3.414	4.828
(1,5)	(2,4)	1.414	3.414	4.828
(1,1)	(2,2)	1.414	3.414	4.828
Continuing the valuation flow of selection cells' neighbor cells from previous step				
(1,2)	(2,2)	1	3.414	4.414
(1,4)	(2,4)	1	3.414	4.414
(1,3)(S)	(2,3)	1	3.828	4.828
(1,5)	(2,4)	1.414	3.414	4.828
(1,1)	(2,2)	1.414	3.414	4.828
Continuing the valuation flow and creation final grid (Fig. 2.25.D)				
(1,3)(S)	(2,3)	1	3.828	4.828
(1,5)	(2,4)	1.414	3.414	4.828
(1,1)	(2,2)	1.414	3.414	4.828

2-2-10- *Com Algorithm*

Com algorithm is used to express the way of leaving the obstacle by the robot, when the conditions for leaving the barrier are met. In this algorithm, the rules of leaving the barrier are clearly set, and hence they're applicable in the development of Bug algorithms. Working principle of Com Algorithm is as follows:

Step 1. Move towards the target until one of the following scenarios occurs:

Step 1.1. Achieve the target, a successful exit from the algorithm.

Step 1.2. Face an obstacle, to follow the border barrier, run step 2.

Step 2. In case of having the ability to move on towards the target, leave the barrier environment, return to the Step 1.

As mentioned above, Com algorithm is the only way to leave the barrier and hence, does not guarantee the robot to attain to the target. For example, applying this algorithm in an environment like Fig. 2.26 shows that the robot could never bring itself to the target and spins around the barrier permanently.

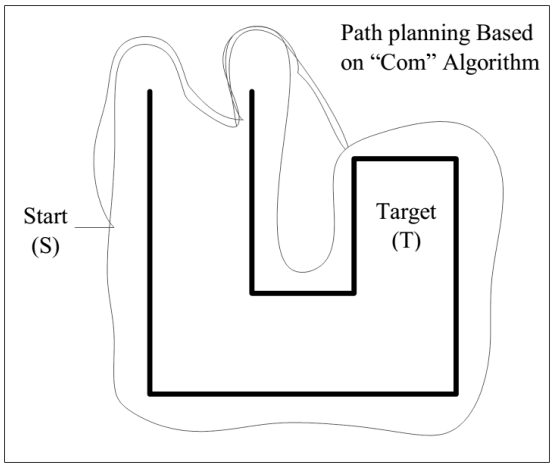

Fig. 2.26. Implementation of Com algorithm in a hypothetical environment.

2-2-11- *Class 1 Algorithm*

Algorithm "class 1" is also a method to study how to leave the barrier, and similar to Com Algorithm, does not guarantee attaining the robot to the destination. In this algorithm, leaving the obstacle is performed in the nearest point to the target relative to the rest of the navigated point. The algorithm class 1 is also used in the development of Bug algorithms like its Com counterpart algorithms, because of having rules for leaving the barrier. The working principle of class 1 Algorithm is as follows:

Step 1. Move towards the target to deal with one of the following scenarios:

Step 1.1. Achieve the target, a successful exit from the algorithm.

Step 1.2. Face an obstacle, follow the border barrier, run step 2.

Step 2. If possible, move towards the target, leaving the barrier environment. Return to step 1.

It must be noted that in step 2, leaving point for the robot is the nearest point to the target compared to all the points that the robot have already met. In Fig 2-27 the algorithm is implemented in an arbitrary environment.

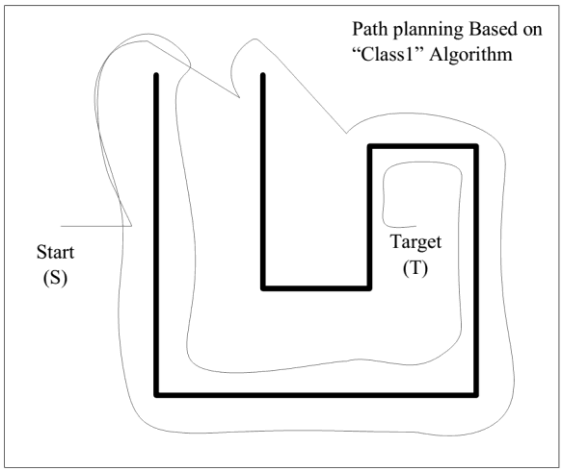

Fig. 2.27. Implementation of Class1 algorithm in a hypothetical environment.

2-2-12- *Rev 1 and Rev 2 Algorithms*

Algorithm "Rev 1" has been introduced by Horiuchi and Noborio (Horiuchi and Noborio 2001). The algorithm is very similar to ALG 1 The only difference is in alternating direction changes in following the robot in each round and also preparing the lists of *H* and *P* in order to capture any better incidences. Rev 1 algorithm acts as follows:

Step 1. Move towards the target until one of the following two conditions occurs:

Step 1.1. Attain the target, successfully exit from the algorithm.

Step 1.2. Encounters an unknown obstacle, the point of collision H_i is specified and its details are recorded in the lists H and P.

Step 2. Move in H_i and consider the list *H*. If both the paths in H_i were already investigated, they would be deleted immediately from the list *H*. Then the robot sticks to barrier and begins to spin around it until one of two scenarios occurs:

Step 2.1. Hit the target, the mission is successfully completed.

Step 2.2. If the distance between the current location of the robot to the target is shorter than the distance of all the past locations to target (metric conditions) and the robot is able to move directly towards the target (physical conditions) the specifications of leaving point will be recorded in the list P and Returns to step 1.

Step 2.3. If the robot returns to previous collision point H_i, the mission has failed. It is the condition that the target is fully covered by the border barrier.

Step 2.4. If the robot returns to the collision point, the previous H_k is recorded as the next Q_l in list *H*. After that, the robot using information contained in the list *H* and List *P*, selects the shortest path to reach the collision point of H_i and chooses the same path to move towards this point. At this time, the robot follows the wall in the opposite direction.

Step 2.5. In the case of returning to a previous point of leaving, this point is recorded as the next point on the list *H*. Afterwards, the shortest route to reach the point of collision H_i is chosen and using the information contained in lists *H* and *P* moves towards it. At this time, the robot travels the wall in opposite direction.

Algorithm "Rev 2" was introduced by the same developers of "Rev 1" (Magid and Rivlin 2004). The difference between Rev 1 and Rev 2 is in step 2.5. Such that in the algorithm Rev 2, if the robot reaches the leaving point in which was located in the past, the prior leaving point is recorded as point as the next point in the list *H*. After that, the robot using information contained

in the list *H* and List *P*, selects the shortest path to reach the point of collision H_i and from this path moves towards this point. At this time, the robot follows the wall in an opposite direction. An example of the performance of these two algorithms is illustrated in Fig. 2.28.

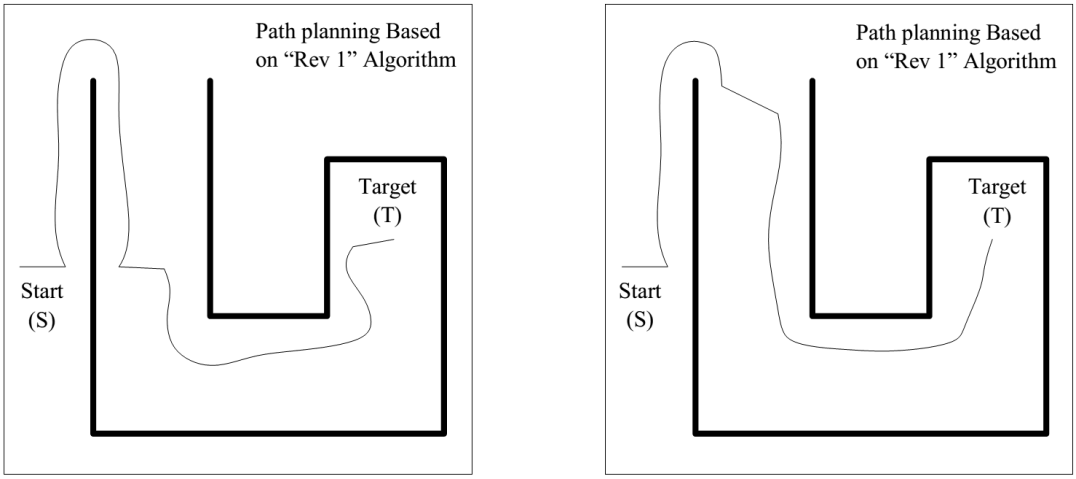

Fig. 2.28. Implementation of Rev1 and Rev2 algorithms in a hypothetical environment.

2-3- Two selected strategies for routing in unknown environments

In this section, two selected strategies in the field of routing in unknown environments will be introduced. The first strategy, histogram of vector field, which is developed by Johan Borenstein and Yoram Koren (Borenstein and Koren 1991). This strategy proceeds to grid the environment using sensors and it assigns a vector to every cell of the grid. Finally the path that is selected by the robot, is obtained from the combination of these vectors and the use of algorithms for bypassing obstacles. The second strategy is called multi-strategy that has been developed by Giovanni Bianco (Bianco and Cassinis 1996). In this strategy, the robot uses specific algorithms which are used in unknown environment, along with predefined maps from the environment.

2-3-1- Histograms of Vector Fields

Consider the case in which the current robot position and the target positions are unknown. In any case, the robot should be able to find the target position. For this purpose we can use

whether optical or audio sensors, or imaging cameras. Also, to circumvent the obstacle we can use algorithms similar to Bug 2. Vector Field Histogram (VFH) method proceeds to grid the environment using sensors and to assign a vector to every cell of the grid. The combination of these vectors, determines the way to achieve the robot to the target, and the robot also can use obstacles bypassing algorithms to get closer to target.

Fig. 2.29 shows an example of a network of two-dimensional environment that can be used to produce the vector field histogram. Of course, considering all the cells in practice is very time-consuming and complicated. As a result, to simplify the calculations, considers only part of the total environment, which is called "active grid" (Fig. 2.29). Selecting this active grid is sometimes done based on effective range. Also, this grid is continuously changed with the robot movements. This two-dimensional grid is used to produce a histogram which determines the angle and the speed in which the robot is controlled.

The histogram is calculated only for the cells existing in active grid. Also, the robot considers just the local information. For each e of the cells, a vector is calculated which has two attributes:

- Direction, from the grid cell towards current cell position in which the robot is located; and
- Magnitude, which is dependent to lucidity of presence of obstacles in that cell.

Vector’s magnitude indicates the value of each cell and it is used as a controlling force required to keep the robot away from the obstacles. Fig. 2.30 shows an example of a vector drawn in an active grid. As can be seen, the number inside each cell represents likeliness of occurring an obstacle in that cell and vector's length based on the magnitude of this value.

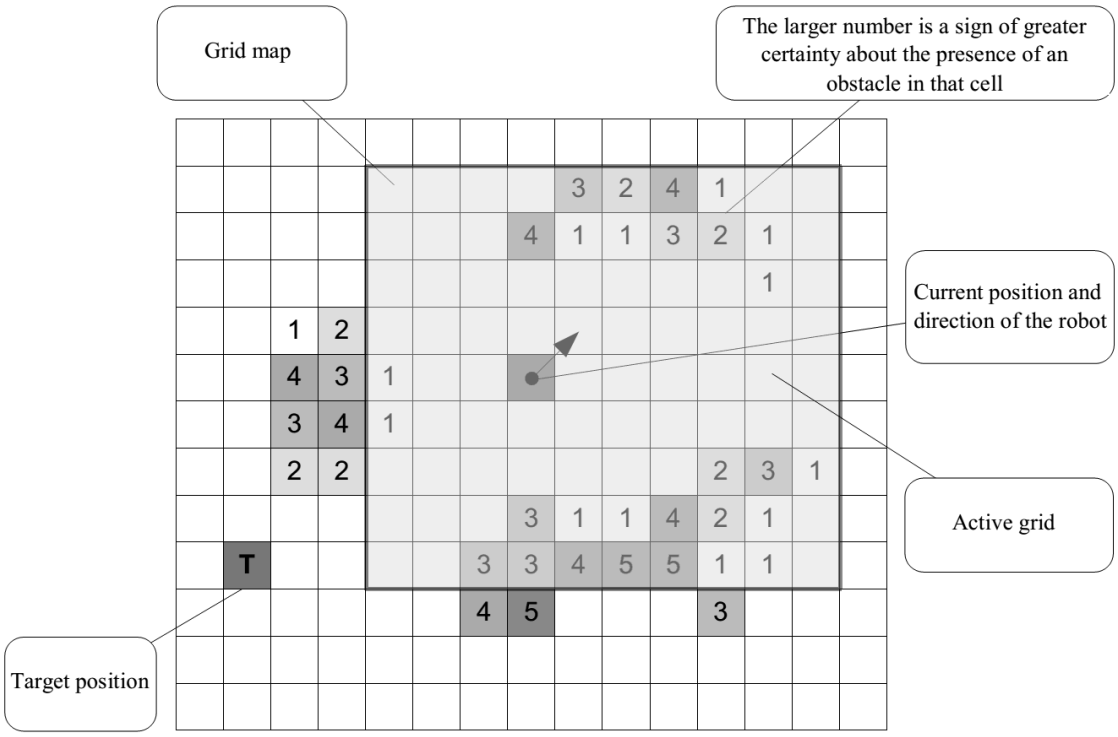

Fig. 2.29. Gridded map in the histogram and its specifications.

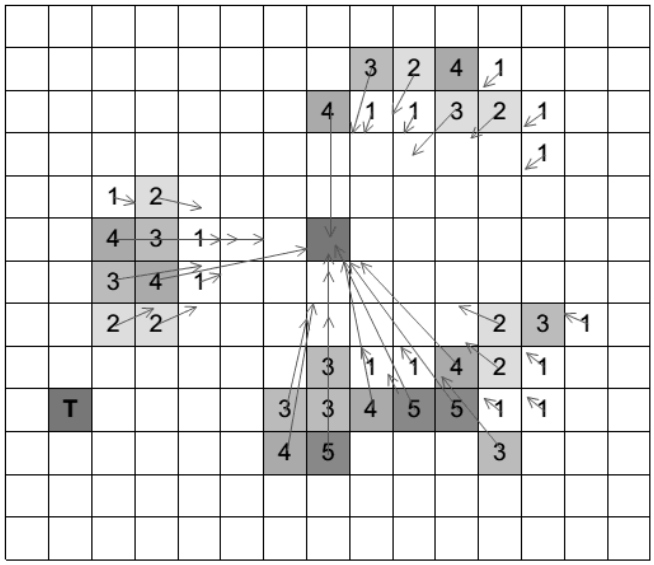

Fig. 2.30. Calculated vectors for cells in an active network.

2-3-1-1- Calculation of each vector

Suppose that $(c_x^{ij},,c_y^{ij})$ is the position of cell (i, j) with value of c_{val}^{ij} and (r_x, r_y) is the current location of the robot. The objective is to obtain the vector v^{ij} cell c^{ij}. Calculation method is as follows:

$$v_{mag}^{ij} = (c_{val}^{ij})^2 \left(\phi - \sigma \sqrt{(c_x^{ij} - r_x)^2 + (c_y^{ij} - r_y)^2} \right) \quad (2.3)$$

$$v_{dir}^{ij} = \tan^{-1} \left[\left(c_y^{ij} - r_y \right) / \left(c_x^{ij} - r_x \right) \right] \quad (2.4)$$

where v_{mag}^{ij} and v_{dir}^{ij} are the size and direction of the vector, respectively and φ and σ are constants used for the normalization. Also, r_x and r_y indicate the center-to-center distance of robot to cell in two directions in Cartesian coordinate system. For this relation it is essential to note that when $c_x^{ij} - r_x \geq 0$ holds, it is necessary to sum up the result with 180.

2-3-1-2- Calculation of Sectors

To calculate the extent of accumulation of vectors that are drawn from obstacles towards the robot, sector principle can be used. Accordingly, angular divisions α is defined. α is in fact the angle division accessible to the robot. This means that the robot's field of view is divided to α parts, which all have the same amount. For example, if the robot's field of view is 360 Degrees and $\alpha = 24$, the size of each sector becomes 15 degrees, and If $\alpha = 16$, the size of each sector becomes 22.5 degrees (Fig. 2.31). The sector s^{ij} associated to each cell, is calculated by:

$$s^{ij} = \text{int}(v_{dir}^{ij}) / (360 / \alpha) \quad (2.5)$$

where “int” is integral part function.

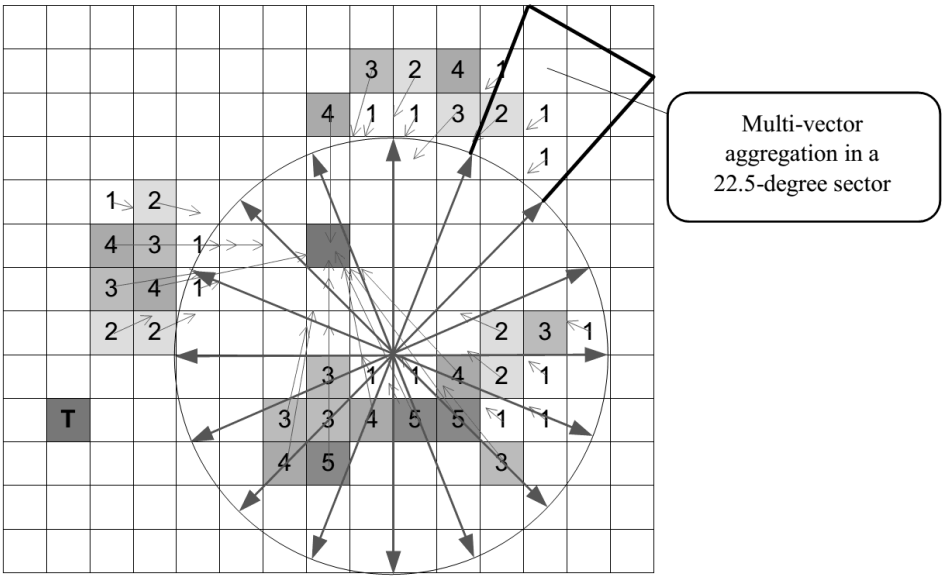

Fig. 2.31. Division of the robot's field of view.

2-3-1-3- Histogram Calculation

In order to calculate histogram, the number of α sectors is taken into consideration. The value of each sector which is shown by h_k and is known as "density of polar barrier", equals the summation of all vectors' magnitudes which have the same s^{ij}. Here h_k is obtained using following relationship:

$$h_k = \sum_{i,j} (v_{mag}^{ij} \mid s^{ij} = k) \qquad (0 \le k \le \alpha) \tag{2.6}$$

where k is the under-consideration sector's number. As a result, all the vectors v^{ij} are assigned to their associated sectors. An example of vector assignments to their associated sectors is shown in Fig. 2.32.

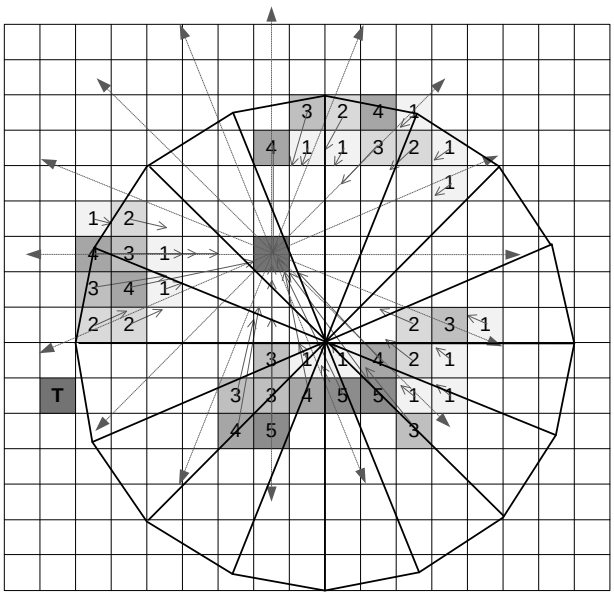

Fig. 2.32. An example of assigning each vector to its own sector.

Histogram graph can be drawn by calculating h_k for each sector. Fig. 2.33 shows the considered histogram grid for two 16- and 72-sector grids. As can be seen, in 16-sector case, the number of slots (having zero amount) in histogram graph is lower; whereas for 72-sector case, the number of zeros is higher, which it is construed as open paths for the robot to cross through. Namely, as the number of sectors increases, the probability of finding an unobstructed path for the robot will increase.

A good idea for matching the histogram, is substituting one value from histogram with the average value of before and after it. This idea is shown in Fig. 2.34. As apparent in the figure, the initial histogram (without averaging) has high scattering. After averaging one time, the size of four neighbors of a sector, the graph will take a more appropriate form. Repeating this operation several times can help to improve the histogram further. It should be noted that the averaging operation must be continued to such extent that border amount ε (which will be explained in the next section) is obeyed.

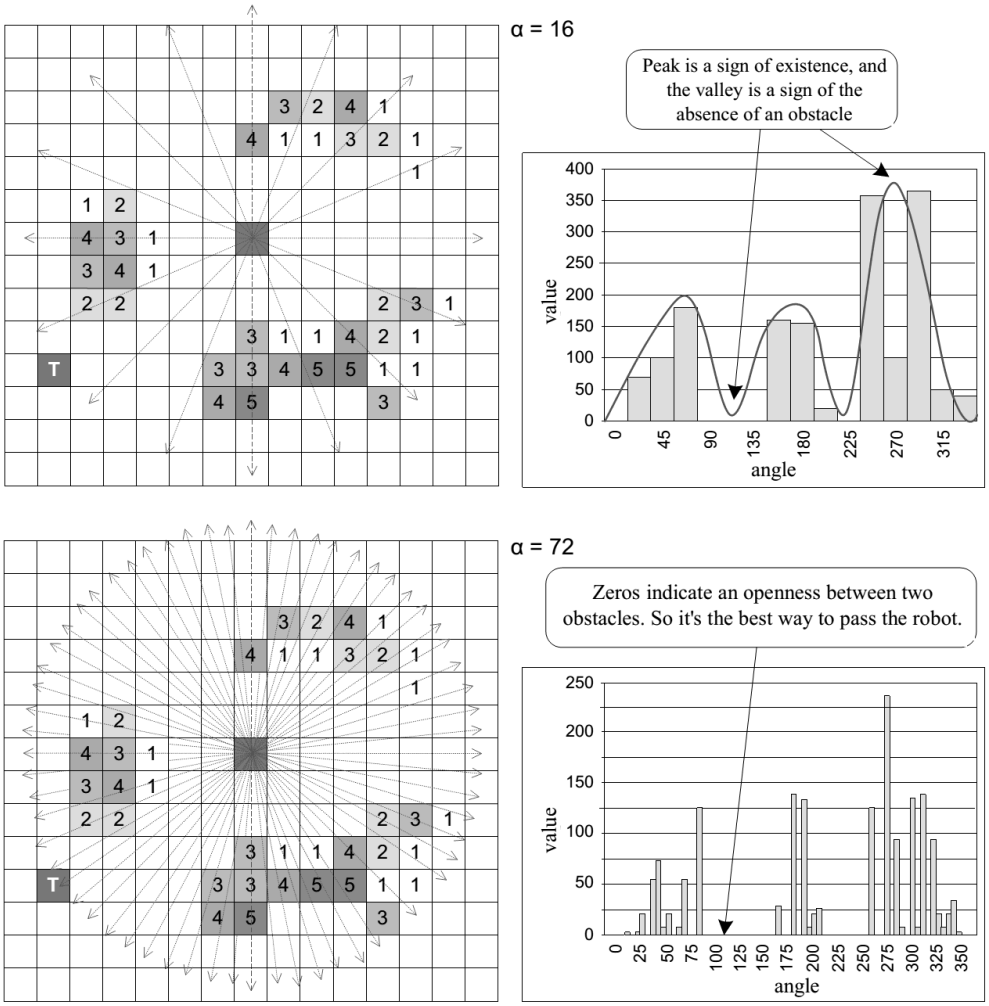

Fig. 2.33. The histogram of the sample environment and its dependence on the number of sectors.

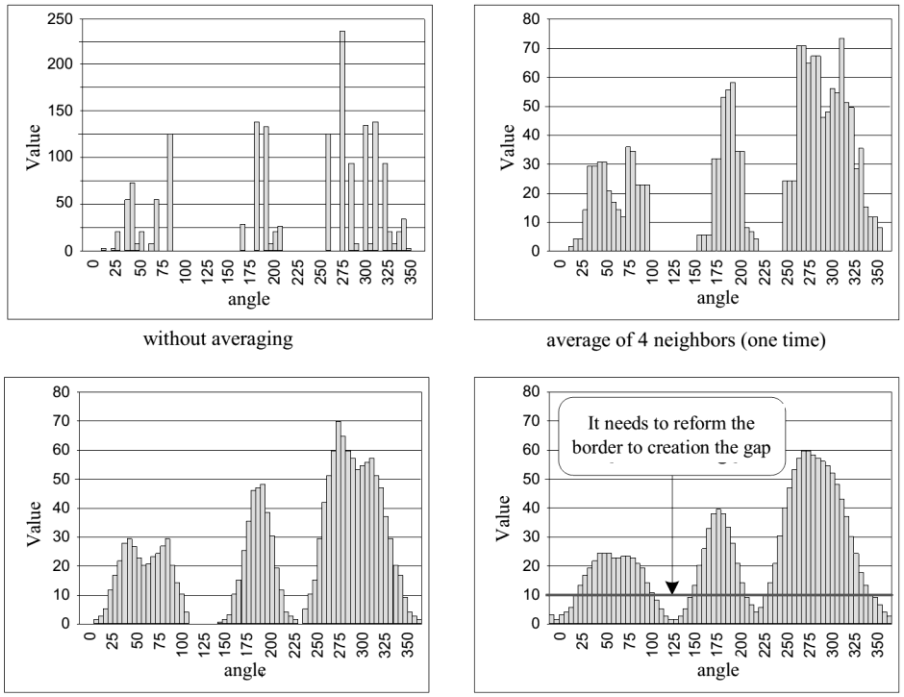

Fig. 2.34. The histogram's dependency on the frequency of averaging the neighbors.

2-3-1-4- How to Use Histogram

At the onset of generating a histogram, it is necessary to specify the sector containing the vector connecting the robot position to the target position. For this, the following formula is used:

$$s^g = \text{int}\left[\tan^{-1}\left(\frac{g_y - r_y}{g_x - r_x} \right) \Big/ \left(\frac{360}{\alpha} \right) \right] \tag{2.7}$$

where s^g is the sector containing the target vector, and (g_x, g_y) is the coordinate of the target position. By plotting a histogram, the nearest valley to the sector s^g can be found among the sectors $s^i, s^{i+1}, \ldots, s^{i+k}$ where i, is the first barrier-free sector and k is the number of barrier-free sectors. For example, the target position in the grid shown in Fig. 2.35, is the sector from 210 to 215 Degrees. The position of this sector in this histogram is also shown in Fig. 2-36 along the corresponding column. The nearest valley to this sector which is usually denoted by S^c is located at position 220 through 225 degrees and is marked with a circle on the histogram. It should be noted that the size of all sectors of a valley must be lower than border amount (ε) (Fig. 37.2).

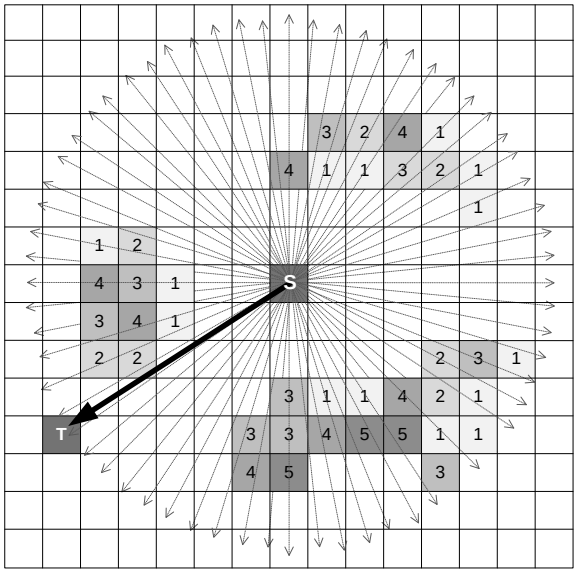

Fig. 2.35. Specifying the sector including the vector of the current position of the robot to the target position.

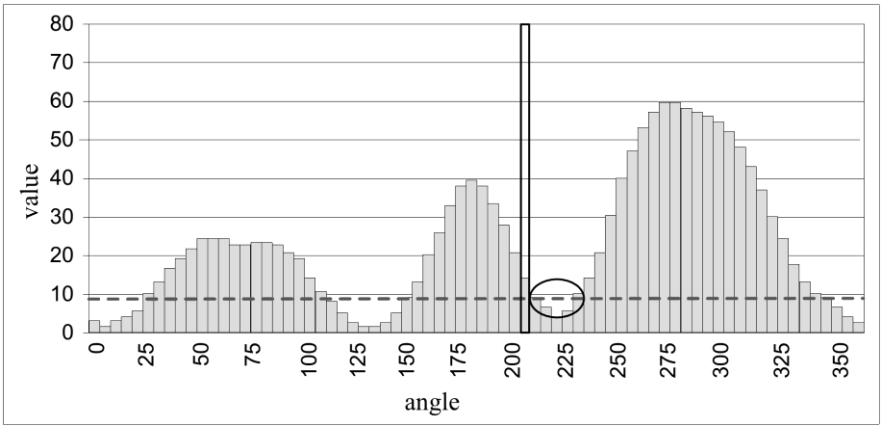

Fig. 2.36. Determining the nearest valley to the sector s^g.

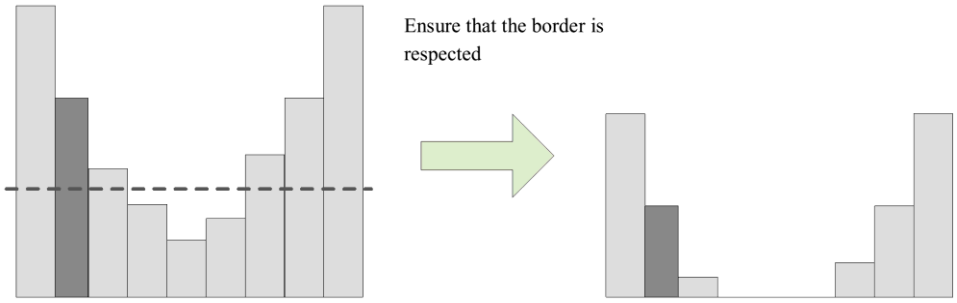

Fig. 2.37. Cutting the histogram regarding the boundary value ε and finding the sectors of a valley.

In order to determine the direction of the robot's movement, several criteria must be considered:

- The number of sectors in a valley which is shown with k.
- The position of border sectors which is denoted by s^i and s^{i+k}.
- The location of the nearest sector of a valley to target sector, which is denoted by s^c.
- The number of neighbor sectors s^c which is shown with ±max (the value for max is determined by user)
- The position of border sectors neighboring s^c is shown with $s^f = s^{s\pm max}$.
- The border value ε showing the maximum size of the sectors inside a valley (value ε is determined by user).

Based on these criteria, valleys can be divided into two categories:

- Vast valleys where $k > max$ and
- Narrow valley where $k \le max$.

Figure 2.38 shows an example of a vast valley with $k = 4$ and $max = 2$. Now, suppose that among all the sectors $s^i, s^{i+1}, \ldots, s^{i+k}$, the sector s^c is closer to s^g. Once s^f is determined, the robot is able to begin its movement along $\theta = \left(s^f + s^c\right)/2$. For example, in Fig. 2.38 the robot will move along the sector s^{i+1}. It should be noted that the higher border value ε, the higher robot movement speed and the less likely to encounter barriers. However, very large values of ε can result in confusion for the robot.

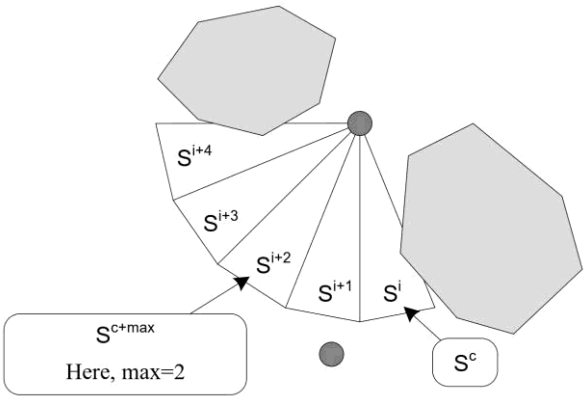

Fig. 2.38. An example of a vast valley (k = 4, Max = 2 and k > Max)

2-3-2- *Designing path based on multi-strategy approach*

In this section, a design for routing robots fitted with independent control system is provided which uses several strategies to reach their target in an unknown environment. This approach has the ability to learn which allows the robot to exploit the results of previous experiments and use them to maneuver better in the future.

As mentioned, robot guidance in an unknown environment has two solutions:

1. Providing a predefined map from the environment with the robot that contains at least something that a robot can see from the starting point.

2. Applying specific algorithms that are capable of dealing with unknown environments.

In this section a combination of both methods with the objective to combine their advantages and avoiding many of the limitations they present is offered. In other words, it seems that remembering some of the characteristics of the working environment, along with the use of algorithms, robust to environmental changes, could be useful.

The proposed approach for designing robot path, uses two main models based on two different assumptions. The first model, taken from reference (Lumelsky 1987a) is built based on information from the environment. Several designs have been formed based on this model, best of which are Lozano-Perez (Lozano-Pérez and Wesley 1979) and Brooks (Lumelsky 1989). The second model, proceeds to design path with incomplete initial information from the environment. Incomplete information, is generally obtained via sensors. Since it is impossible to consider the environment thoroughly from the very beginning, path designing is divided into several time intervals (Lumelsky and Stepanov 1984).

Suggested strategies for "unknown from beginning" environments will result in defining path planning algorithms that will not necessarily lead to converged and optimum paths. As a result, researchers have suggested various approaches to improve converging and optimum strategies. For example, in reference (Lumelsky and Stepanov 1986), Bug 2 Algorithm which guaranties converging to target was used as the first strategy, and if failed, Bug 1 Algorithm was applied. Some other researchers also developed path designing using intelligent training; such that redesigned paths can use the information of prior successful paths (Spandl 1992).

2-3-2-1- Concepts and definitions used in the proposed multi strategic method

In this section, some kind of multi strategic approach is provided for path designing which considers not only failure conditions (divergence) of one strategy in some environments, but also some limitations such as the kind of under used sensors. As it is known, failures (loops and more generally, divergences) are not the only characteristics that lead to inefficiency of a strategy in some environment. In fact, there are many limitations for robot in evaluating its surrounding environment. For example, take into consideration a strategy which incorporates acoustic sensors. These sensors work well in open environment; but will become inefficient in narrow and tight environments.

In order to formulate a relationship for this concept, two sets S and C and one impact factor function η, are used which are defined as follows:

Set S, which its elements are possible strategies in path design and are shown with $s_1, s_2, \ldots, s_n$;

Set C, which its elements are possible environmental properties;

Function η, which indicates impact factor of a strategy identified in travelling a given path *P* and its value is within [0, 1].

If under consideration strategy fails on given path *P* (it means it doesn't reach the target or the path is a loop) η is assumed to be zero. But if the path to reach the target is optimal, η will take the amount of 1 (the optimal route is defined with the shortest route and maximum possible velocity). In all other cases ($1<\eta<0$) the defined strategy always reaches the target, but not through optimal way. If $s_n(c)$ ($s_n \in S$ and $c \in S$) is the optimum route, the following relationship for this hypothesis is written:

$$\forall s_n \in S \quad \Rightarrow \quad \exists \bar{c} \in C,\ s_m \in S : \eta(s_m(\bar{c})) > \eta(s_n(\bar{c})) \tag{2.8}$$

where $\bar{c}$ is a specific environmental element belonging to "*c*"'s. This means that for each strategy, there is an environmental parameter that leads to its more effectiveness than the current strategy. In other words, it is assumed that no strategy is absolutely optimal.

Here, the applied method to divide the environment, is transforming it into square pieces; such that their dimensions are approximately equal to the robot dimensions in size. This process has been shown in Fig. 2.39.

The full path from the starting point to the target, can be a sequence of cells or boxes that are not necessarily adjacent to each other ($A_S \to A_1 \to \ldots \to A_n \to A_T$). Thus, the path consists of a sequence of consecutive paths which are shown with $A_i \to A_j$. As a result, paths can be designed according to different strategies.

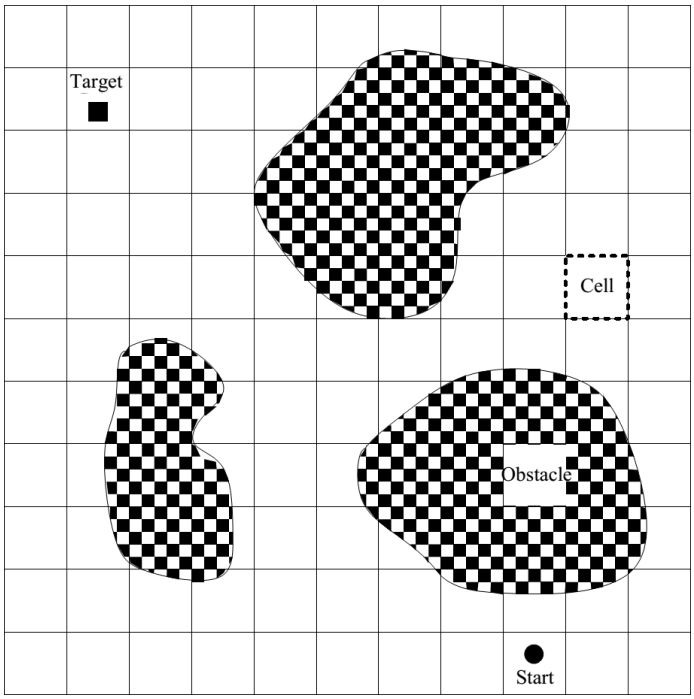

Fig. 2.39. The division of the environment into cells.

Choosing a specific strategy for designing each path depends on the robot itself. Robot does it based on a set of information, which are stored in form of features of each strategy. These features, which allow comparison of a strategy with other strategies, are as follows:

- Usability in a specific local environment,
- Possible efficiency of path traversal,
- Actual efficiency of path traversal.

Defining usability criteria is very difficult for a certain strategy. In contrast, we can define unsuitability as "for every specified strategy s_n, there is at least one environmental parameter c_{ij} that guaranty the failure of strategy s_n. That means:

$$\eta\left(s_n(c_{ij})\right) = 0 \tag{2.9}$$

where c_{ij} belongs to effective environmental parameters and it is planned using strategy s_n (from a cell A_i to cell A_j). For a better understanding, some points about impact factor function η are provided.

Presumable impact factor: this factor is defined as minimum ratio of navigation time (t_μ) to presumable Navigation time (t_σ). Thus, for each path $A_i \rightarrow A_j$, by defining an minimum time ($t_{\mu ij}$) and a possible time ($t_{\sigma ij}$), presumable impact factor can be calculated as follows:

$$\eta_p = \frac{t_{\mu ij}}{t_{\sigma ij}} \tag{2.10}$$

Minimum navigation time occurs when the robot travels a direct path from starting point (located in the cell A_i) to the target point (located in the cell A_j) with a maximum speed.

Whereas, presumable time is the period the robot needs to reach the target point in a specific strategy.

Actual impact factor: This factor is defined as ratio of minimum navigation time (t_{μ}) to actual navigation time (t_{μ}) and for each route $A_i \rightarrow A_j$ from the following equation is obtained:

$$\eta_a = \frac{t_{\mu\, ij}}{t_{\eta\, ij}} \tag{2.10}$$

In this relation, $t_{\eta\, ij}$ is actual navigation time, which is needed to follow a path by the robot. In fact, presumable time can be calculated prior to design step; whereas the actual time will be determined only after robot reaches the target.

By using environmental information, the robot can select the most effective strategy among stored strategies in the memory to go from cell A_i to cell A_j. So, for each known functional strategy ($\eta\left(s_n\left(c_{ij}\right)\right) \neq 0$), the robot selects a strategy that has the highest actual impact factor. If no such strategy was found, a strategy is selected that has the highest presumable impact factor.

2-3-2-2- Building an Environmental Representation Matrix

In multi strategic approach, the robot conducts selection based on environmental presentation information. Environmental presentation, is a square matrix which its rows and columns indicate the identity of cells. Each element of the matrix is associated with a table that includes a list of all the known strategies. The robot has access to three types of information from the environment which are obtained by three virtual sensors:

Virtual sensor Applicability (VSA): This sensor provides a binary response (zero or one) about the applicability of a specific strategy a localized environment.

Virtual Sensor Presumable Efficiency (VSPE): This sensor calculates a number in interval [0, 1] according to the presumable impact factor ($\eta_p = t_\mu / t_\sigma$).

Virtual Sensor Actual Efficiency (VSAE): Similar to estimated efficiency, this sensor also calculates a number in interval [0, 1], this time according to the actual impact factor relation ($\eta_a = t_\mu / t_\eta$).

This virtual sensors are achievable with a general knowledge of the environment or using active sensors (how to incorporate active sensors in path designing approaches are discussed by Lumelsky and Skewis (Lumelsky and Skewis 1990)). The reason to use information of active sensors and environmental knowledge, is finding environmental factors that may impact negatively on usability of a strategy.

For this, at first, t_σ is calculated that often depends on the maximum time consumed by the robot for receiving information from the environment. Using mathematical equations (to calculate the time required to get information any time at a situation specific environment) or using statistical data from previous applications, are the two main ways to do this work. However, VSA is a simple set of rules gained from human experience.

Figure 2.40 shows a matrix representation of the path. As can be seen, for each element of the matrix, a table is created consisting of usability, and actual and presumable impact factors.

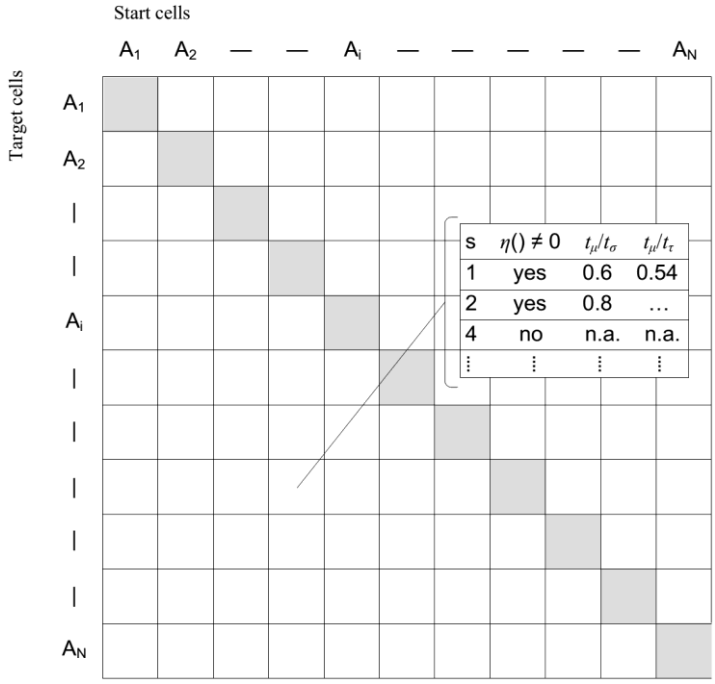

Fig. 2.40. Matrix display of the path.

2-3-2-3- Path design methods based on multi strategic approaches

Path design based on multi strategic approach based on collected data from sensors obtained from local environment, is applicable with three following methods which are different in terms of complexity and efficiency:

Minimal method: The robot continues planning all its path based on only one strategy as long as it doesn't fail. Robot can use other strategies for replanning and can use sensors for finding failure locations.

Median approach: The robot changes its strategy after finding an environmental factor that is incompatible with implementation of the current strategy. The robot uses sensors to detect the local environmental conditions.

Full Methods: In this method, the robot changes its current strategy immediately after finding a strategy with better efficiency in each local environment. The method used in every cell to calculate efficiency of each strategy by the robot, is receiving information from the sensors.

Here, the default approach is minimal approach. This way, initial information is stored in each element of the matrix. This information can be used after any time the robot passes an element. As a result, there is no need to calculate all the information again. The experience of successes and failures of each strategy can be stored and can be used optimally during solving next navigation problems in the same environment.

In Figs. 2.41 to 2.43, three examples of applying multi strategic approach are provided. In Fig. 2.41, the strategy s_1 is applied until prior to failure (the robot caught in an infinite loop). After that, the robot uses another strategy (s_2). In Fig. 2.42, strategy s_1 until failure time (in this case lack of continuity) and then the other strategy (s_2) is used. In Fig. 2.43, strategy s_1 until superiority over other strategies will be used. As soon superiority over another strategy, the robot uses a more effective strategy (at the beginning s_2 and then s_3). In Fig. 2.43, the strategies s_2 and s_3 have better performance than strategies s_1 and s_2.

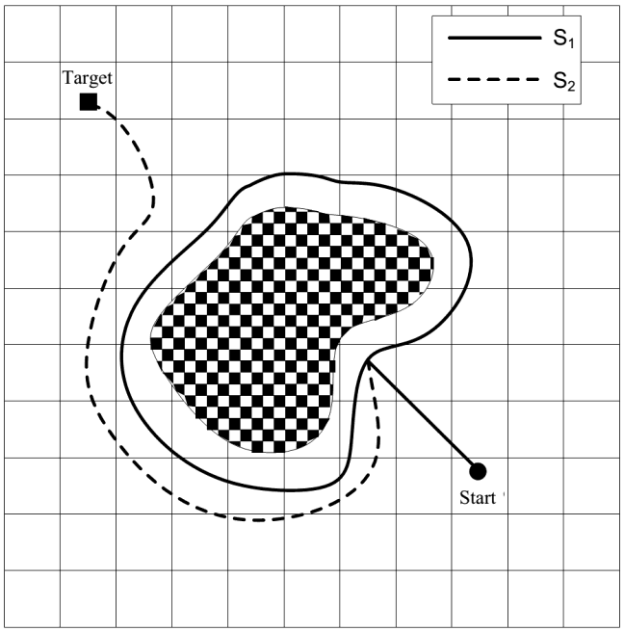

Fig. 2.41. Change of strategy in case of being placed in a loop

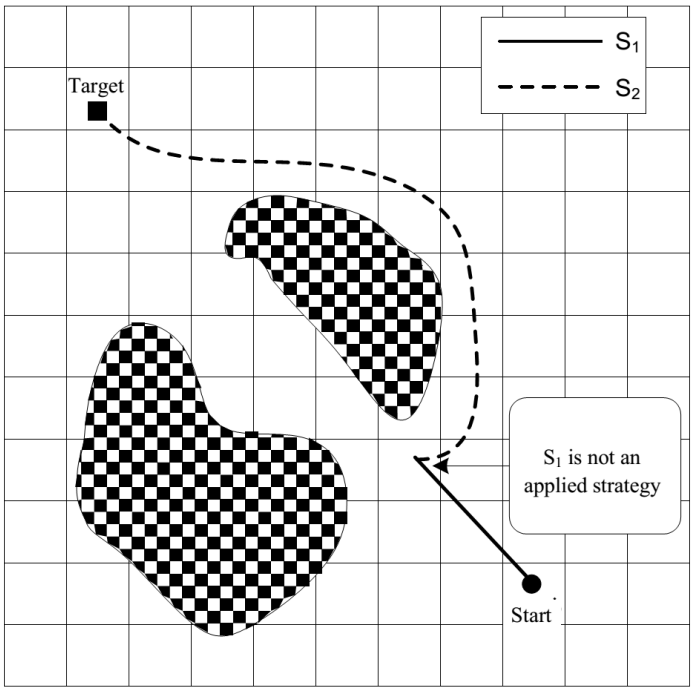

Fig. 2.42. Changing the strategy by breaking it.

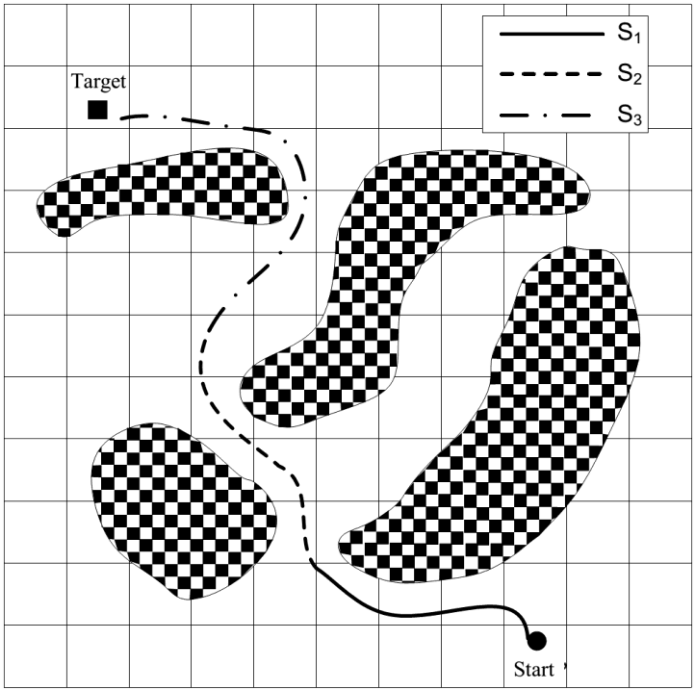

Fig. 2.43. Applying the best strategy.

2-3-2-4- Output of proposed multiple strategy approach

The multi strategic method, is not a path design "strategy", but is "a way" for "improved" path planning". In fact, by using current strategies sometimes we can improve path efficiency or

address the problems of a specified design strategy in certain environmental conditions which result in the robot not reaching the target.

It is necessary to compare multi strategic approach with other improved design approaches (not with specific path design strategies). Accordingly, the main difference between multi strategic approach and its classic types is that for reaching the target, every cell has its own strategy which necessarily doesn't include all the path. This is that difference which can be seen between intelligent training in classic approach and behavioral training in multi strategic approaches. Behavioral training allows the robot to take into consideration qualitative (not quantitative) information about surrounding environment. Hence, in total, obstacles movements and environmental changes, have less effects on multi strategic approaches than their classic counterparts.

Multi-strategy approach, is beneficial particularly in the case of little environmental corrections. For more explanation, consider an unknown environment in which the robot moves. This can be a static environment (where there is no change) or dynamic (which contains changes).

To extract a relation for environmental classes, one can take N as the number of cells existing in the partitioned environment E with the condition $C_{E_t} \subset C$ in time t. If t_1 and t_2 $(t_2 > t_1)$ refer to periods during which the robot must plan a route and M refers to the number of cells with $C_{E_{t_2}}$ variables, with considering $C_{E_{t_1}}$ the under study environment conditions can be defined as follows:

- The environment is static, if $M = 0$;
- The environment is fully dynamic environment, if $M = N$;
- The environment is partially dynamic, if $0 < N < M$.

Therefore, there will be a link between environmental changes and environmental representation. Since in multiple strategy approach, information of every cell is needed, we can evaluate the behavior of the multi-strategy approach in a variety of static and dynamic environments as follows:

Static environments: in this environment, efforts to improve the environment designed using multiple strategy is useless. In contrast, other methods relying on preparation of geometry maps from the environment can have better results.

Full dynamic environment: Regarding the fact that the environment changes completely each time the robot passes the environment, saving environmental information has no benefit. For those environments, a multi strategic method is considered a suitable one for dealing with unknown environments. However, the capacity of training system has failed completely.

Partial dynamic environment: In this environment, no part from environment changes and previous performed experiments could be useful for the design of the leading paths.

2-3-2-5- Multi strategic in action

The use of multi strategic allows designing routes dynamically and usable in environments with slight modifications. In each of the three methods: minimum, median and full, for each cell, a set of impact factors (e) are defined as follows:

$$PE = \{e_1, e_2, \cdots, e_n\}$$

This set can be expanded with statistical analysis as follows:

$$D = \{e_1 * V, e_2 * V, \cdots, e_n * V\}$$

Where V is the numbers of times the robot passes from the corresponding cells.

With random selection of i ($i \in \{1, 2, \ldots, n\}$) and creating strategy s_i, the robot sometimes selects a strategy which is not seemingly optimal. This selection, can be a great help in selecting the robot direction in initial designs that sensors have not already obtained extensive information from the environment and the environment is unknown to a large extent.

Chapter 3- **Path Planning in Known Environments**

3-1- Introduction

In this chapter, path planning in an environment with predefined barriers will be addressed. For this purpose, the robot makes use of maps provided by external resources, or, on its own, prepares maps from its surrounding environment. In the first case, the robot may utilize satellite photos or might have a predefined fixed map at its disposal. In this case, it is assumed that positions of the robot and the target have been specified beforehand. For example, a GPS receiver is able to identify the required positions. There exists a very important issue and that is heavy dependence of existing algorithms to the type of map. With regard to this issue and with given positions of barriers, three strategies to guide the robot towards the target are suggested. With these assumptions, the robot gains extensive information from all the barriers existing in the environment and can utilize a set of pre-computed data to guide itself towards the target. Three major guidance strategies under discussion are as follows:

- Feature-based guidance
- Guidance with potential field
- Vector Field Histograms

In the previous chapter, vector field histogram approach, which is considered as a common approach in both known and unknown environments, was introduced in detail. In this chapter I will proceed to introduce the two remaining approaches.

3-2- Feature-based Guidance

Feature-based guidance is based on preparing features maps and drawing its corresponding graph. Guidance towards the target is based on a process that applies on the graph. In this section, the process of preparing features maps, drawing graphs and completing it until the robot reaches to the target are detailed.

3-2-1- Preparing Feature Maps

The first challenge in guiding the robot based on features is that the robot must traverse the barrier's peripheral completely. There are several approaches to do this. For example, if according to Fig. 3.1, all the corners of a barrier are different in size, the robot can look for some corners by which it already has passed to terminate its search. Also, the robot can, according to Fig. 3.2, use an indicator (such as a circle) to mark its searching starting point until it reaches to its previous indicator again, ensuring that the barrier is completely traversed. Of course, this method will fail in cases where the passages' width is narrow. For example, placing an indicator in a narrow passage (Fig. 3.2) causes the robot to sense the indicator while crossing again from the passage, and stopping its movement though it still hasn't traversed the barrier completely. Another way to ensure that it completely traverses the barrier is taking into account the maximum perimeter of the barrier and stopping the robot after traversing it. This approach has been shown in Fig. 3.3.

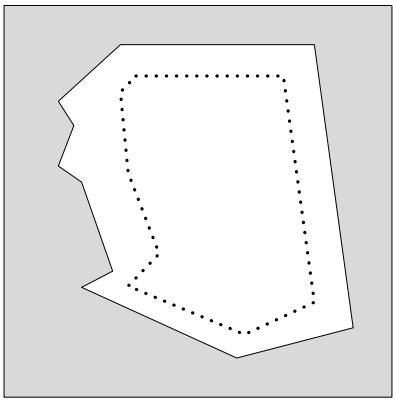

Fig. 3.1. A barrier with different types of edges; allowing robot's transverse regarding the edges.

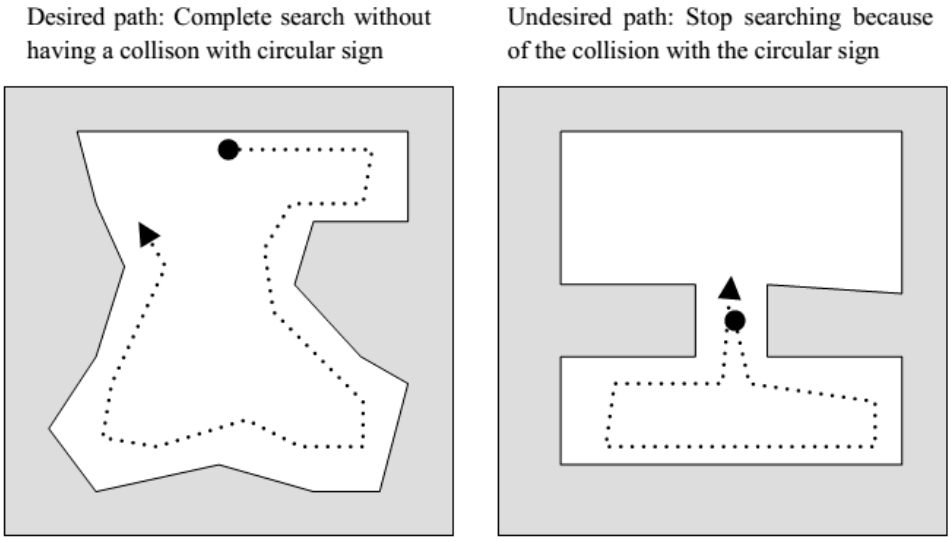

Fig. 3.2. Resulted desirable and undesirable situations due to using a circle indicator for traversing barriers.

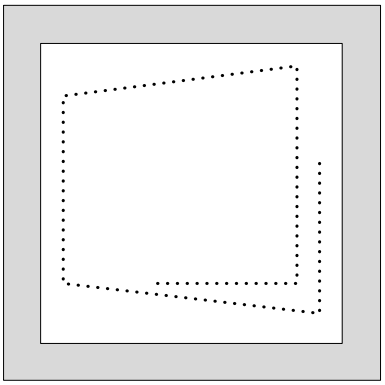

Fig. 3.3. Suspension of robot's movement, having travelled the maximum perimeter.

3-2-2- Storing Feature Maps

There are two ways to store Feature Maps. In the first method, the robot stores their correct number in memory while passing by each corner and edge, (Fig. 3.4a). In the second method

(Fig. 3.4a), a graph or a grid, which can be similar to neural networks, is depicted for each object separately.

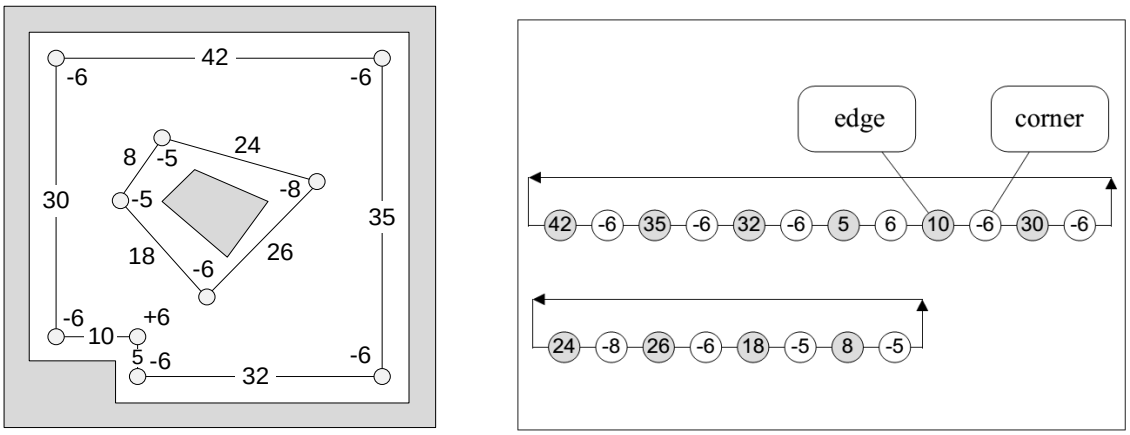

a) Assign integer to corners and edges b) Draw a graph corresponding to the environment

Fig. 3.4. Two different ways of storing feature maps.

3-2-3- *Coinciding Edges*

This section starts with evaluating how to coincide corners on each other. At first, consider those two different ways of pursuing a same environment shown in Fig. 3.5.

The task begins with searching for the first corner by using the procedure to follow the new one. The boundary is chosen as the coincidence's starting point. In this work, all the angles and edges are evaluated sequentially until reaching full coincidence or otherwise failure. Once this occurs, one of these two states can happen:

- Pursuing the new one, leads to formation of new edges and corners.
- Pursuing the new one, does not recognize existing circulations in the main map.

In the first case, one must find a coincidence for edge number 10 and without considering the edge number 3 (Fig. 3.7). In this step, new edges are introduced into the map (Fig. 3.8). But in the latter case, one should search for a coincidence for the edge number 3 (Fig. 3.9).

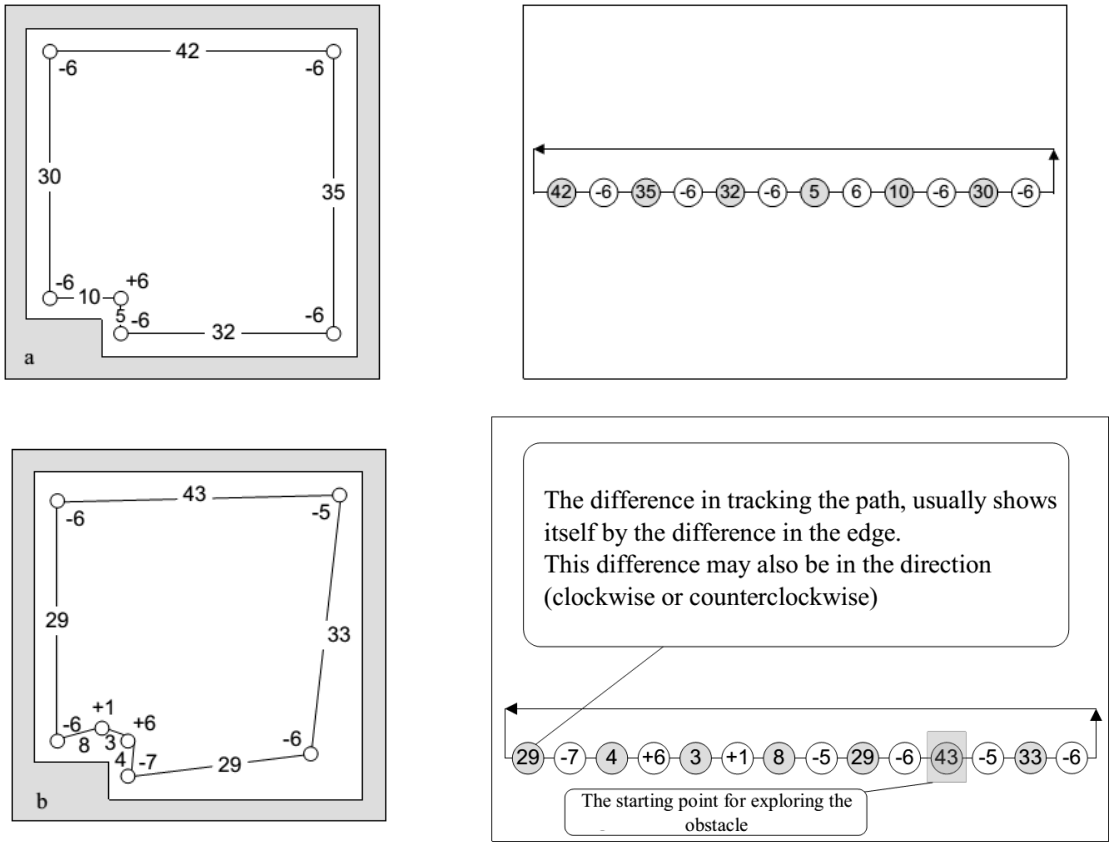

Fig. 3.5. Two different ways of pursuing a same environment and its corresponding graph.

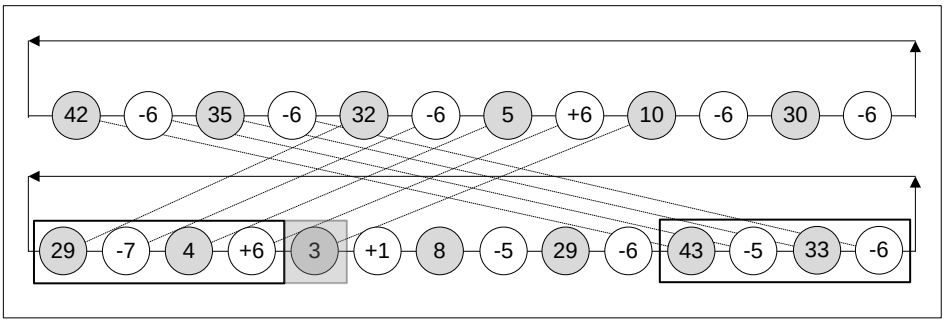

Fig. 3.6. Evaluation of all angles and edges for coinciding.

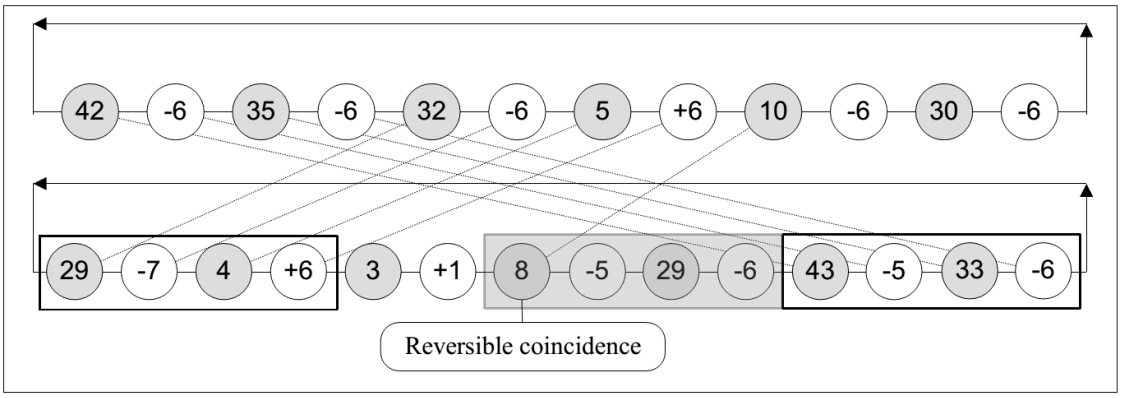

Fig. 3.7. Coinciding edge 10.

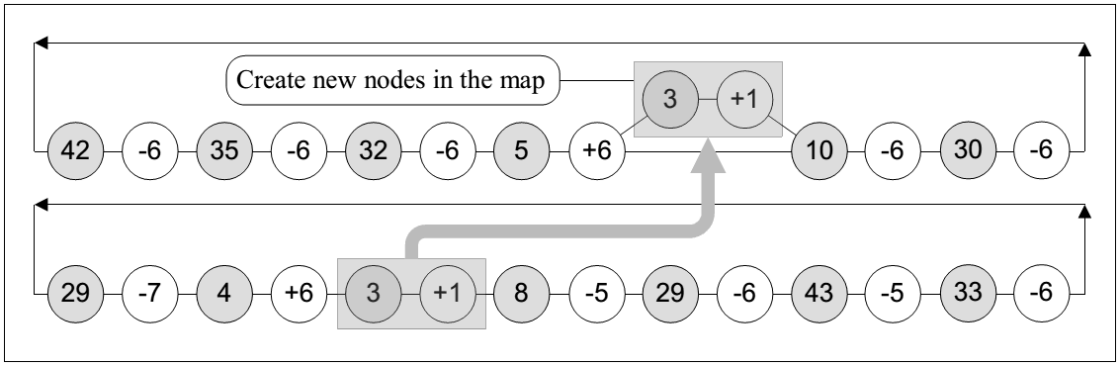

Fig. 3.8. Introduction of the new edges.

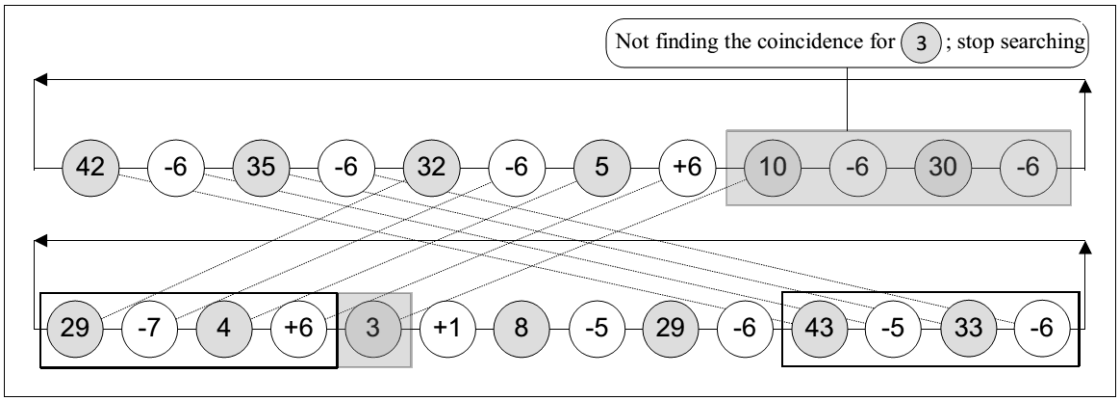

Fig. 3.9. Coinciding edge 3.

3-2-4- Adding Bridges

While drawing graphs, bridges can be considered as edges connected to barrier (Fig. 3.10). Where there doesn't exist a necessary connection between two barriers, in order to transvers all the barriers, it is necessary to add some bridges between them. As seen in Fig. 3.11, before adding a bridge, there were no connections between the graphs of these two barriers and once these two bridges are added, the connection between the graphs is also established.

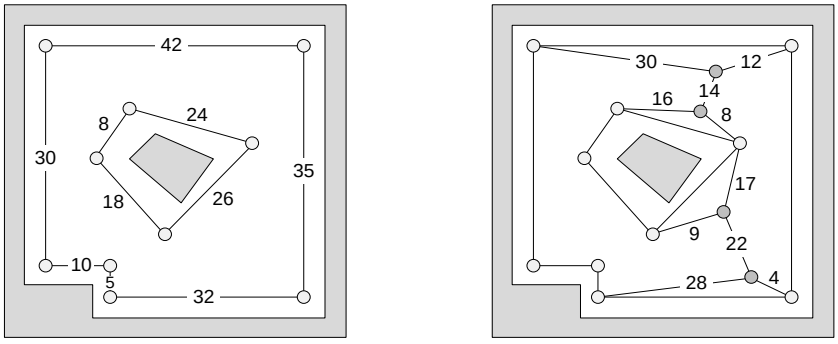

a) before adding the bridge

b) after adding the bridge

Fig. 3.10. An environment including convex and concave barriers, before and after adding bridges.

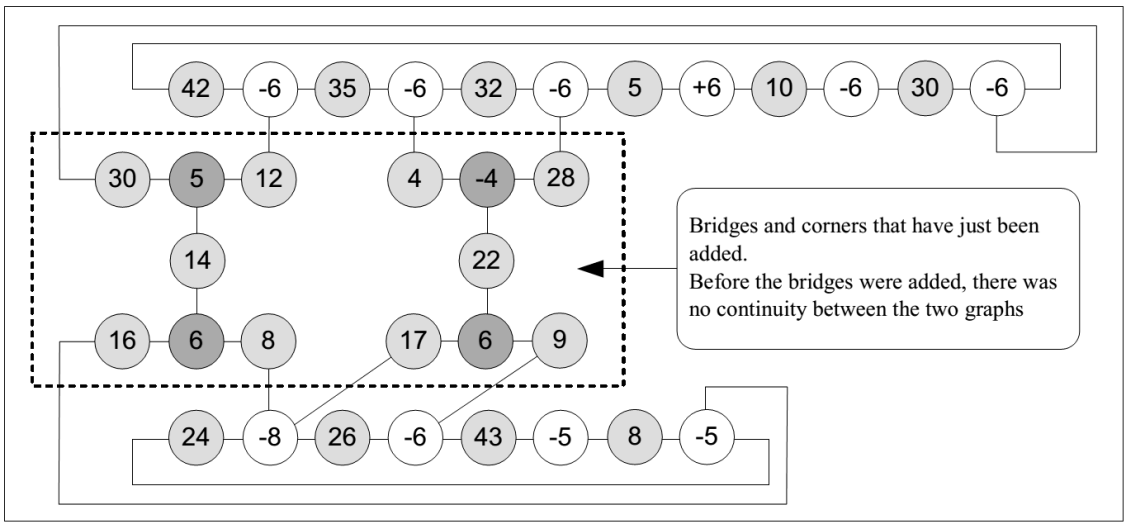

Fig. 3.11. The environment's graph including two barriers, having added the bridges.

3-2-5- Graph-based guidance towards the target

With the formation of feature map, by searching for graph the robot can be guided towards the target. One way to guide from the current position to the target position is to search for the graph and check the length of the edges to find a shorter route. Afterwards, the robot passes by the barrier in a clockwise or counterclockwise manner (Figs. 3.12 and 3.13). To do this, the position of an object in the graph is set to zero value and movement starts from there. With the passage by each vertex, the length of edge of barrier enclosed between two vertices is added to the value of the stepping. This trend can be seen in Fig. 3.14.

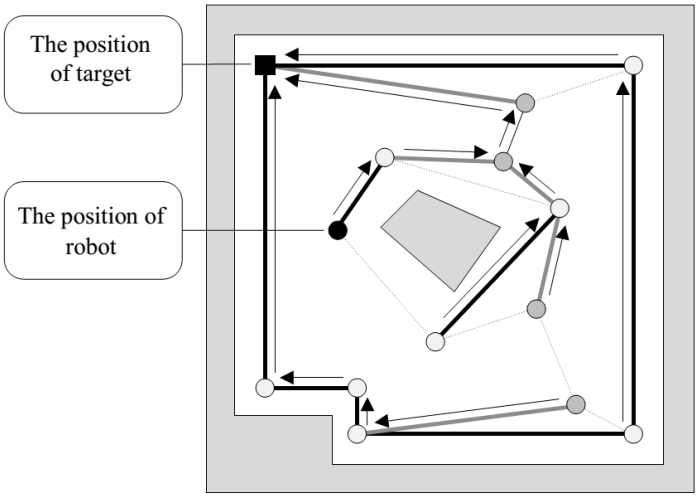

Fig. 3.12. The environment's feature map including two barriers, guided using guidance map.

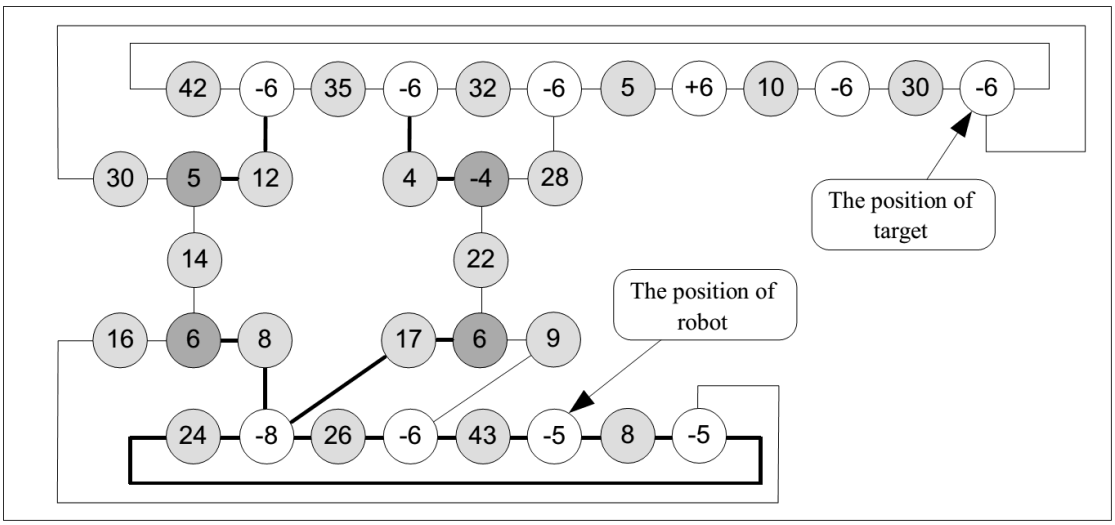

Fig. 3.13. Graph of the feature map shown in Fig. 3.12.

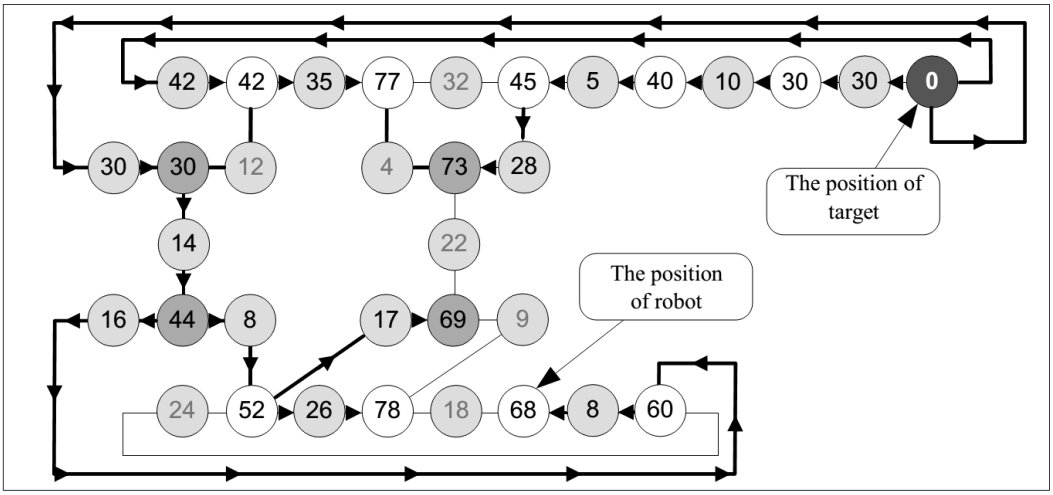

Fig. 3.14. Guidance graph of Figs. 3.12 and 3.13.

Here one must decide about how to choose the path of the robot. This means whether the robot should move to left or right after being located at a vertex. For this purpose, a mark is considered for any edge; a plus sign is assigned to the edges located on the right side of the robot and a minus sign is assigned to the edges on its left side. However, it should be noted that during value setting for the graph, absolute values of the edges are taken into consideration (Figs. 3.15 and 3.16).

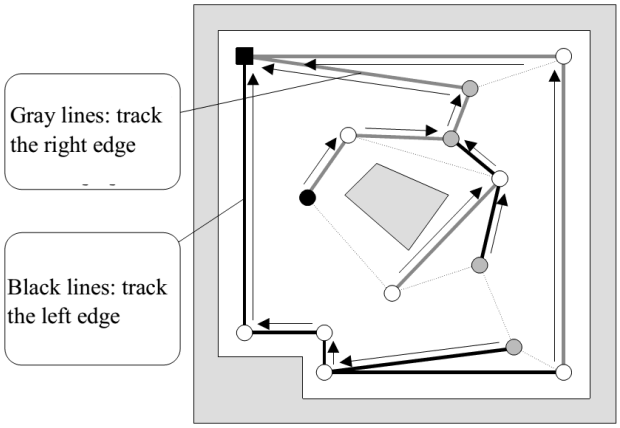

Fig. 3.15. Feature map's graph.

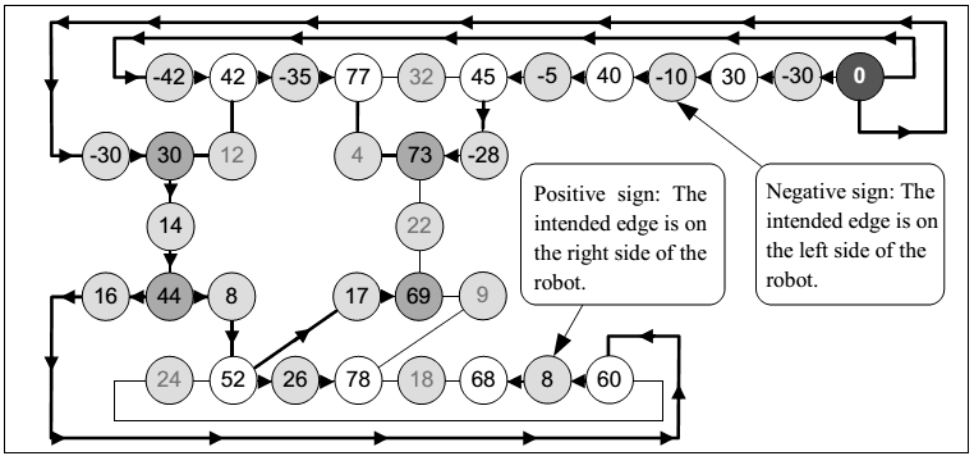

Fig. 3.16. Guidance graph of choosing path.

3-3- Guidance in potential field

Guidance in potential field is consistent with the principle that objects and situations cause to attract or repel the robot during its movement in their environment like a magnet. Robot so as to be guided to the target, conducts vector calculation which is a function of the final desired position and position of barriers. Movement along this vector continues until the target is achieved and the vector calculated at any time will also be updated. Changes in robot path in the potential field is based on three principles:

1. Attraction to the target point

2. Repulsion from reference point (to avoid the robot remain in just one position)

3. Repulsion from barriers

These three principles are shown in Fig. 3.17.

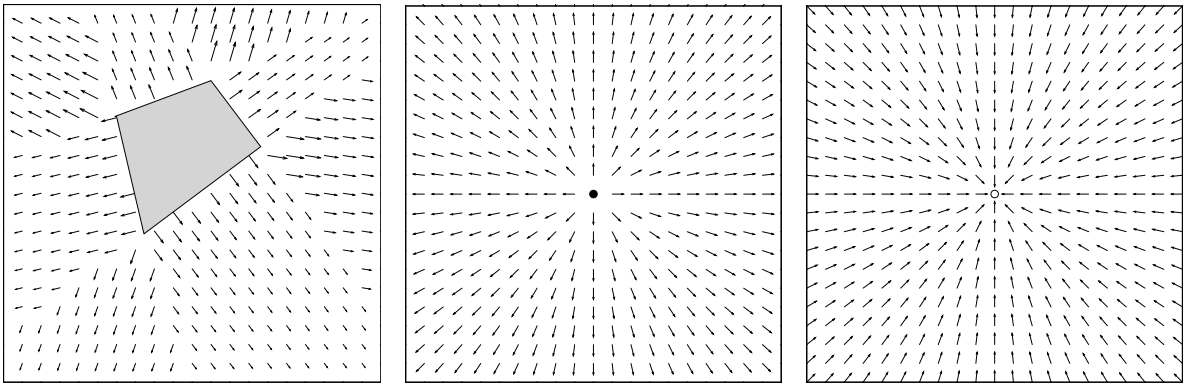

Fig. 3.17. Three principles of changes in robot path in the potential field.

Each vector in potential field has two properties of "orientation" and "magnitude". Vector orientation at any point in a potential field represents direction and alignment of robot's movement and its magnitude presents the extent of its importance in guidance along that orientation. For example, Fig. 3.18 shows a potential field around a barrier and the position of the robot in this field. Vectors' direction is such that results in making the robot go away from the barrier. Besides, near the barrier the magnitude of vectors becomes larger and at distances far from the barrier, vectors' magnitude become smaller.

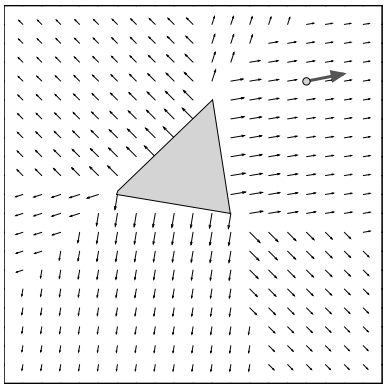

Fig. 3.18. Vector orientation and magnitude in potential field represent the extent of its orientation and importance in guidance.

3-3-1- *Calculating potential field vectors at target and reference points*

Calculating potential field vectors at reference and target points is very simple. For each point of the field, a vector can be defined as follows:

$$\vec{v}_g = v_{g,mag}(v_{x,g}\mathbf{i} + v_{y,g}\mathbf{j}) \tag{3.1}$$

where $v_{g,mag}$ is vector's magnitude and $v_{x,g}$ and $v_{y,g}$ are the components of potential field vector in the target point. The components of this vector can be obtained with the knowledge that the direction of resultant vector must be from the point (x, y) towards (g_x, g_y) as follows (Fig. 3.19a):

$$\begin{cases} v_{x,g} = g_x - x \\ v_{y,g} = g_y - y \end{cases} \tag{3.2}$$

The magnitude of the target vector $v_{g,mag}$ at each point is also calculated as follows:

$$v_{g,mag} = \frac{\alpha_{goal}}{\sqrt{(g_x - x)^2 + (g_y - y)^2}} \tag{3.3}$$

where the constant value of α_{Target}, is amplification factor of target vectors determined according to the complexity of the environment and the number of barriers.

Calculations for potential field vector at reference point is also similar to the target point, with the difference that this time the vectors' direction is from the reference point (r_x, r_y) to the point (x, y) (Fig. 3.19b). If necessary, amplification factor *src* at reference point vectors can also be determined independent of target point in order to guide the robot in a proper manner towards the target point using the resultant potential field.

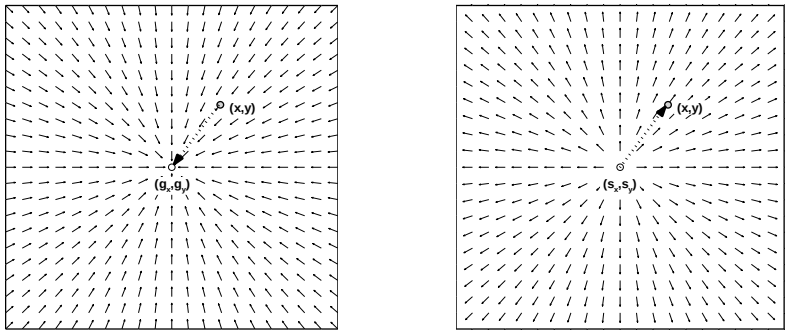

a) the vectors of potential field of target point b) the vectors of potential field of reference point

Fig. 3.19. The position of the field points relative to the reference point and the target.

3-3-2- *Calculating potential field vectors of barriers*

The calculations for potential vectors of the barriers is a bit more complicated. Independent vectors must be formed for each edge of a barrier, and then must be combined with each other. Each edge of the barrier divides the plane into two parts, one of which contains the barrier and the other side hasn't any barrier (Fig. 3.20). For any edge, potential vectors are produced only in a part that does not include a barrier. The position of a point with respect to any edge of the barrier, can be demonstrated with a set of clockwise vectors, as shown in Fig. 3.20.

Accordingly, any point of the plane where forms a counter-clockwise composite edge along with the vector, will be affected by that edge and for it, a non-zero vector is calculated. The vector will be zero for the rest of the plane points with respect to this edge. For example, rotation direction at the points (x, y), (d_x, d_y), and (s_x, s_y) in Fig. 3.20 is counterclockwise, and we must define an appropriate vector for this direction. Type of rotation can be specified using the right-hand rule and determinant operator as follows:

$$\begin{vmatrix} s_x & s_y & 1 \\ d_x & d_y & 1 \\ x & y & 1 \end{vmatrix} = s_x d_y + s_y x + d_x y - d_y x - s_y d_x - s_x y \qquad (3.4)$$

where, if

- The resulting determinant is negative, it means counterclockwise;

- The resulting determinant is positive, it means clockwise;
- The resulting determinant is zero, it indicates alignment of those two vectors.

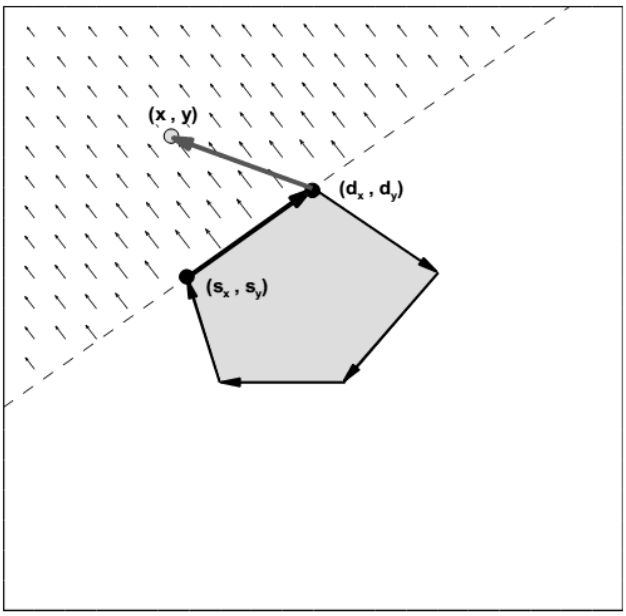

Fig. 3.20. Vector representation of a barrier with a collection of clockwise vectors.

After it became clear that a point on the plane must be affected by an edge, its vector can be defined as follows:

$$\vec{v}_{obst} = v_{obst,mag}(v_{x,obst}\mathbf{i} + v_{y,obst}\mathbf{j}) \tag{3.5}$$

where, $v_{obst,mag}$ is the vector's magnitude, and $v_{x,obst}$ and $v_{y,ob}$ are the components of the unit vector of potential field for any edge. Unit vector components can be calculated by knowing that the resultant vector must be perpendicular to the edge and away from it, as follows (Fig. 3.20):

$$\begin{cases} v_{x,obst} = \dfrac{s_y - d_y}{L_{sd}} \\ v_{y,obst} = \dfrac{d_x - s_x}{L_{sd}} \end{cases}, \quad L_{sd} = \sqrt{(d_x - s_x)^2 + (d_y - s_y)^2} \tag{3.6}$$

The magnitude of potential field vector, $v_{obstacle,mag}$ is also obtained from the following equation:

$$v_{obstacle,mag} = \frac{\alpha_{Obstacle}}{1 + \frac{d}{\varepsilon \alpha_{Obstacle}}} \tag{3.7}$$

where d is the minimum distance from the point (x, y) along the edge, $\alpha_{Obstacle}$ is the amplification factor of barrier and ε is the growth factor of vector's magnitude with increasing distance from the edge. The amount of d depending on whether the point (x, y) is within the range perpendicular to the edge or outside of this range, is calculated with equations (3.8) and (3.9) respectively:

$$d = \frac{|ax + by + c|}{\sqrt{a^2 + b^2}}, \quad \begin{cases} a = d_y - s_y \\ b = s_x - d_x \\ c = bs_y - as_x \end{cases} \tag{3.8}$$

$$d = \min\left(\sqrt{(x - s_x)^2 + (y - s_y)^2}, \sqrt{(x - d_x)^2 + (y - d_y)^2}\right) \tag{3.9}$$

Parameters $\alpha_{Obstacle}$ and ε can be determined in terms of complexity of the environment and the number of barriers. By changing these parameters, different potential fields are formed, and Fig. 3.21 shows its impact on potential field of an edge. As can be seen, as $\alpha_{Obstacle}$ increases under constant ε, results in larger vectors magnitude, and as ε increases under constant $\alpha_{Obstacle}$, it makes smaller vectors with increased distance from the edge.

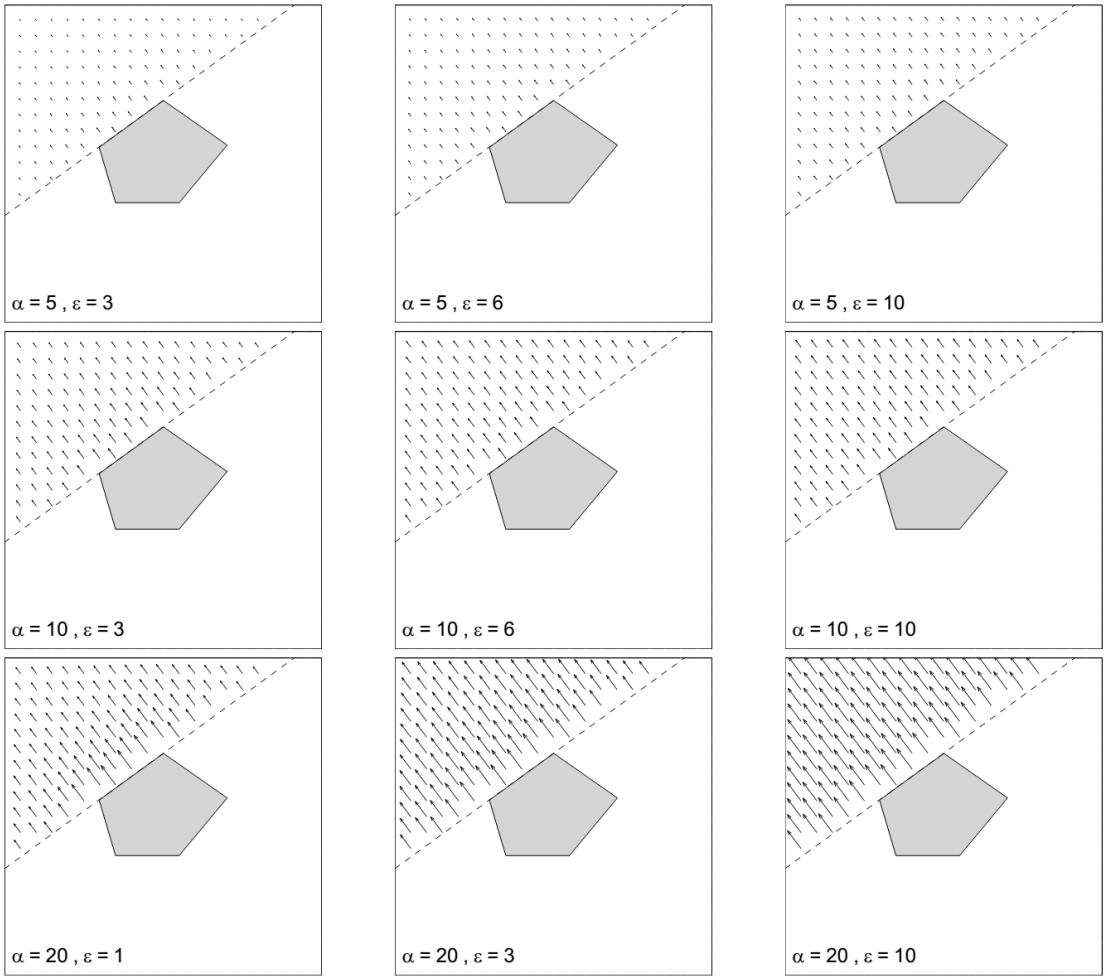

Fig. 3.21. The impact of the parameters; coefficient of amplification (α) and ε, the growth factor, on the potential field of a barrier.

3-3-3- *Combining potential vectors*

After the potential vectors of the different components of an environment, were formed independently ranging from reference and the target points to edges of the barriers, by using the vector sum (Fig. 3.22) we can combine them and obtain final potential field. To combine two vectors, one can decompose them into *y* and *x* components, and then combine them together.

An example of combining potential field, relates to edges of a barrier. Fig. 3.23 shows independent potential field of a barrier's edges, and Fig. 3.24 shows the combination of potential field of its edges. As can be seen, in combinational potential field, the vector situation

or state at any point in the field with respect to that barrier is characterized well and if the robot is in the vicinity of that barrier, it will find its movement direction away from of the barrier.

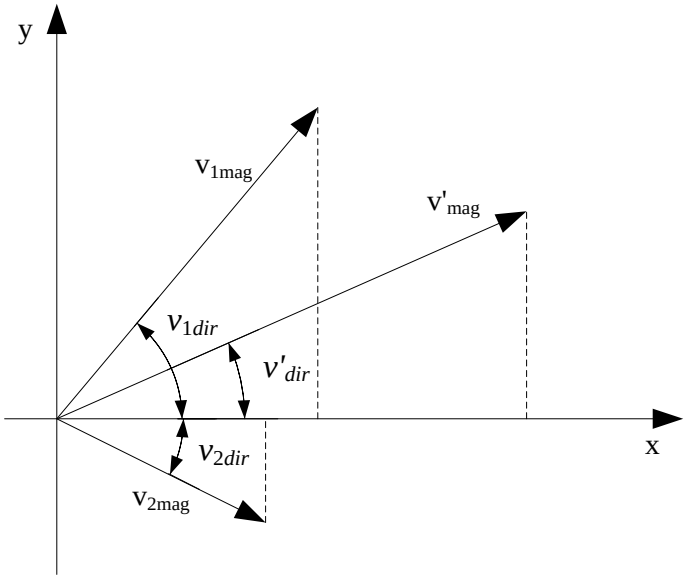

Fig. 3.22. Vector sum of two vectors in the potential field.

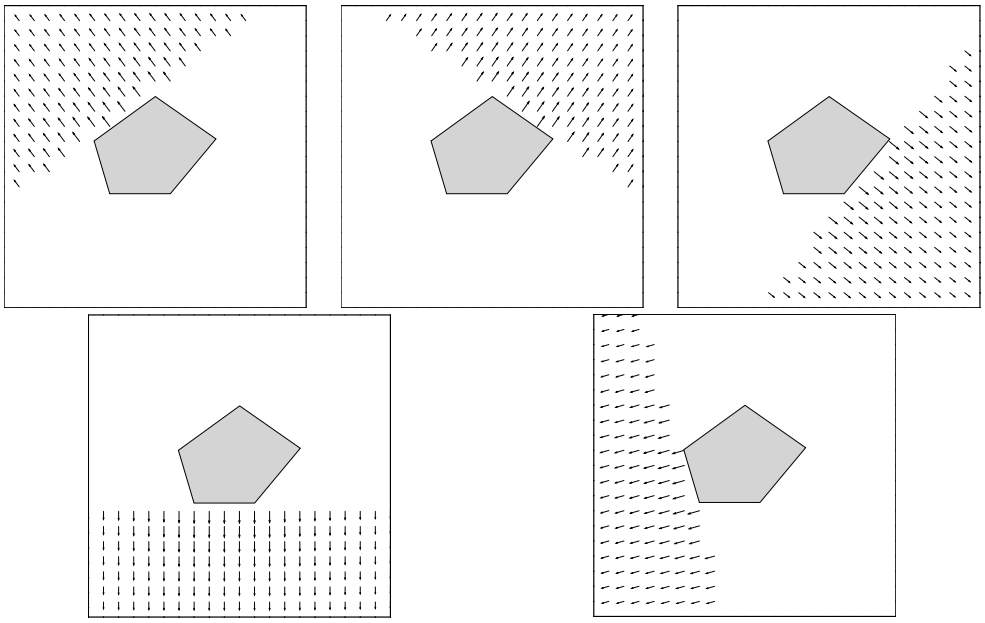

Fig. 3.23. Independent demonstration of potential fields near the edges of an obstacle.

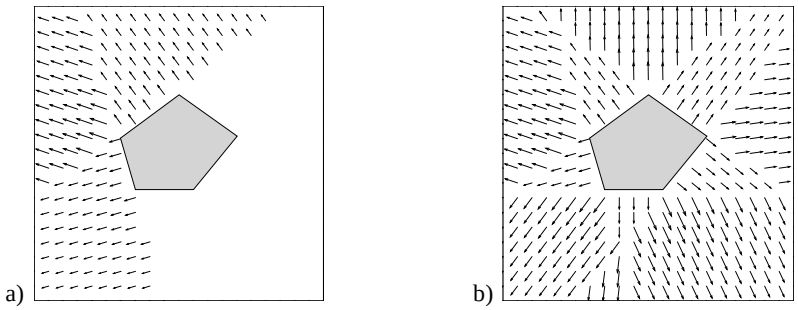

Fig. 3.24. Combination of vector fields near the edges of an obstacle; a) two edges b) all edges.

Figure 3.25 shows potential field of a complicated barrier with multiple edges, and convex and concave corners, which are formed from combining potential field of each of the edges. In this potential field as the distance from barriers increases, the vectors magnitude become significantly smaller which indicates a small amount of number ε in determining the vectors of this field.

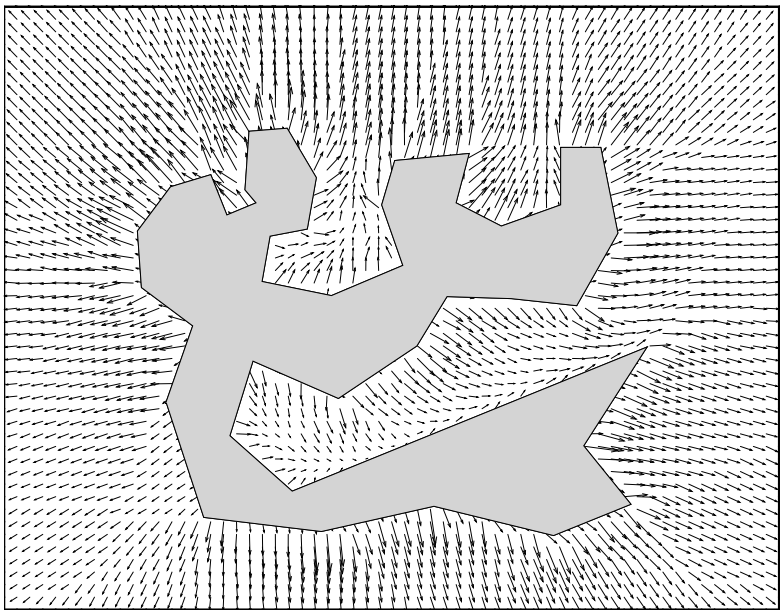

Fig. 3.25. Applying left turn method for unjust obstacles.

3-3-4- Path planning based on combinational potential field vectors

By combining potential fields of barriers and reference and target points, one can determine the robot's movement path from the reference point towards the target point. For example, Fig. 3.26, shows an environment with three barriers, and reference and target points. As can be seen,

the combination of the potential fields of these five components has caused the robot to determine the appropriate path direction towards the target with very simple calculations.

Of course, sometimes repulsion force in the field at reference point is such that makes achieving a solution a bit difficult. Fig. 3.27, shows an example of such a field. As can be seen, the magnitude of the vectors around the reference point is very small and effectively prevents the robot from moving to the target. Sometimes, amplification factor of repulsion from barriers could be such that the combination of vectors around a point of reference be towards the point of reference rather than going away from it. In such cases, guidance of the robot towards the target depends on the strength of the created field. Fig. 3.28 illustrates a field with medium attraction strength, and Fig. 3.29 shows a field with high attraction strength. Such fields can be created by increasing the amplification factor at targets and reference points. However, excessive increase in field strength can result in collision of the robot with barriers. For example, in Fig. 3.29, the vectors' orientation in some edges of barriers is such that the resultant vector actually drags it to the barrier rather than making robot away from barrier and can result in a collision with it.

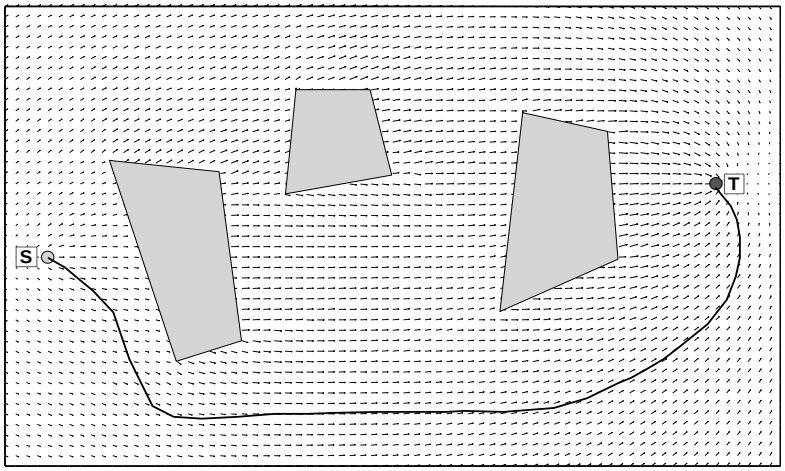

Fig. 3.26. Combination of potential fields in an environment including a few obstacles, to determine the direction of the robot.

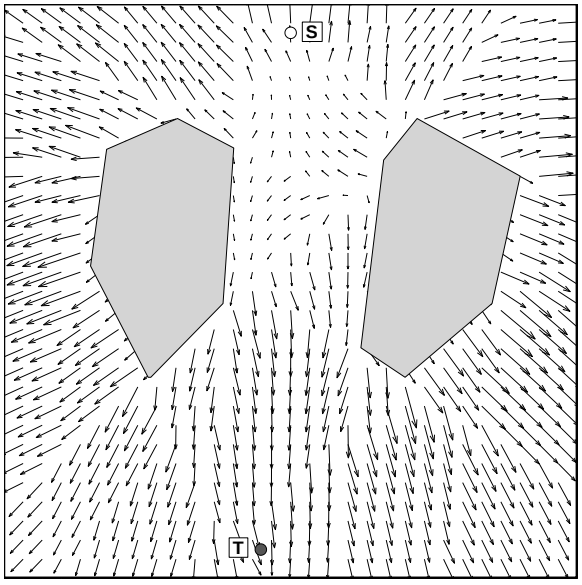

Fig. 3.27. A potential field with a weak target attraction.

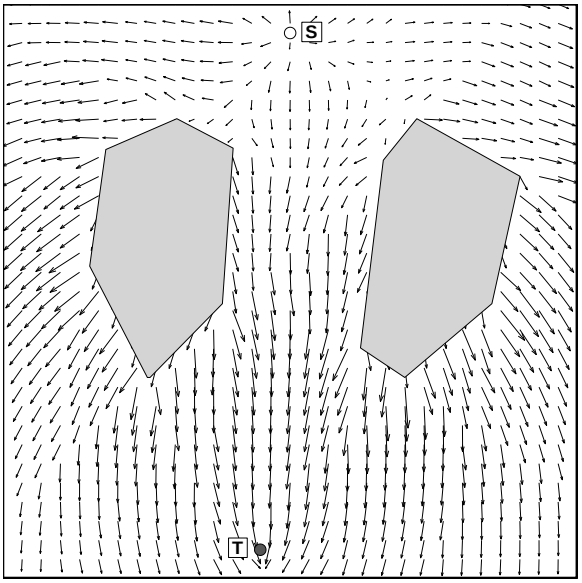

Fig. 3.28. A potential field with a mediocre target attraction.

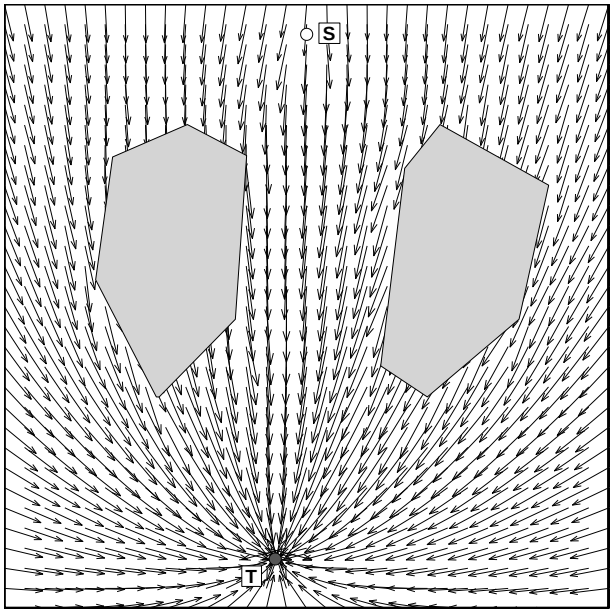

Fig. 3.29. A potential field with a strong target attraction.

3-3-5- *Local minimum*

Sometimes the magnitude of the vectors around point of reference in combination with other components of the field is so small that in practice it becomes incapable of determining the path. Such a situation which is shown in Fig. 3.30, is called local minimum. There are two ways to escape from being trapped in a local minimum:

- Increasing field intensity at reference point
- Introducing noise to the environment

In the first method, some intensity value is added to the reference point that in fact, causes more repulsive force from that point and prevents the robot from being static (Fig. 3.31). In the second method, some noise is introduced into the environment. This noise is usually defined as a vector with fixed size and random direction (Fig. 3.32).

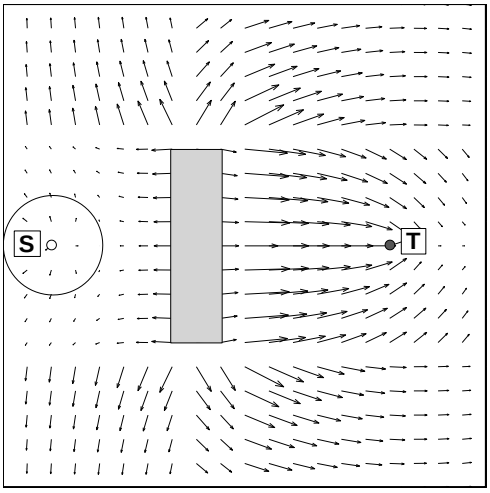

Fig. 3.30. Existence of a local minimum around the reference point of a potential field.

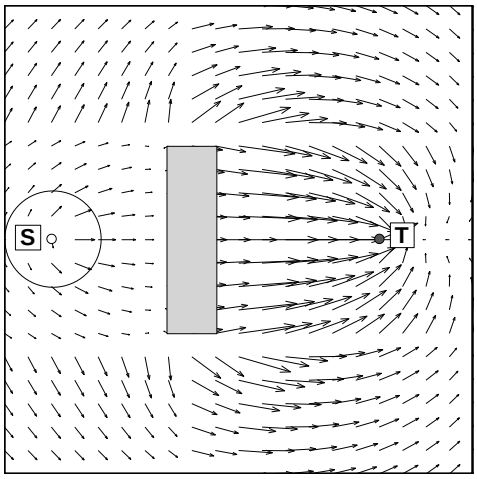

Fig. 3.31. Prevention of being trapped in a local minimum by creating repulsive force from the reference point.

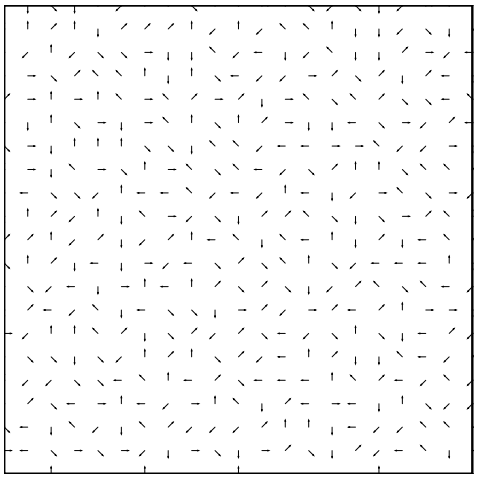

Fig 3.32. Creating noise (vectors of the same size with random orientation) to prevent being trapped in local minimum of a potential field.

Adding reference field strength in many cases does not create a path to move the robot toward the target and sometimes results in trapping into local minima as well. But adding noise in most

cases (but not always) leads to overcome the local minimum and to find a path to guide the robot towards the target. Fig. 3.33 shows an example of the effect of noise field on opening up a path to the target.

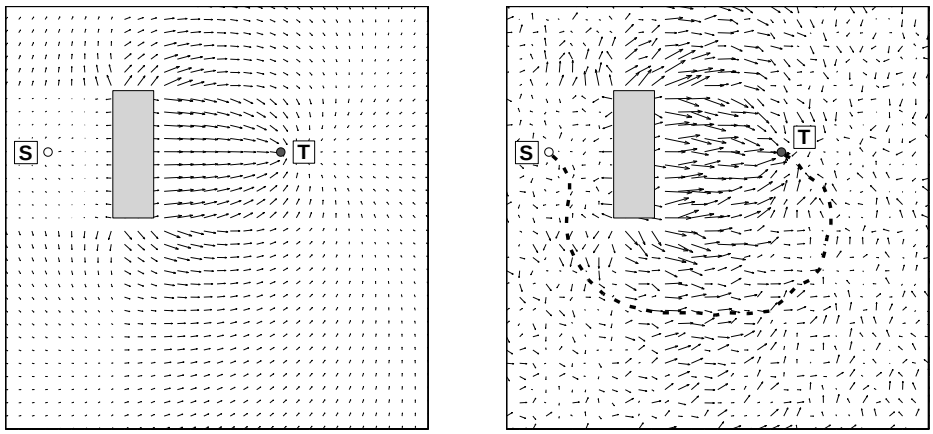

Fig. 3.33. The impact of creating noise on finding the best choice of reaching the target.

It should be noted that while the robot looks for the target point, movement path is constantly changing in consistent with random noise vectors. Fig. 3.34 indicates this situation very well. In addition, excessive magnitude of noise vectors leads to their inefficiency, so that the robot cannot find its way to reach the target. Such a situation is also shown in the Fig. 3.35.

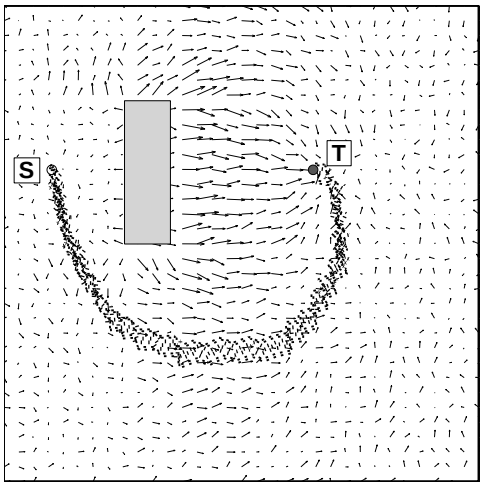

Fig. 3.34. Continuous change of the path by changing the noise vector during the robot's movement towards the target.

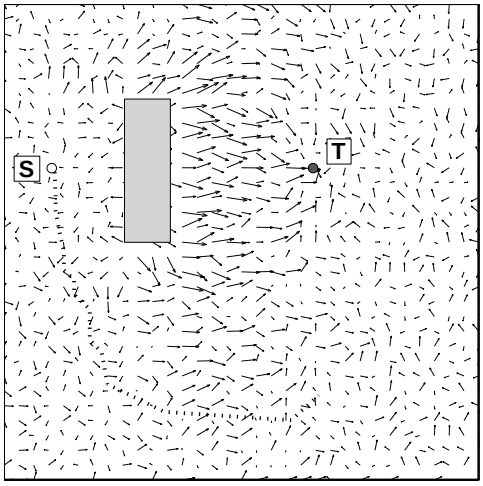

Fig. 3.35. Failure of the robot to find the path due to excessive noise.

Chapter 4- **Path Planning and Robot's Hardware**

4-1- Introduction

In this chapter, we will deal with path planning based on the robot's sensors and computing hardware. In unknown environments, in which at first there exists no map, needed information is collected through the sensors. Depending on robot hardware, path planning can be as the following:

Path planning is based on mapping functionality including: without memory (without a map) with the capability of mapping the traversed path, and with capability of mapping its environment.

Path planning based on sensor data, includes:

- Based on distance, ultrasound and laser sensors
- Based on attendance sensors: infrared and contact sensors
- Based on vision sensor: single-vision, bi-vision and multiple vision
- Combinational (data fusion)

The first part of this chapter deals with introducing path planning based on mapping capability. In this section, three mapping methods, including polygon, gridding and hierarchical mappings will be described and the advantages and disadvantages of each will be analyzed. In the second section, path planning is examined based on visual sensors. As mentioned above, path planning based on sensors includes three methods of "distance-finding", "attendance-finding" and "vision-based", which each one has its own features. Vision sensors are the best according to

information which is made at their disposal for path planning affairs. This section will provide explanations on the nature of light, and then the stages of recording, storage and recognition of light using the visual sensors are described. In the fourth section of this chapter, movement of two-dimensional robots in environments with two-dimensional obstacles is provided (Lengyel et al. 1990). Two-dimensional robots can have two or three degrees of freedom (i.e. movement in directions x and y and/or θ). In this section, how to model robots in such environments will be explained. Two methods of configuration; space and potential field, which are more common, are briefly described, and according to them, a combinational method having high speed and reliability is introduced and its implementation results in various conditions are provided.

4-2- Path planning based on mapping capabilities

The environment in which the robot is located, may change over time. Hence, by map we mean to show the environment at specified times. Accordingly, the robot must have the several abilities: planning guidance strategies, preventing from collisions with obstacles while moving, detecting the changes in the environment, detection of achievable and unachievable areas, and the ability to pinpoint its current location on the environment.

Maps are in fact an estimation of the environment. This estimation is often inaccurate or even incorrect. An example of such a map can be seen in Fig. 4.1. Consequently, the robots have to rely on their sensors in addition to the map to avoid a collision.

Fig. 4.1. An example of a map that provides an uncertain estimate of the environment.

In this section, we assume that the maps are accurate, legible and constant (unchangeable) over time (time invariable) and then discuss how to plan paths using them. The way in which a map is prepared from an unknown environment will be discussed in the next section. There are different types of maps:

- **Geographical maps:** These maps usually record the relationship between the obstacles, or in the other type, they record voids in the environment.
- **Obstacles Maps:** these types of maps record location of obstacles and unattainable places.
- **Outdoor Maps:** determining safe locations for movement of the robot in an environment is one of the applications of these maps.
- **Path maps:** recording the routes in which the robot can move safely is the responsibility of these maps. These maps have industrial application and guide the robot in known paths.

- **Hierarchical Maps:** relations between obstacles or cells are recorded into hierarchical maps. These kinds of maps which are mostly referred to as locational maps represent the relationship between different parts of an environment.

In this book, discussing about Two-dimensional maps (such as Fig. 3.1) is sufficient.

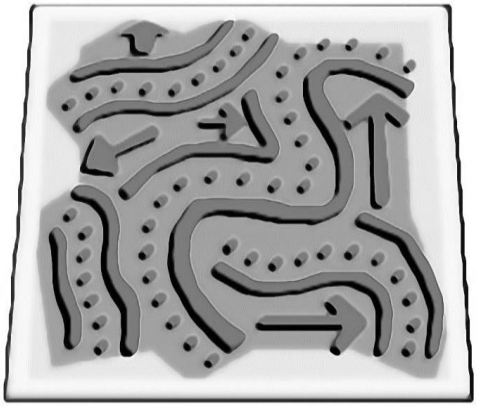

Fig. 4.2. An example of a two-dimensional map of the environment.

4-2-1- Mapping obstacle maps using polygonal and gridding methods

Obstacle maps are prepared in two ways: In the first method, straight lines which form polygons are used for detecting border obstacles. While in the second method, the environment contexts in the form of a two-dimensional image are grid and the obstacles are specified through grid cells. Fig. 4.3 shows an example of these two maps for a similar environment.

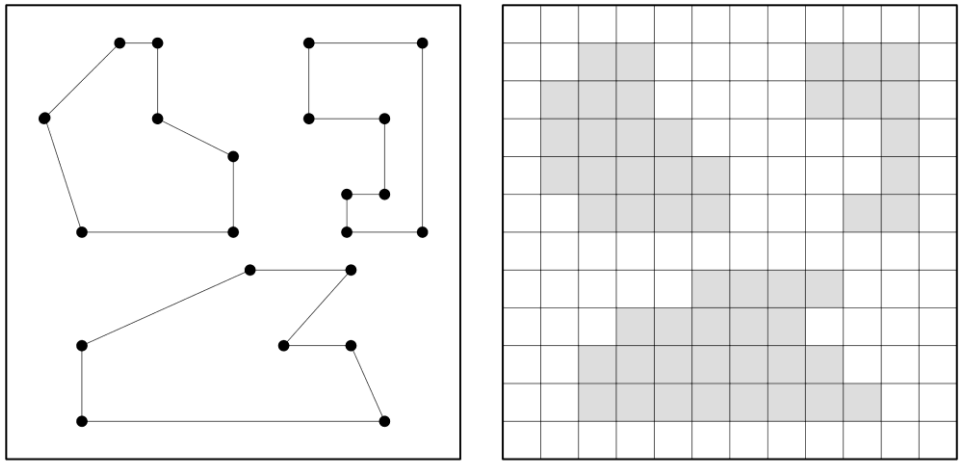

Fig. 4.3. An example of a map of the environment and obstacles based on polygonal and networking methods.

The main difference between these two methods is in memory requirement to store the image, algorithm complexity and execution time of the algorithm. In large areas with low numbers of obstacles, in the first method which is called vector storing, little memory space is required to save image. But in the second method, apart from whether the cells are empty or filled, memory space is occupied, and therefore storing the image requires a relatively large storage memory. But, it is clear that in environments with many small obstacles, the second method (environment gridding) is preferred. The difference between these two methods is in the environment which they are used (with few and many numbers of obstacles), as can be seen in Figs. 4.4 and 4.5.

But the memory required to store the image by gridding method which is called raster maps, depends on the size of the network. For example, the required memory for storing a grid with the size of $M \times N$ is at scale of $O(MN)$. In this way, for each $m,n << M,N$, vector maps demonstrate a higher performance. By taking m obstacles with n vertexes for each, the space required to store the image using vector method is obtained using the following equation.

$$storage = (m \times n) \times 2 + 2 \times (m \times n) = O(mn) \tag{4.1}$$

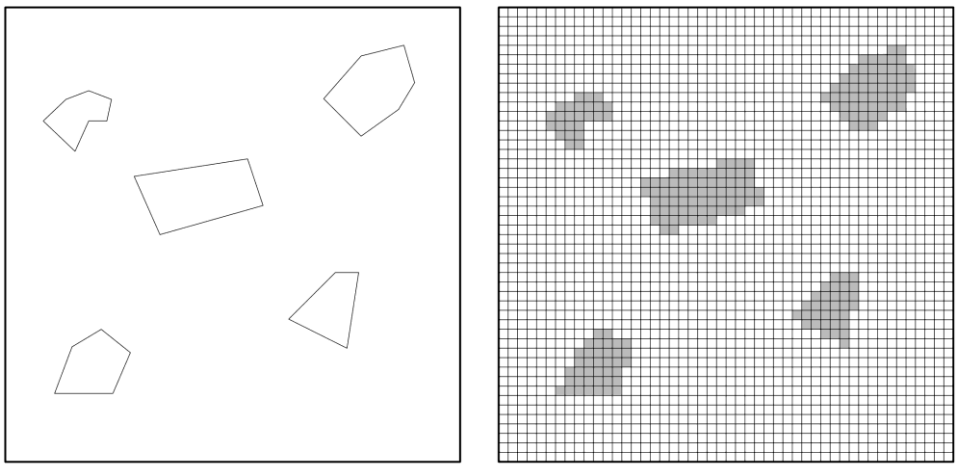

a) Polygonal method

a) Gridding method '

Fig. 4.4. Polygon and networking maps from an environment with a low number of obstacles (less required memory for the polygon method).

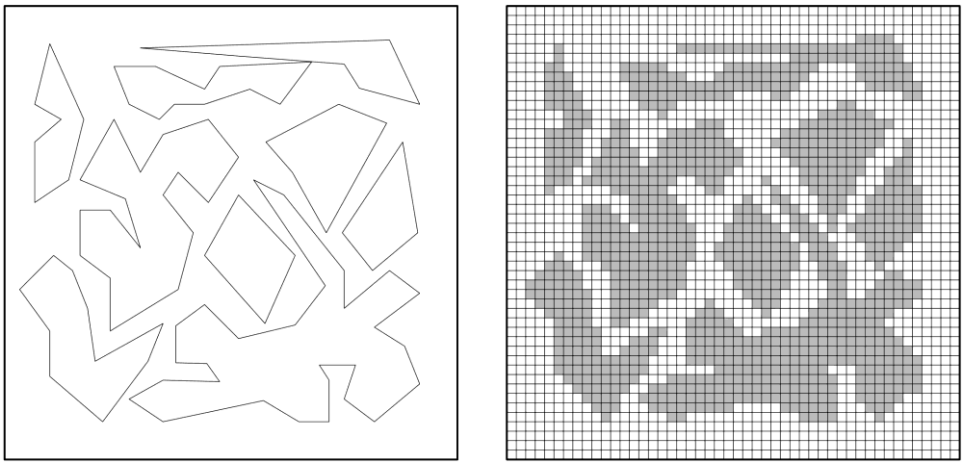

Fig. 4.5. Polygon maps and networking from an environment with high number of obstacles (less memory for networking).

Image's resolution in gridding method depends on accuracy. By looking at Fig. 4.6, one can observe the difference resulted from resolution. Reduction in resolution of images while reducing the memory required to store the maps, also leads to loss of precision. This loss has effects on problem solving. For example, in an environment with three resolutions of low, medium and high, as shown in Fig. 4.6, finding the path towards the target can be impossible, single-path or multi-path, respectively. However, in the vector maps, problem solving is not dependent on memory resolution, in contrast, it heavily depends on the numerical method.

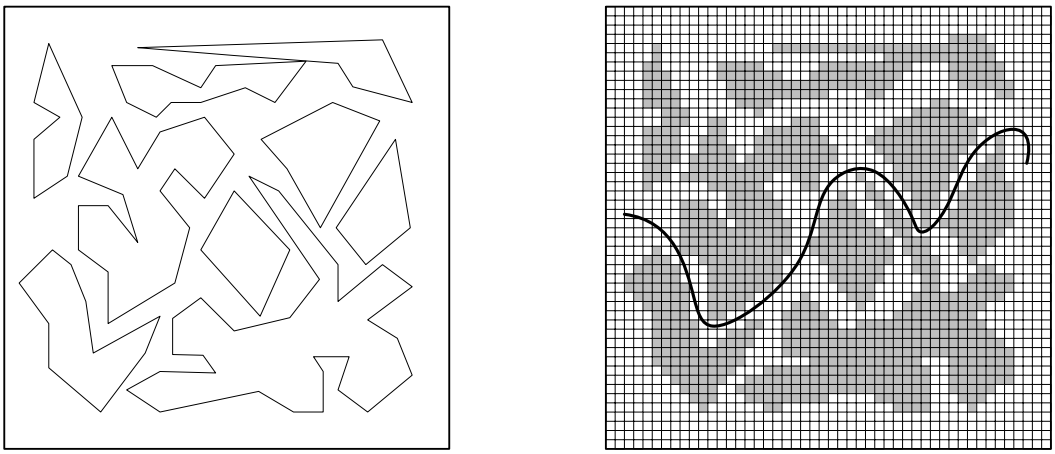

a) Real image

b) Map with 45 * 45 resolution (There are several paths towards the target)

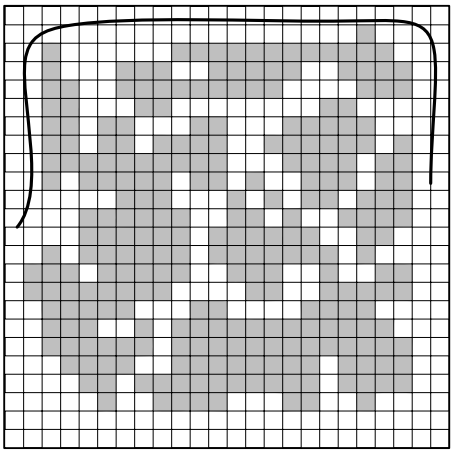

c) Map with 24 * 24 resolution (There are two paths towards the target)

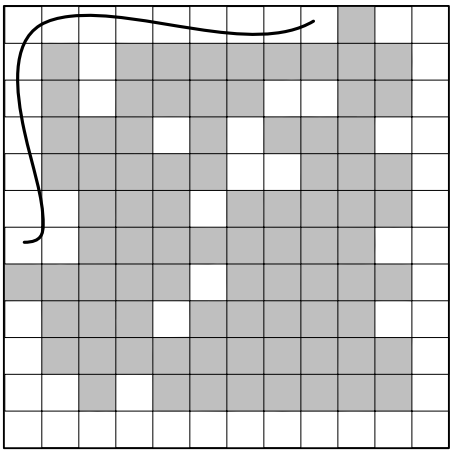

d) Map with 24 * 24 resolution (There are two paths towards the target)

Fig. 4.6. Changing the number of paths to the target in maps with different resolutions.

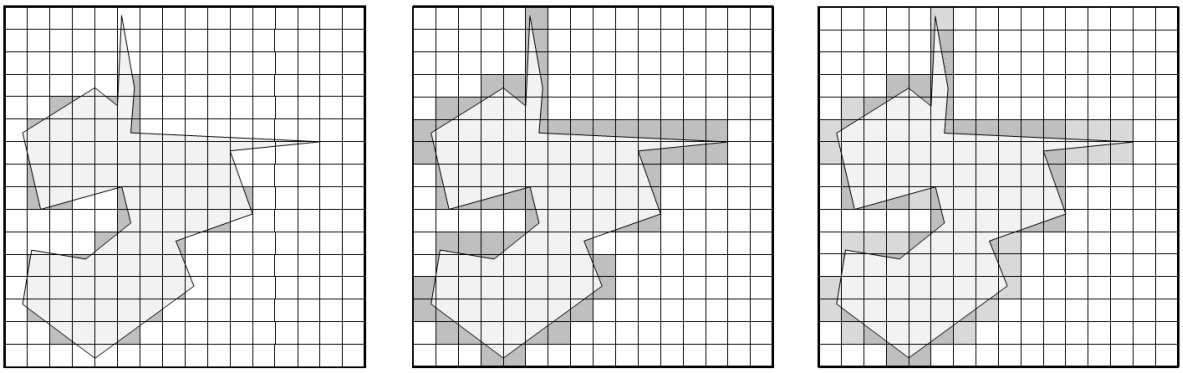

Gridding is based on occupying more than 50% of cell space

Gridding is based on occupying at least 1% of cell space

Gridding with considering the amount of space occupied by each cell

Fig. 4.7. Determining the presence of an obstacle in a cell from the network using its occupancy rate with the obstacle.

Safety of robot is one of deployment targets of using grid-based maps. The level of occupation of each grid cell, indicates the presence of obstacles at that part of the map. Fig. 4.7 shows three ways based on the extent of presence of any obstacle. For example, in Fig. 4.7.a, at least 50% of a cell must be occupied by obstacle for that cell to be filled, but in Fig. 4.7.b, 1% occupation of a cell space is enough to fill it. In Fig 4.7.c also the level of cell occupied by obstacle is stored as a part of information in that cell. In practice, most of robots use the type of maps in Fig. 4.7.c, this map allows using fuzzy algorithms to determine the position of obstacles. Therefore, occupation level of each cell presents the presence possibility of an obstacle into that cell.

4-2-2- *Hierarchical maps*

Another type of maps, are called hierarchical, which store relationships between obstacles or cells. In this section two types of these maps called “topological maps” and “feature maps” will be introduced.

4-2-2-1- Topological Maps

Topological maps represent the relationship between different parts of an environment. For example, there may exist an obstacle in an environment that has one or more holes in its midst (Fig. 4.8). Obviously, the robot must refrain from moving towards these holes or cavities. While in vector maps, if there be a hole between the obstacles, the robot is allowed to move towards it.

In topological maps, these holes are shown with empty cells. These maps utilize a structure called "square tree" to reduce the required memory. Thus, both horizontal and vertical lines, as shown in Fig. 4.9, divide the environment into four equal sub-zones and gridding is only done in areas where there are obstacles. The result of this division is a tree like structure similar to Fig. 4.10, in which neighboring cells are read from left to right.

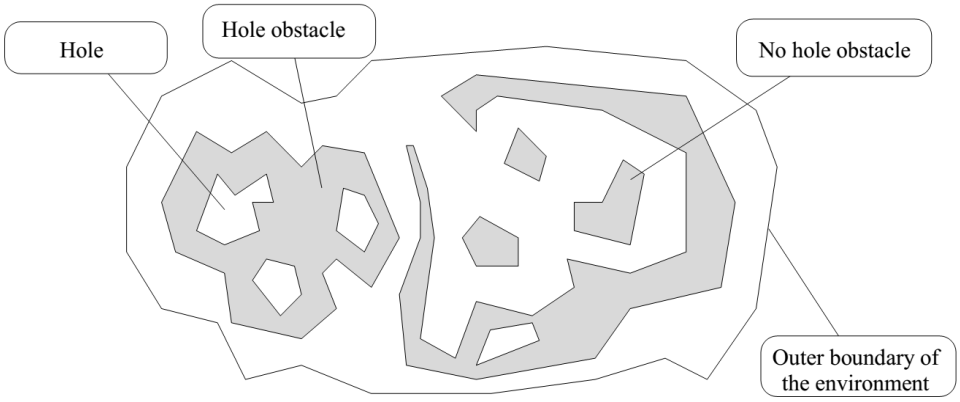

Fig. 4.8. Obstacles with or without holes in topological maps.

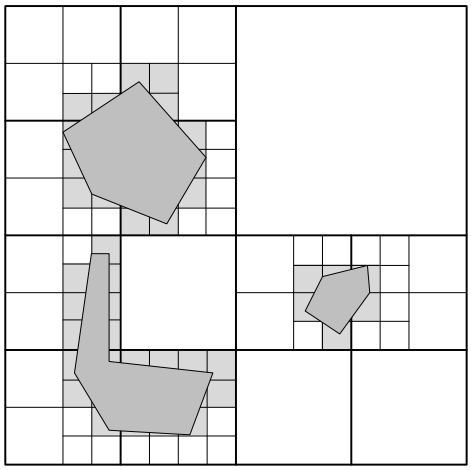

Fig. 4.9. How to divide the environment by rectangular tree in topological maps.

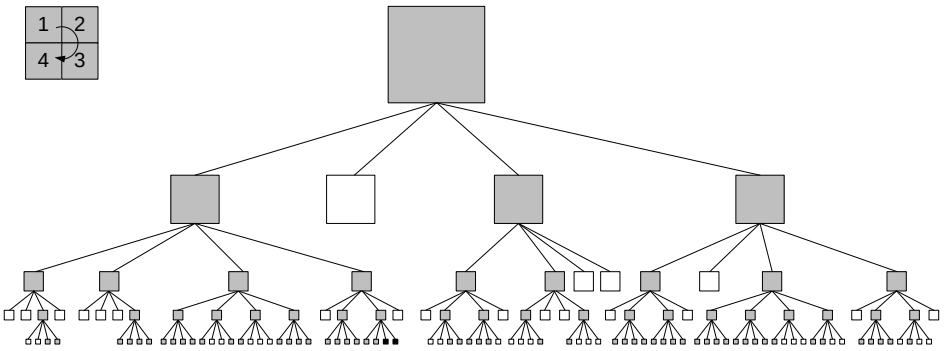

Fig. 4.10. The tree of the environment cells in the topological maps.

Square tree method in environments with low density of obstacles can reduce the memory required for storing images. Since it considers cells with various sizes, application of this method requires special programming arrangements in the path planning algorithm.

4-2-2-2- Feature Maps

Feature Maps are a form of hierarchical maps that store environment characteristics, such as free spaces or boundaries. Fig. 4.11 shows an example of maps that were prepared by following borders of the obstacle and storing corners and edges. The way in which this kind of mapping is provided was described in detail in Chapter 2.

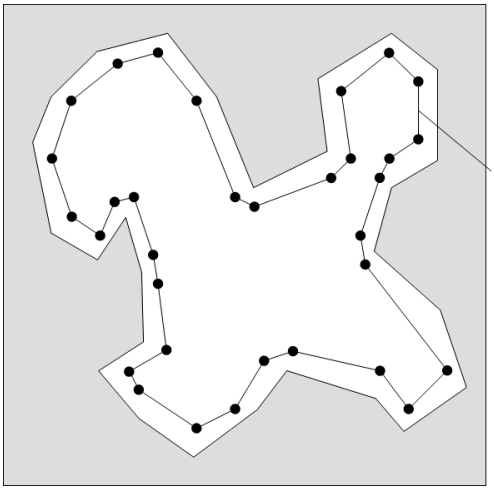

Fig. 4.11. Recording corners and edges by tracking obstacles.

The accuracy of prepared maps depends on the parameters such as minimum rotation angle of the robot. This feature of the robot manifests itself at the corners of a map. For example, note at Fig. 4.12 which is being used to prepare a feature map from minimum rotation angles of 15, 45 and 60 degrees. The more this angle, the less the accuracy in storing the corners and edges, to such extent that it may result in collision of the robot with obstacles.

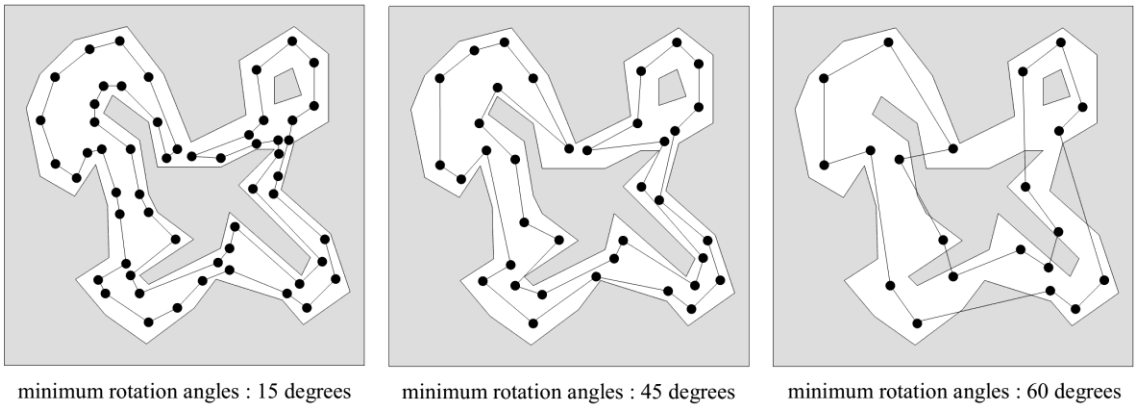

Fig. 4.12. Effect of the minimum angle of rotation parameter on the accuracy of feature maps.

Different stepping methods around the obstacles can also lead to the creation of different maps. Fig. 4.13 shows two different environments that were traversed once in clockwise and once again in counter-clockwise direction. The differences in recording corners and edges in the two methods of traversing is quite evident.

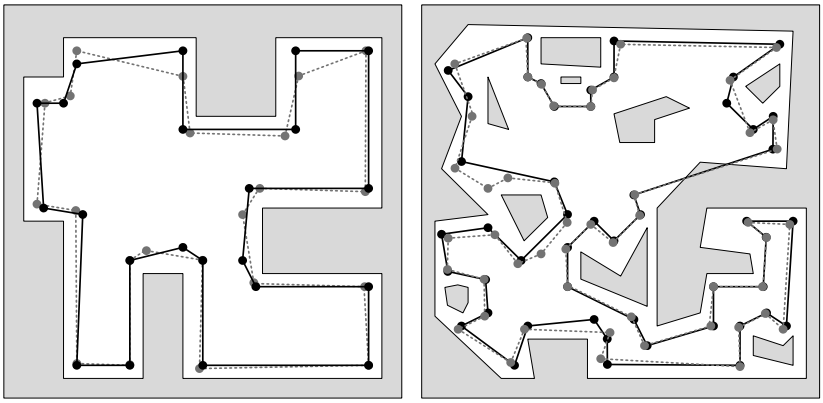

Fig. 4.13. Comparison in the map taken from clockwise and counterclockwise shooting in two environments mapping.

The robots get confused during guidance towards edges in symmetrical environments. For example, in Fig. 4.14, a series of obstacles with symmetrical edges are shown in which the robot gets confused passing by them (marked with a thick line).

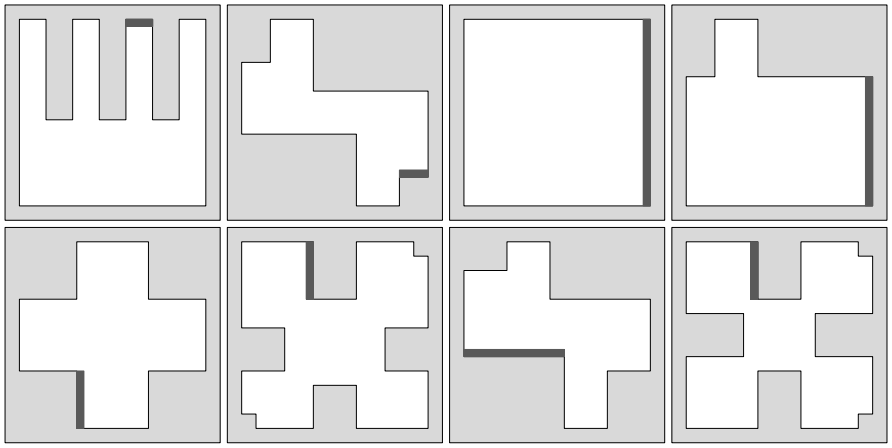

Fig. 4.14. Symmetric environments.

Besides, the robot doesn't have the ability to determine the rotation direction of edges in widespread coordinates, unless an external source or a wide reference coordinate system is at its disposal. For example, three environments of (a), (b) and (c) shown in Fig. 4.15 appear to be similar in terms of length of consecutive edges for robot; since the only difference between these three environments is in a rotation without having a wide coordinate, it is not possible to make distinction between them for the robot. But the position of the interior obstacles in the environment (d) is not the rotation of three environments, and therefore, it is distinguishable for robot.

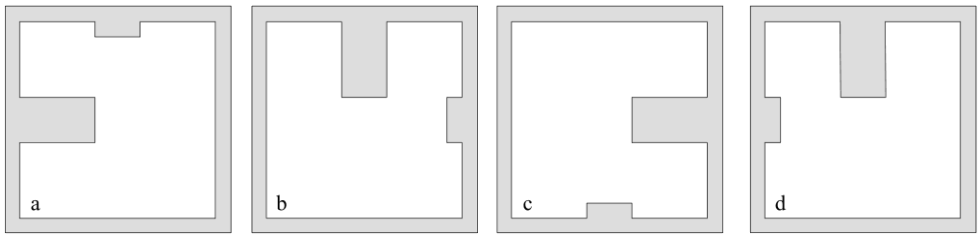

Fig. 4.15. Rotated environments, with similar lengths (a, b, c) and different (d).

In addition, without any coordinating information and by only relying on footprint of the robot, not many wide rotation parameters, relative rotation and relative location can be determined. For example, in the environment maps of Fig. 4.16, because of the similarity of the obstacles and lack of access to coordinate information, it is not distinguishable for the robot. In such cases, by creating a number of bridges or shortcuts between the obstacles, according to Fig. 4.17, one can estimate the obstacles' distances in the environment and consider the effect of rotation.

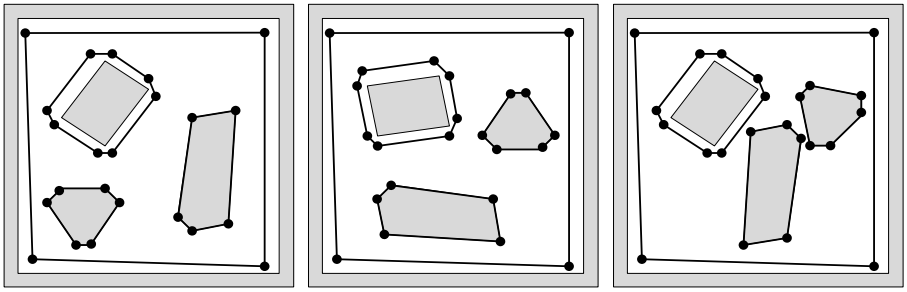

Fig. 4.16. A demonstration of the impossibility of determining the wide rotation, relative rotation, and relative location.

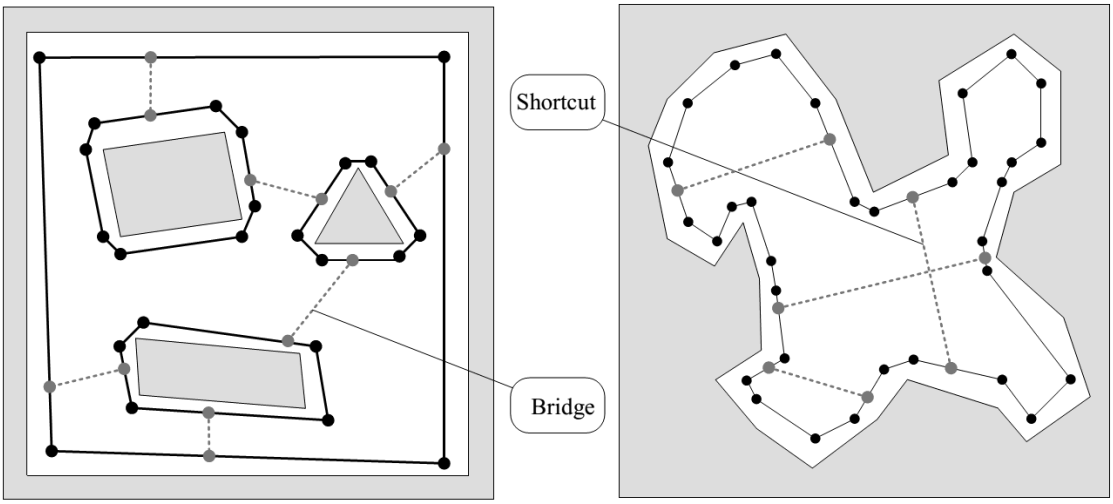

Fig. 4.17. Shortcut and bridge.

In the end, it should be noted that drawing complete maps where the robot travels a short path, is justifiable, but over long distances, because of need for high memory and also increased processing load for finding the optimal path, application of these maps is not possible in practice. For medium distances, the method of mapping the traversed path which is a method in between these two extremes, appears to be reasonable.

4-3- Robot path planning using vision sensors

As mentioned in the introduction to this chapter, routing based on sensors includes three methods of "distance", "attendance" and "vision", each of which has characteristics. Attendance sensor usually extends the path and provides the least information to the robot. For this reason, methods that rely solely on sensors are obsolete. The distances sensors provide good data for routing, but the extracted data does not provide the ability to identify the danger zones for the robot. Also, due to the "activation" of these sensors, their use during wartime (due to rapid identification by the enemy) is not wise. The sensors are the best sensors in the routing topic, given the information they provide. This section first describes the nature of the light, and then describes the light recording, storage, and diagnosis of visual sensors.

4-3-1- Nature of the light

Light is a range of electromagnetic waves. In general, all the bodies glow light, but since the range of these radiation is not necessarily in the range of human vision, it is not always possible to see them. The bodies exhibit three different behaviors in contrast to the light that they receive: absorb a part, pass through a part, and reflect the rest. Attracted light is a sign of objects around. In fact, the image is an optical set that shines on a curtain. The human eye senses the image created on the retina of the eye with the help of sight cells. In fact, vision is a perception that comes from the images (Fig. 4.18).

4-3-2- Discoloration of light

The light has a continuous range; however, it is individually received when it is received by the sensor. Images with discrete range are called digital images. Digital images are, in fact, two-dimensional digital signals that vary both in color and in position. Regarding this, images are usually stored in a few matrices. The smallest (discrete) image component is called pixel. In other words, digital images are composed of several pixels, each pixel can be a non-image (a gray image) or a vector (color image).

4-3-3- Color model

The difference in color is in frequency difference or wavelength. Therefore, a way to display pixels is storing the frequency vector or the corresponding light intensity. Unfortunately, current technology does not allow such sensors to be built. As a result, different methods have been developed to measure and store pixels. The most famous color model is called the RGB model, in which the intensity of the three red, green and blue colors is stored. Yellow, turquoise and purple are three subclasses produced from the combination of each pair of these original colors. The white color represents the presence of all three of the original colors and the black color indicates all of them. Typically, the color intensity is shown with integers between 0 and 255. To obtain light intensity (regardless of color), it is enough to measure the mean intensity of the three main colors. The human eye has cells susceptible to the frequency of red and green light, as well as light-sensitive cells, and therefore functions similar to the RGB model.

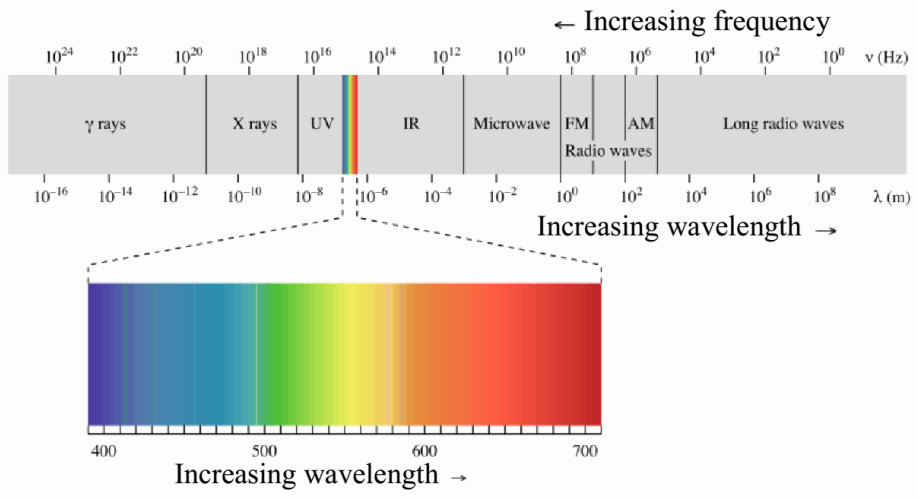

Fig. 4.18. The range of electromagnetic waves.

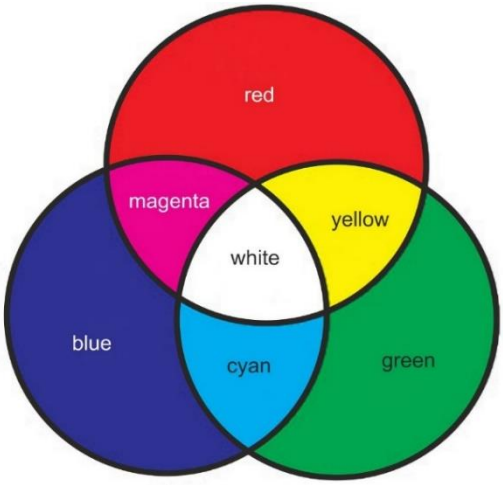

Fig. 4.19. The combination of red (R), blue (B), and green (G) colors in RGB color model.

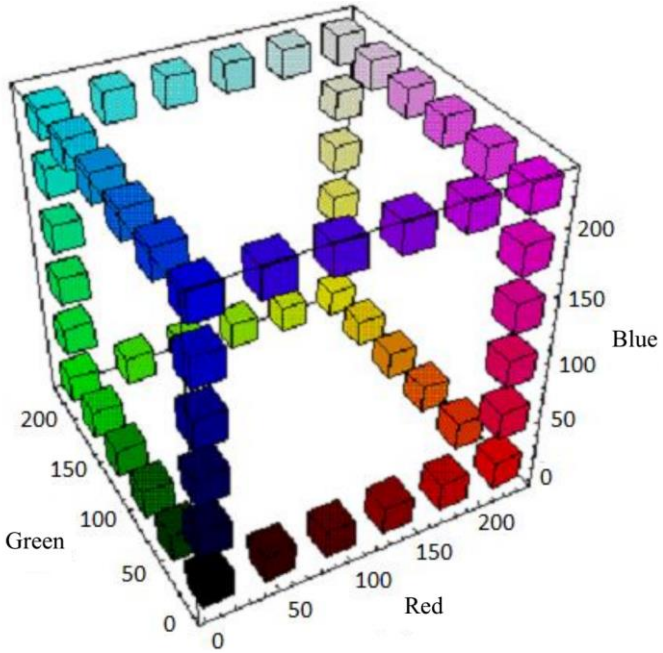

Fig. 4.20. Color Spectrum Changes in RGB color model.

The vision sensor-equipped robots use different models depending on the type of sensor used. As a result, in the first step, there should be a tool for transforming their color model. For example, Nao's humanoid robot uses the 422 YUV color model, where Y expresses the intensity of light, U represents the difference in blue color, and V indicates the difference in red color. Using the following equation, you can convert 422 YUV images to RJB.

$$\begin{bmatrix} R \\ G \\ B \end{bmatrix} = \begin{bmatrix} 1 & 0 & 1.13983 \\ 1 & -0.39465 & -0.58060 \\ 1 & 2.03211 & 0 \end{bmatrix} \begin{bmatrix} Y \\ U \\ V \end{bmatrix} \tag{4.2}$$

4-3-4- *Low pass filter*

Due to the electromagnetic nature of light, the noise in the sensors is normal. Due to the continuity of the bodies, there is also an approximation of the color. As a result, the presence of a high-frequency signal (the color difference of one pixel relative to its neighbors) is likely to be a noise. As a result, you should delete the noise by using the downstream filter.

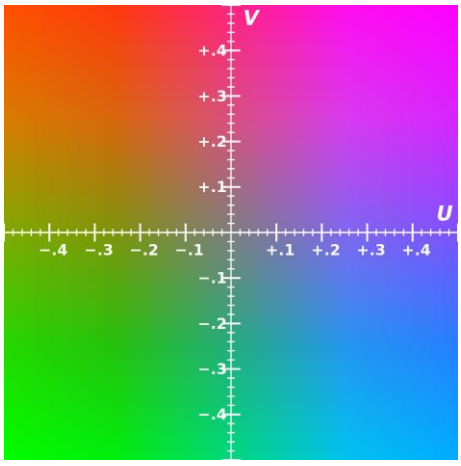

Fig. 4.21. YUV color model.

4-3-5- *Segmentation and modes filtering*

As mentioned, each pixel represents three intensity levels of red, green, and blue, which range between zero and 255. Although these data are needed to display the image, they do not play a

role in routing. A robot needs only knowing the type of pixel to determine its path. To this end, it must be determined that each pixel indicates which obstacle, risk, free or target spaces? To convert the image from the color space to the space of the segmentation environment is called segmentation.

Various ways to segment images are suggested. Selecting the appropriate segmentation method depends on the location of the robot. The quality and complexity of these methods can begin with the Euclidean method in the laboratory and end in a war along with water, smoke and fire. All segmentation techniques can have error (noise). As a result, after the end of segmentation, images must be passed through the mode filter so that their noise is taken.

4-3-6- *Expansion*

During the recording process, parts of the outer boundary may be blocked in the form of other spaces (usually free space). As a result, to avoid collisions with the robot, at this stage, obstacles are slightly widened. Also, expansion of obstacles increases the effect of fine obstacles. Figure 4 shows the stages of image expansion.

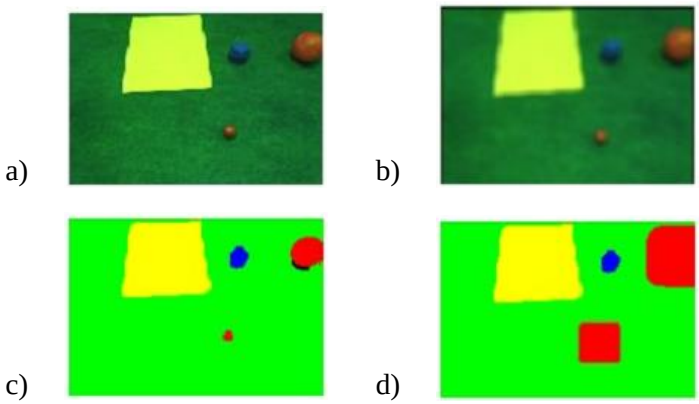

Fig. 4.22. Image expansion to enhance obstacle effect (a: main image; b: filtered image; c: split and filtered image; d: expanded image).

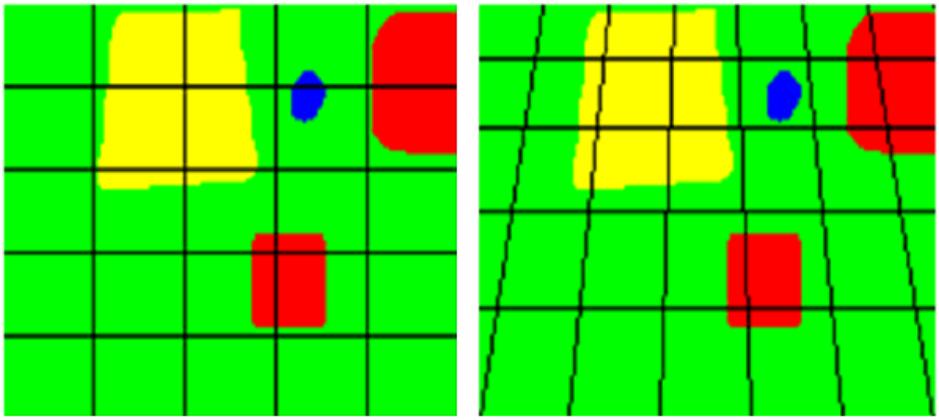

Fig. 4.23. Homogeneous (left) and heterogeneous (right) networks.

4-3-7- Network segmentation

The robot camera collects images at constant altitudes and angles relative to the ground. Therefore, the location of pixels can provide an estimate of the equivalent position. Finding the approximate position of a cell (a set of pixels) has less error; hence, network segmentation must be done after image segmentation. In most cases, in the case of an image with a desired angle to the ground, instead of a homogeneous network, a heterogeneous network is used (Fig. 5.1).

4-4- Robot path planning using rasterizing

Movement of two-dimensional robots in such environments with big and small obstacles is one of the major challenges in path planning towards the target. In these problems, usually the robot is modeled as a point which can lead to override the limitations of the two-dimensional robot. To deal with this error, some corrections and modifications are also done in modeling the environment, and in particular obstacles, to prevent a possible collision of the robot with obstacles. Two-dimensional robots can have two degrees of freedom (movement in the directions of x and y) or three degrees of freedom (movement in the directions x, y, and θ). One of the issues in this field is Piano Mover's problem that can be solved in various ways. However, both configurations; space and potential field methods are more popular than the others. In this section, I first introduce each of the two methods mentioned above, their

advantages and limitations will be discussed and then the corrected algorithm based on configuration space which is of higher speed and flexibility is introduced. This path design algorithm can be run for any type of polygonal geometry of robots and obstacles, including discrete components and convex angles, and if there is a path towards the target, it certainly will find that path. At the end of this section, some examples of implementation of this algorithm in different environments and different circumstances are provided, illustrating its operational capabilities.

4-4-1- *Configuration space method*

4-4-1-1- Definition of configuration space

Consider a moving object on a plane surface. The object's position can be described using its coordinates along x and y axes and its orientation towards θ. The configuration space of this object, is a set of all possible situations (x, y, θ) where $(x, y) \in R^2$ (real plane) and $\theta \in S^1$ (Unit circle). For this reason, configuration space of a moving object on a plane surface can be defined with $R^2 \times S^1$ (Fig. 4 .24). In robotics literation, configuration space is also called *C*-space in brief.

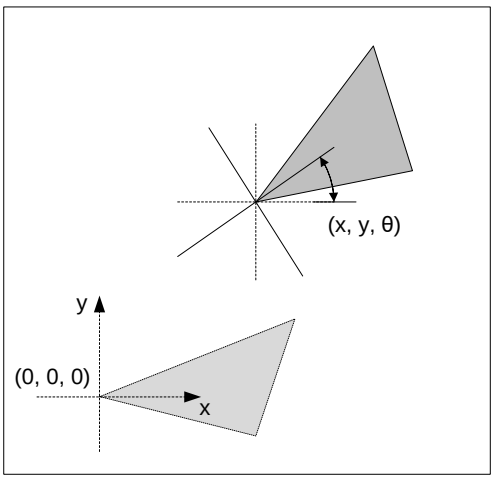

Fig. 4.24. A two-dimensional object in $R^2 \times S^1$ configuration space.

As another example of configuration space, consider a robot or a dual interface arm at (x, y) which is connected to a support, as shown in Fig. 4.25. According to this figure, the two angles θ_0 and θ_1 (with denote base arm angle and free arm angle, respectively) define the position of the robot completely. Configuration space for this system is $S^1 \times S^1$ and its point position is specified by $(\theta_0, \theta_1) \in S^1 \times S^2$.

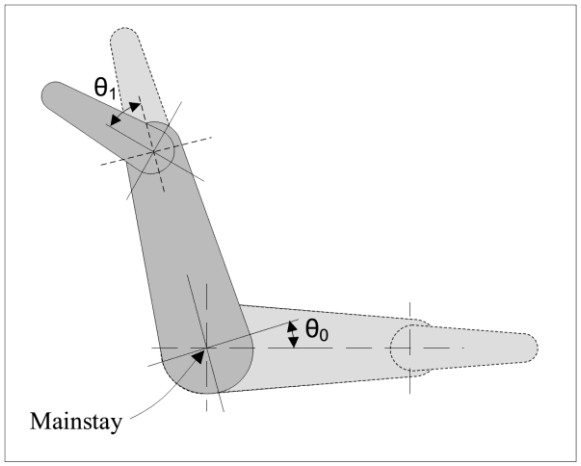

Fig. 4.25. Dual interface arm at (x,y), with the position (θ_0,θ_1) ϵ $S^1 \times S^1$.

4-4-1-2- Making c-space equivalent with Physical space

The motion problem of a complex robot at a physical environment can be made equivalent with the problem of a point's movement in *c*-space (This point is also called the robot reference point). In order for the border of obstacles in real *c*-space to be followed and observed in configuration space (*c*-space), we can consider obstacles in wider space of *c*; it means that compacting dimensions of the robot from a two-dimensional object to a point can be offset by widening obstacles. It is clear that when the robot's reference point is located outside the wide obstacles, in physical space the robot itself also is placed outside the obstacles.

Lozano-Pérez (Lozano-Perez 1987) used Minkowski summation of robot and environment for adjusting the obstacles' borders in *c*-space. In Minkowski summation, all the points of a set are

moved by points of another set and transferred to a new position. Minkowski sum is written as follows:

$$A + B = \{a + b \mid a \in A,\ b \in B\} \tag{4.3}$$

where a and b are members of sets A and B, respectively. For example, consider the following two sets, which are in fact coordinates of the vertices of two triangles:

$$A = \{(1,0),(0,1),(-1,0)\} \quad ; \quad B = \{(0,0),(1,1),(-1,1)\}$$

Minkowski sum of these two sets will be as follows:

$$A + B = \{(1,0),(2,1),(0,1),(0,1),(1,2),(-1,2),(-1,0),(0,1),(-2,1)\}$$

which demonstrate itself in a hexagonal form (Fig. 4.26).

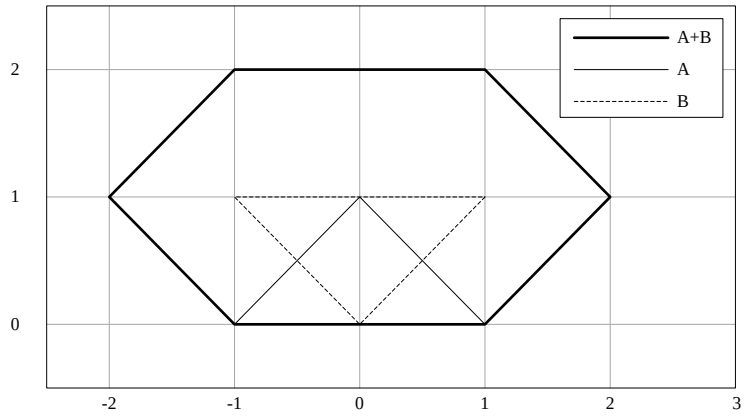

Fig. 4.26. Minkowski summation for the two sets; A and B.

For the sets that are defined with polygons, Minkowski sum can be considered the same as convolution (set summation) of the obstacles edges; it means that polygon of the obstacles can be summed with negated polygon of the Robot. For example, negated polygon of triangular robot is shown in Fig. 4.27.a. To model the robot's environment, its convolution with obstacles is used in order to produce c-space in the form of Fig. 4.27b.

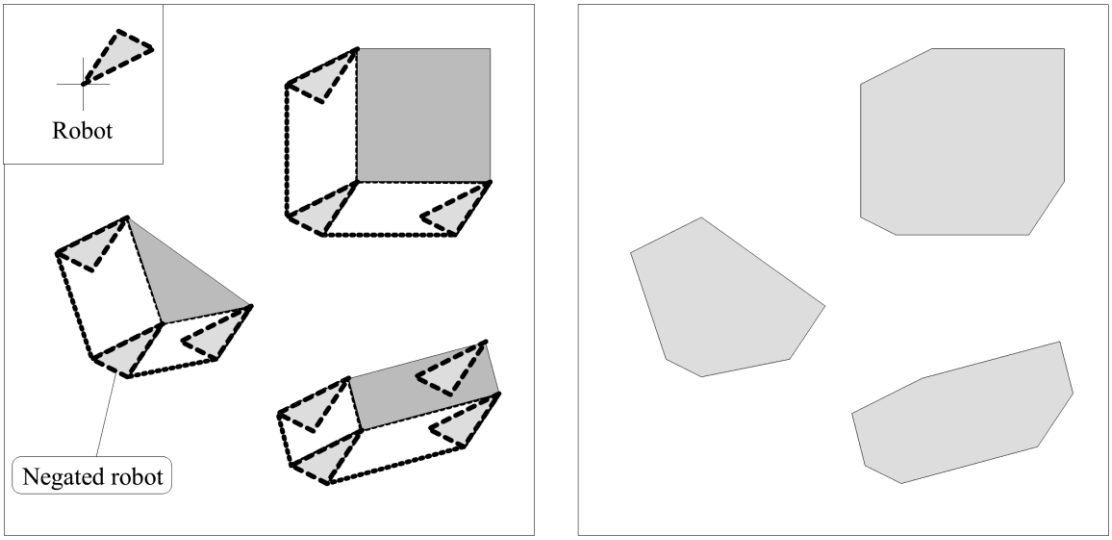

a) Minkowski sum of robot and obstacles b) The polygons derived from Minkowski sum

Fig. 4.27. Minkowski sum of robot and obstacles and the resulting polygons.

So as to calculate this convolution, convex hull algorithms can be used. However, since the time scale of execution in this algorithm is $O(n\ logn)$ (n is the number of points) and at a plane with no optimum convex polygon, Lozano-Perez proposed an alternate method that its execution time scale is $O(n)$. More information about the basics of this algorithm are provided in (Udupa 1977; Lozano-Pérez and Wesley 1979; Lozano-Perez 1983); but the way of its implementation will be described in the remainder of this section.

Note that what is meant by convex set or polygon is a set where connecting line between any two arbitrary points within it is completely located within the same set (polygons). Otherwise, interest set is called concave or non-convex set. Fig. 4.28 shows an example of two sets of convex and concave.

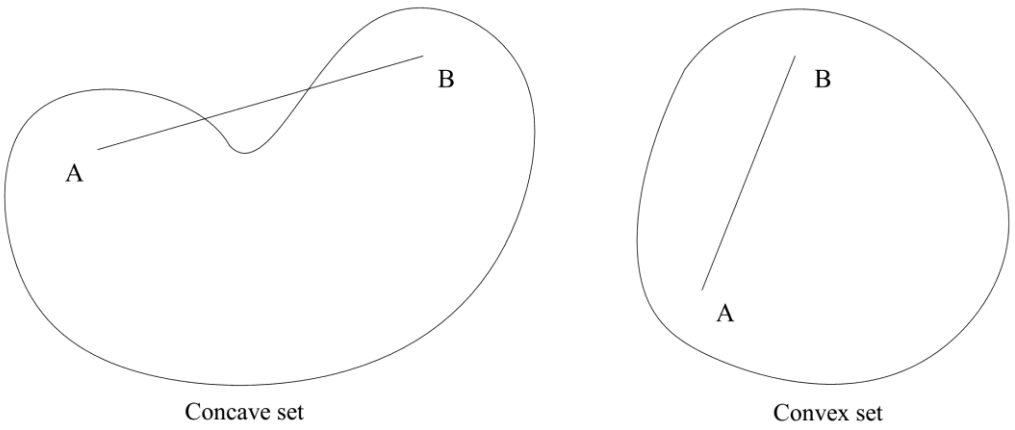

Fig. 4.28. Convex and concave sets.

4-4-1-3- Rasterizing Methods in c-space

Other researchers have used rasterizing method in *c*-space. For example, Luzano-Perez (Lozano-Perez 1987) utilized the research conducted by Lozano-Pérez (Lozano-Perez 1983) and Donald (Donald 1987) and encrypted them in a bitmap format in *c*-space. However, this algorithm was one with non-local search, heterogeneous, non-parallel able and with no hardware support.

Dorst and Trovato, also used a *c*-space-based rasterized approach for planning two-joint arms (Dorst and Trovato 1989). They described motion planning problem in a differential geometric framework with a metric topology applied on the space configuration and calculating the shortest corresponding paths with optimum paths. For this reason, they first made *c*-space discrete and then used cost wave propagation and gradient following to find the optimal routes. The third and fourth parts of the algorithm in this section are very similar to this work. With the important difference in the work of Dorst and Trovato, the problem of creating obstacles in c-space is not discussed. Besides, in the algorithm discussed in this section, it was focused on the hardware aspect which it is not considered in Dorst and Trovato's work.

Also, Donald proposed a motion planning algorithm with good approximation, that in an environment with a certain resolution, guarantees finding at least one path (if any) and besides,

all the proposed way(s) is (are) secure (Donald 1987). Among other features of his algorithm, were the use of constraint equations to display obstacles in *c*-space, applying *c*-space gridding and finally, using local multi-experts for guiding searches in c-space. The noteworthy advantage of this algorithm is the guaranty to find the path in a given resolution. However, its software implementation, particularly in a non-parallel machine, is very slow. In the remainder of this section we will see that using parallel processors can significantly increase the speed of the algorithm.

4-4-2- *Potential field methods*

4-4-2-1- Vector presentation in potential field method

The potential field method was first introduced by Khatib and Lemaître (Khatib and Le Maitre 1978). In this method, the obstacles are shown in the form of scalar analytic functions with zero value ($f(x,y,z)=0$). Then, the local potential field of every obstacle is generated with a relationship inversely proportional to the square of the distance from the position of each obstacle by another obstacle. Besides, an optional cut value f_0 is also defined, in order to specify some points with a value less than f_0 (Long distances from the obstacle) (Fig. 4.29.a). Accordingly, potential field $P(x,y,z)$ is expressed mathematically by the following equation:

$$P(x,y,z)=\begin{cases}\dfrac{\alpha}{f^2(x,y,z)} & , \quad f(x,y,z)\le f_0 \\ 0 & , \quad f(x,y,z)> f_0\end{cases} \tag{4.4}$$

where α is amplification factor of potential field, which is determined with regard to that if an interest point is affected by target field, obstacle or the robot. A moving particle which is moving in the potential field in accordance with Newton's laws, will never hit the obstacle. Khatib, regarding the law that the sum of gradients is equal to gradient of sum, showed that the

sum or total potential fields of several obstacles results in a unique function, which under its effect, the particle will not hit any obstacles. Since the real moving object is not a spot or a point, Khatib specified some distinct points on the object, in order to use linear combination of their potential to determine the position and orientation of rigid body.

The potential field method, has been successful in avoiding momentary collisions with obstacles in variable environments, but for motion design it suffers from some limits. A fundamental problem is forming a fictitious (bad) local minimum in particular for robots with convex shape. Random methods or other methods that are described below should be used to escape from local minimum.

4-4-2-2- Bitmap representation in potential field method

Barraquand and Latombe expanded the concept of potential method and used bitmaps to represent obstacles. They formed a separate potential field for the robot which starts from target point (Fig. 4.29b) (Barraquand and Latombe 1991). In this method, the potential field is not a function of distance from one point to the target, but it is a function of the path length which is obtained from bypassing obstacles along the path to the target.

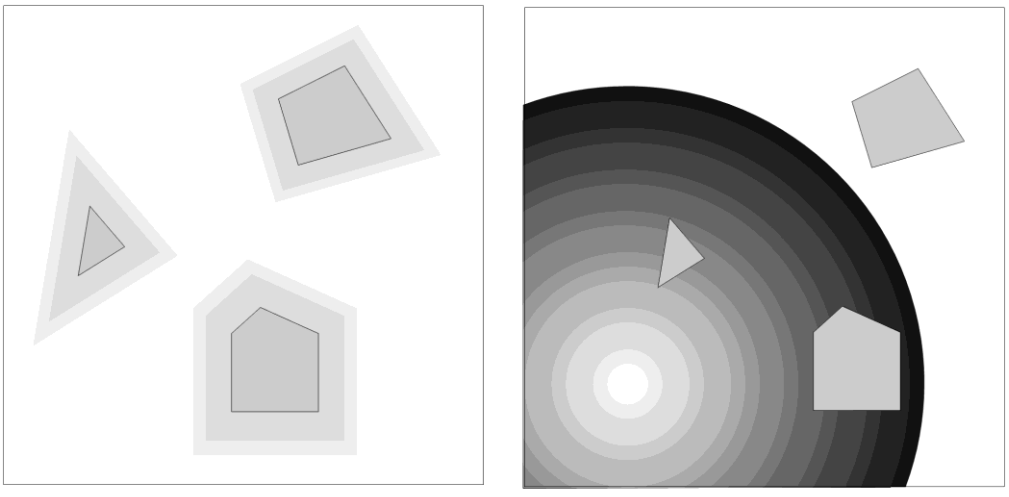

a) Potential field of robot and obstacles

b) Bitmap potential field of target

Fig. 4.29. Potential field resulting from obstacles and target. The higher the density, the higher is potential sign.

Then, in a manner similar to Khatib's method, they combined potential field of separate points together in order to achieve a single potential field. Although, potential field doesn't have any local minimum for a point robot, the combined potential field for more complex robots may contain several local minimums caused by competition of distinct points. Barraquand and Latombe proposed two methods to avoid the local minimum, both of which search for a route in *c*-space using potential fields. Their first method, which is filling local minimum, will result in a complete design in a given resolution. In this regard the interest algorithm offered in this section is very similar to their method.

4-4-3- *Combinational algorithm*

Motion design algorithm used in this section, is a combination of capabilities of above algorithms mentioned in configuration space and potential field. From an algorithmic perspective, this method, is based on Donald's network-based approach (Donald 1987) along with Lozano-Perez's configuration space approach (Lozano-Perez 1983) and consists of four distinct parts as follows:

1. **Creating *c*-space:** In this section, a voxel (Volumetric pixels) is assigned to display *c*-space and obstacles of *c*-space are quickly computed in this array using standard graphics rasterization hardware.

2. **Calculating navigation function:** in this section, c-space navigation function (Koditschek 1987) is calculated using a dynamic programming (such as expanding wave-front solutions). The navigation function, is in fact a function with discrete vector value, which by having instantaneous position of robot voxel in *c*-space, determines the direction along in which the distance to target is reduced.

3. **Determining the optimal path:** in this section shortest path is determined from every starting position of voxel to the target (if there is any suitable solution). Since the navigation function determines the motion direction in every cell, this section can quickly calculate the path and if there is a path, detect it in a fixed time.

4. **Drawing motion path:** this part, creates real-time kinematic simulation for robot motion.

As follows, each one of these parts are explained in detail.

4-4-3-1- Creating configuration space representation

In this phase, at first, the polygons related to obstacles of configuration space are calculated using Minkowski sum of obstacles and robots (Lozano-Perez (Lozano-Perez 1983)), which an example is shown in Fig. 4.27a. Afterwards, polygon filling graphics hardware is used to fill the polygons of the obstacle's space configuration (Fig. 4.27b). When the robot is restricted to two degrees of freedom (translation in plane), this representation contains only one bitmap, but if the robot rotations are permitted, space configuration is represented by a series of bitmaps, where each bitmap is a sector picture of space configuration in the angular interval of $[\theta_1, \theta_2]$. *c*-space representation in one direction is an easy task but creating a conservative and discrete representation from c-space over several angular intervals is a difficult task. The aim of this method is to ensure that in a bitmap sector which represents the c-space in an angular interval $[\theta_1, \theta_2]$, no pixel with a penetrated obstacle is labeled "free". To create a discrete representation from *c*-space angular interval of $[\theta_1, \theta_2]$, the *c*-space is divided into *n* equal parts, each part of which is specified with angular development $\theta = (\theta_2 - \theta_1)/n$. Therefore, the bitmap sector for

angular interval $[\theta_1, \theta_2]$ is shown using by union of all the subintervals. The Pseudo-code for this method is as follows:

```
GENERATE C-SPACE ()
 For theta = 0 to 2π by 2π/N  (N  is # of theta slices)
  Foreach robotpoly in robot polygon list
    For t1 = theta – dtheta to theta + dtheta
      Rotate robotpoly by t1
      Foreach obstaclepoly in environment
        Generate the minkowski sum of robotpoly and obstaclepoly
        Fill minkowski polygon with obstacle color.
  Read filled polys from frame buffer
  Move bitmap into voxel array.
  Clear frame buffer.
 Return bitmap voxel array.
```

It should be noted that bitmap sectors are conservative, it means that, once any part of an obstacle penetrates into the cell, all those cells are labeled "obstacle". This task excludes some of potential routes, but it strengthens the fullness property of resolution of the algorithm. Thus, if two cells stuck together, they are labeled "obstacle-free", the path between them is open, because otherwise, one or both of them are labeled "obstacle". With this, motion is permitted only between free cells and as a result, all the resultant paths will be valid (collision free).

4-4-3-2- Calculating navigation function

In this algorithm, a dynamic path planning approach has been used for expanding wave-front solutions which starts from the target point, and by forming a queue of voxels and their characteristics, records the location of the wave-front (Dorst and Trovato 1989). Each element in the queue, records the location of a cell from the environment as well as the length of its

traversed path until the target location. After each cell occupies an element from the queue, their other neighboring cells not already in the queue, are added to the remainder of queue. The first element in the queue, is the target cell with zero length path. This algorithm, takes out this cell from the queue and fills its position in the pixelated (rasterized) environment with zero values. Then, it brings all the adjacent cells with path length of 1, to the beginning of the line. Thus, the wave-front advances until covers all the obstacles in *c*-space (Pavlidis 1981). It should be noted that in this way, every cell available to the target point is initialized just once. The following pseudo-code and Fig. 4.30 show this process:

```
FILL NAVIGATION FUNCTION (target location)

   Enqueue target location with distance = 0

   While queue is not empty

      Dequeue element F

      Label F´ s location with F´ s distance

      Enqueue all neighbours of F that are not obstacles and that have not yet been
filled with distance = distance +1
```

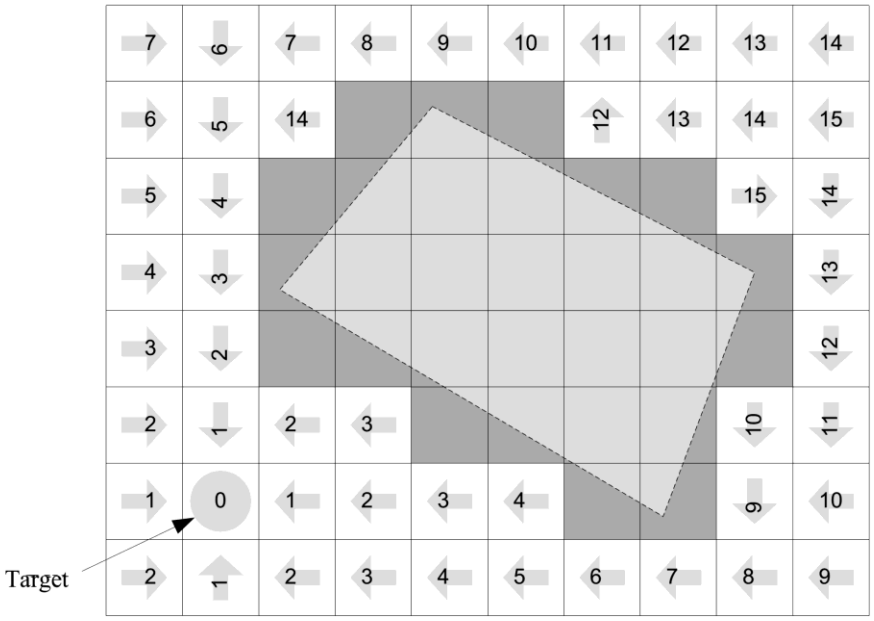

Fig. 4.30. Calculating navigation function.

The duration required to run the calculations is proportional to the number of free cells in the environment. More complex parts of the field in which there exists high numbers of obstacles, have much fewer free cells and as a result, will be filled faster.

In a robot with three degrees of freedom (two translational and one rotational motion), the process of filling cells is conducted in the upward direction and also along θ in peripheral manner (direction), just like expanding along directions *x* and *y*.

4-4-3-3- Path design

Since the navigation function is created using a breadth-first-search (BFS) in the entire *c*-space, the shortest route from target to any accessible location in c-space can be found (the shortest path, is a path that passes from fewer voxel) (Dorst and Trovato 1989). To get closer to the target point from any starting position, the robot moves to an adjacent cell which has the least figure. If there are multiple cells with the lowest figure, it is likely for any of them to be selected; because each are the origin to begin a path with equal numbers of movements to reach the target point. If two options of rotation (movement along θ) and translation (movement along *x* or *y*) were available, this algorithm chooses the latter option (translation) in order to minimize rotation. The following pseudo-code and Fig. 4.25 show this process:

```
GENERATE PATH (start location)
    let C = cell corresponding to start location
    let P = NULL
    if C was not reached by fill (label is blank)
       return cannot reach target
    else
       while C is not at target
           add C to path P
           pick lowest numbered neighbour, L
           let C = L
       return P
```

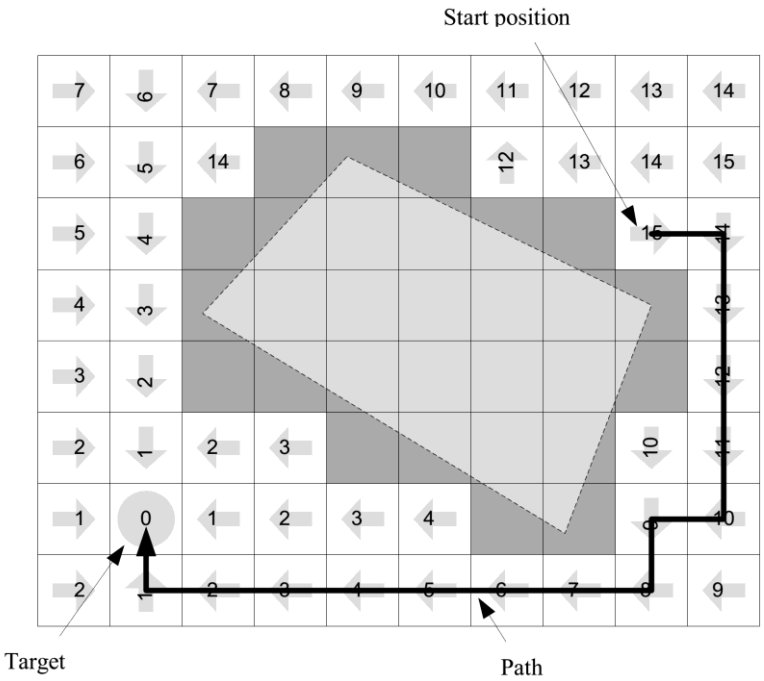

Fig. 4.31. Generating paths in the desired algorithm.

Each cell achievable from target, has a neighbor with lower figure than itself (the cell that has been placed in the queue for labeling). So, no local minimum exists in navigation function. The robot can follow the broad initial search tree to the target, without having any concerns about being trapped. Seeking search tree in terms of duration of the run, is linear and fast.

4-4-3-4- How to display

To demonstrate this method, a program including standard graphics hardware acceleration is used to represent real-time movement of the robot, which brings about the capability to correct the position of the observer. For graphical representation, two preprocessing steps, including rasterizing c-space and calculating navigation function are required. C-space is created at the beginning of the calculation and until a change has not happened in the position or geometry of the obstacles, or the geometry of the robot is not changed, there is no need to redefine open space. Navigation function is only recalculated when a change has occurred in the target position. As mentioned, navigation function calculations are linear and therefore their running

speed is high. However, the calculations related to graphical representation can be conducted almost simultaneously while observing the robot's movement.

4-4-3-5- Hardware utilization

Running this algorithm in non-parallel processors is very slow, however by using a dedicated hardware or parallelism, its speed becomes extremely high. During running, the first part (creating *c*-space obstacles) and fourth part (simulation, kinematic) require graphics hardware. Second part (flood like expansion) is a local performance and is of optimized calculations (Barraquand and Latombe 1991). The third part (extensive initial search tree) is also inherently a fast-sequential operation.

4-4-3-6- Testing algorithm

The proposed algorithms have been tested in environments with multiple obstacles, and with robots and obstacles with various convex and forms. Duration of the test for each of the samples is shown in Table 4.1. Every time that preprocess steps are completed for configuration space and navigation function, path planning algorithm is executed in real time, and real-time motion will be possible.

Processing and displaying the results are executed on a *HP 835* system with *turbo-SRX*. Pre-calculations have been done for Fig. 4.36 and Fig. 4.37 (Marked with * in the table 4.1) similar to Fig. 4.33, and there is no need to repeat it.

Table 4.1. Run time for each example

problem	Figure	Pixel netting	Run time			
			c space	fill	search tree	display
two-dimensional robot with direct path traversing	4.33	256×256×120	22.6	44.1	0.11	35.8
two-dimensional robot with reverse path traversing	4.36	256×256×120	*	*	0.11	50.3
trammeled two-dimensional robot	4.37	256×256×120	*	*	0.01	0
piano (environment 1)	4.39	192×192×180	26.0	50.2	0.05	27.1
piano (environment 2)	4.40	92×92×90	8.1	8.1	0.04	7.2

Example 1: Two-dimensional robot motion in $R^2 \times S^1$ space

In this example, movement of a two-dimensional robot with three degrees of freedom (translation and rotation) will be examined. Under consideration, robot and its physical space have been shown in Fig. 4.32. The obstacles occurring in the path of robot include rectangular and triangular appendages over intermediate walls and two small triangular obstacles which can be seen in the top left corner. Target position is labeled with the letter (d) and light gray color on Fig. 4.26. To evaluate the performance of the algorithm, three cases of (a), (b) and (c) are set aside for starting position of the robot and are shown on the figure.

The result of traversed path for starting position (a) has been shown in Fig. 4.27. Carefully looking at this figure, we can see that after a few initial steps the robot, conducts a 45-degree clockwise rotation in the top right corner of the environment and then, preserves its status almost until reaching small triangle obstacles of the upper left corner obstacles.

The robot, to cross from triangular obstacles, starts another counter-clockwise motion and continues up to 180° rotation in order to take itself to the target position. As can be seen, all these traversing paths are conducted without any backwards stepping or returning. In other words, because the respective algorithm starts its path by searching from the target side and continues until the starting point and situation, it can find existing path(s) and select the most efficient one.

In the starting position (b), the robot has an interesting situation. As seen in Fig. 4.34, for the robot to move to the target point, it must pass through triangular obstacles, and to do so needs to rotate counterclockwise.

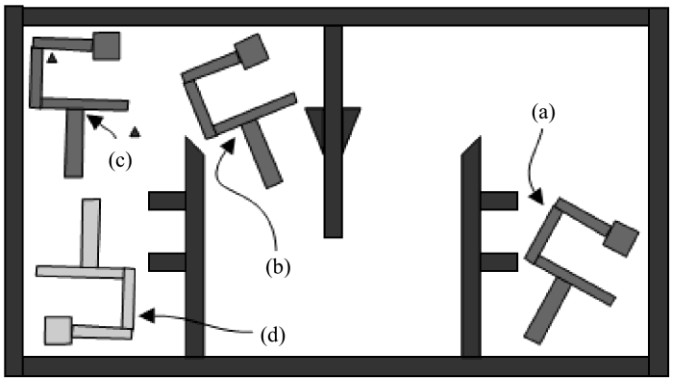

Fig. 4.32. Robot's positions;
Start position of a) Fig. 4.34, b) Fig. 4.34 c) Fig. 4.37 and d) target

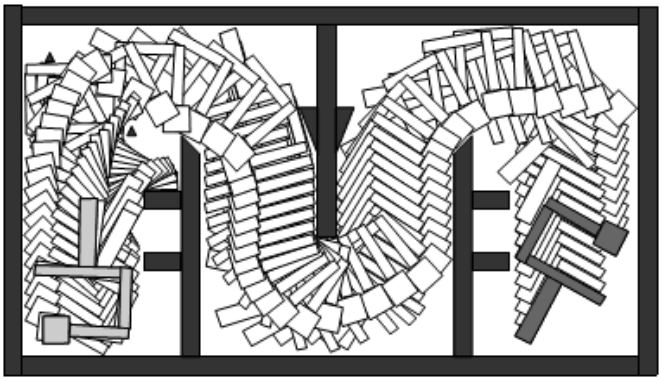

Fig. 4.33. Mobile two-dimensional robot without going back to the target.

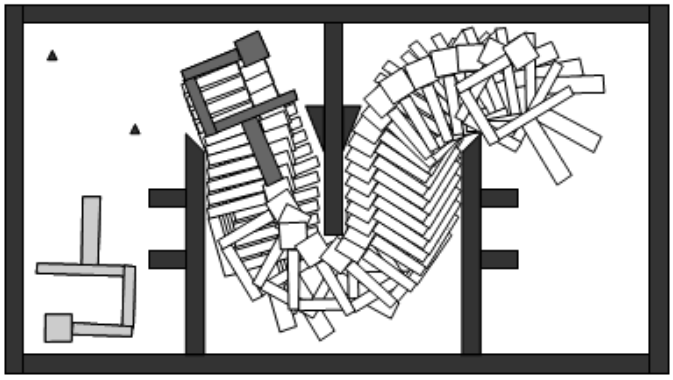

Fig. 4.34. The first step to move the robot towards the target in mode (b) (reverse scroll to correct the situation).

But, as can be seen, positioning state of robots and obstacles is in such a way that there is no possibility of rotation at the starting point. For this reason, the algorithm guides the robot to a

reverse path in first step until it reaches to the top right corner location of the environment where there is the possibility to rotate. Afterwards, in second step (Fig. 4.35) the necessary rotation places the robot in a situation similar to state (a) so it can continue its path towards the target point. This feature of the algorithm which doesn't limit itself to the path from starting point to the target, is considered as a significant feature. Since, without this feature, there wouldn't be any paths towards the target.

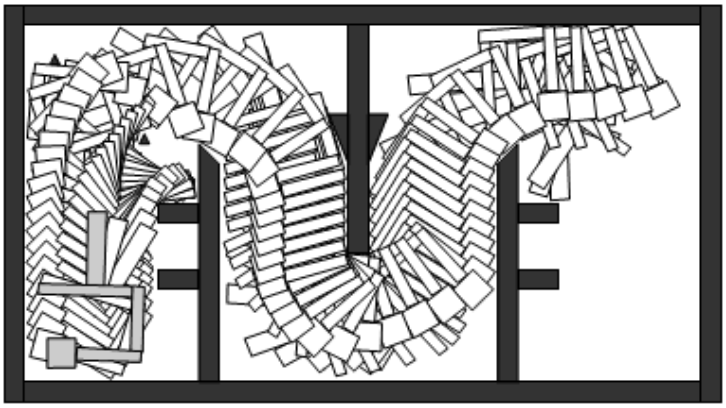

Fig. 4.35. The second step to move the two-dimensional robot toward the target in state (b) (state correction and direct scrolling).

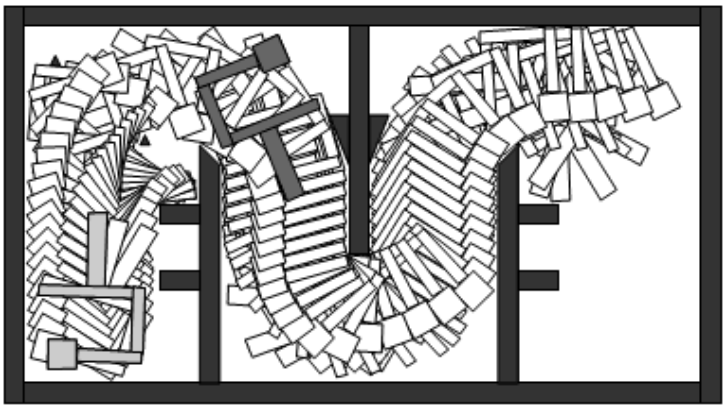

Fig. 4.36. Combining the first and second steps to move towards the target in mode (b) (inverse and direct scrolling).

Nevertheless, in location (c), the conditions are quite different. As in Fig. 4.37, the robot situation is so that the occurrence of triangular obstacles, prevents any maneuver from the robot. Thus, there does not exist any paths to the target position (c).

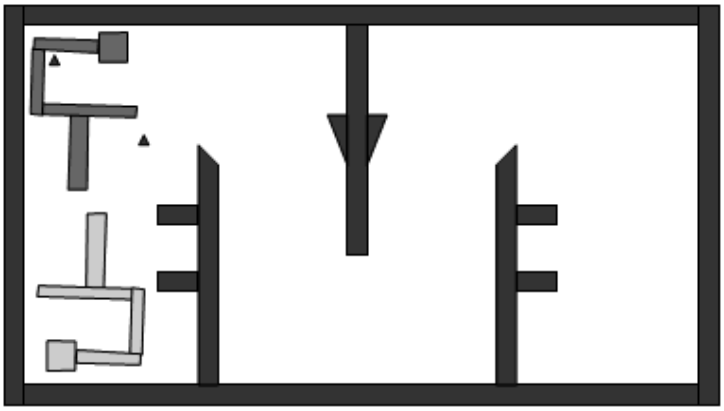

Fig. 4.37. The trapped two-dimensional robot in mode (c).

Example 2: Three-dimensional Robot Motion (Piano) in $R^2 \times S^1$ space

A lot of three-dimensional robots have some parts that differ from each other vertically. For example, the piano in Fig. 4.32 has small bases and the main part is large. By defining two short and long types of obstacles, one can distinguish them. Short obstacles limit the movement of bases and long obstacles limit the body of piano. Thus, this algorithm which in fact is designed for two-dimensional problems, can be run for such three-dimensional ones which can be separated into two or more two-dimensional problems.

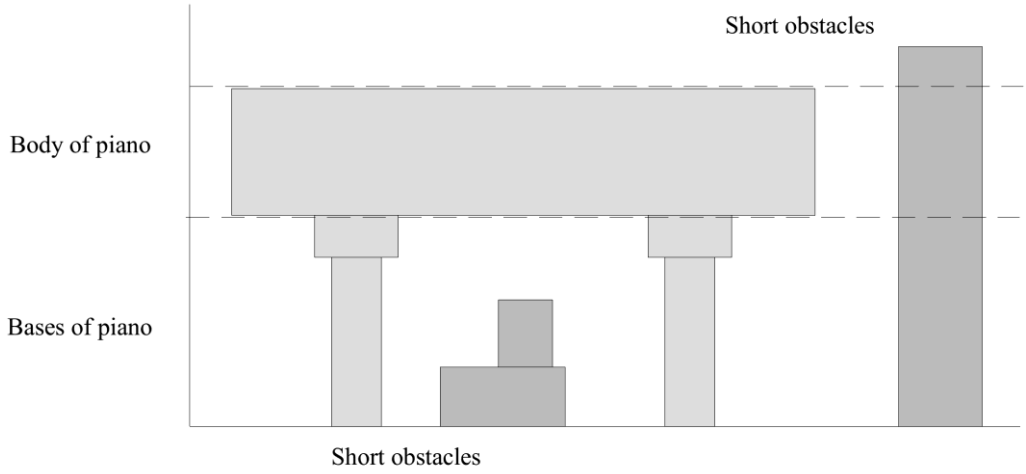

Fig. 4.38. The piano's division into two types of bases and body.

Rasterizing the environment is done as before, except that for creating c-space in this case, the body and bases will be only summed by Minkowskily method with high obstacles and low obstacles, respectively. In this way, by union of low and high obstacles, a single bitmap will

be created. Since the short obstacles didn't sum Minkowskily with the piano's body, that body can move over it, but the bases maneuver around them.

Experiment of piano movement was done in two different environments and in each environment, was done from two different starting points. In the first environment (Fig. 4.39) both long and short obstacles (body and base Obstacles) exist. High (long) obstacles are distinguished with dark squares and short ones with white squares. The positions of bases are also shown from top view with three small squares on it. As can be seen, the piano from each both starting points with direct movements and necessary rotations crosses over short and high obstacles to reach the target position.

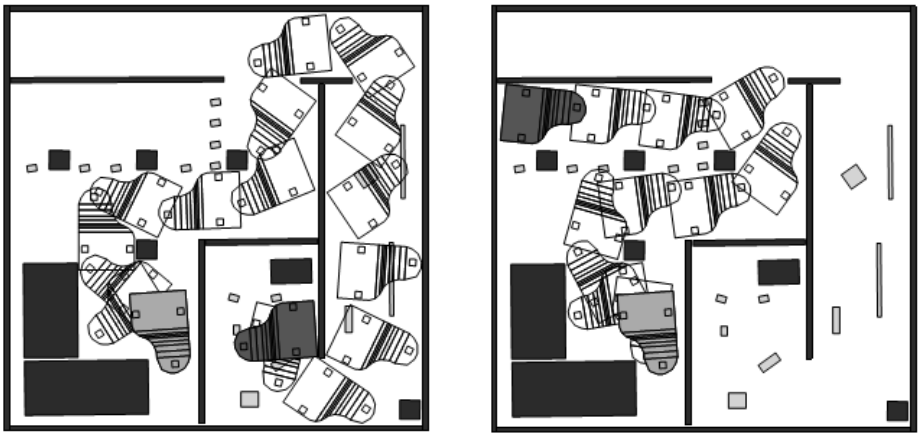

(a) (b)

Fig. 4.39. The piano's movement in the first environment, including both short and long obstacles, from two different starting points.

In the second environment (Fig. 4.40) just short obstacles (bases) are there. In the first starting position (Fig. 4.40a), there are two paths towards the target. The first one is direct path until the end of the isle and the other is direct motion towards left side of exit. Regarding that path selection in under consideration algorithm is based on minimizing rotation, the first path (direct motion toward the end of isle) is selected. In the second starting position (Fig. 4.40b) also piano chooses the direct path and along the way, does necessary rotation to align with the target status.

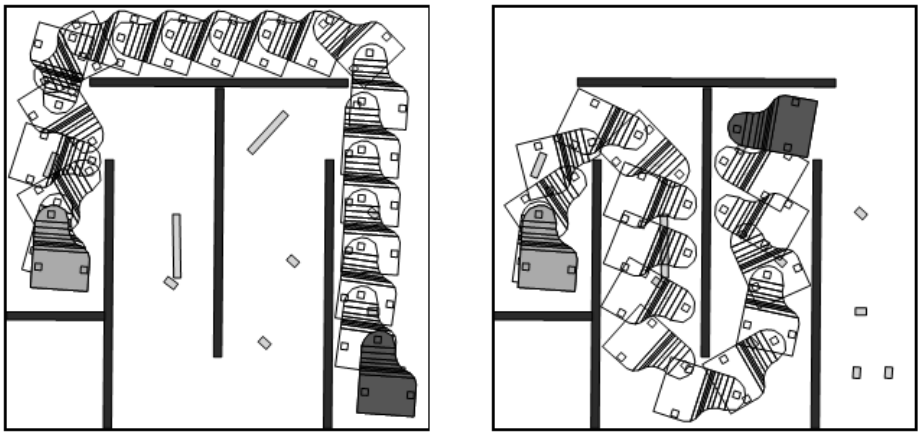

(a) (b)

Fig. 4.40. The piano's movement in the second environment, including short obstacles, from two different starting points.

Chapter 5- **Examples of Path Planning Algorithms' Testing**

5-1- Introduction

In chapters 2 to 4, all the variety of path planning approaches and algorithms in known and unknown environments and how to rely on the audio and visual sensors were introduced in detail and their working principles were described.

In this chapter, I will proceed to implement some of the most important methods. The second section of the chapter is dedicated to implementing Bug 1, Bug 2 and DistBug algorithms on the Pioneer Robot, where their traversed path and practical advantages are compared (Alpaslan and Osman 2009). In the third section, an analytical approach to improve the performance of the robot to avoid collision to obstacles is presented. This method tries to cross the robot through a variety of obstacles with convex and concave corners (obstacles with Z, V, U and zigzag shapes), on the basis of tangential escape (Brandão et al. 2013). In the fourth and fifth sections of this chapter, I proceed to plan paths in the environments with and without risk space. As you're aware, there may be three kinds of spaces in robot's paths: free, risk and obstacle. The robot must avoid obstacles and cross through open spaces. But decisions about risk areas (like muddy paths, water holes and ...) depends on existence of selected options. The line space could be the only path to cross or perhaps there might be some other paths to cross through. Four approaches: artificial fuzzy potential field, lingual method, Markov decision process and fuzzy Markov decision process, are introduced in these two sections and will be implemented on Nao humanoid robot. Performance results of these methods in the form of images generated from traversed paths and the robot decisions when encountered with obstacles will be presented.

5-2- Comparisons among Bug Family Algorithms

In this section, path planning algorithms; Bug 1, Bug 2 and DistBug will be simulated on mobile robots and their results will be compared with each other. Path planning algorithms mentioned above are applied on a Pioneer robot in a simulated environment. In these experiments, acoustic sensors are to be used.

As noted in the second Chapter, Bug algorithms are simple ways that guarantee high performance and once the robot faces obstacles, they are able to follow a path towards the target (if available). In this category of algorithms, there are three assumptions about robots: 1) Robot is supposed to be as a point body. 2) The robot has full localized knowledge from its environment. 3) The robot's sensors are accurate.

5-2-1- Implementation

The codes for Bug algorithms are offered in various references. Here, these codes are written in C++ and ran by using the Aria libraries in the Linux environment. The simulation environment is 10 meters long, 8 meters wide and has two convex obstacles (Fig. 5.1). To prepare a map, Mapper ver.3 described in reference (Sankaranarayanan and Vidyasagar 1990) is used.

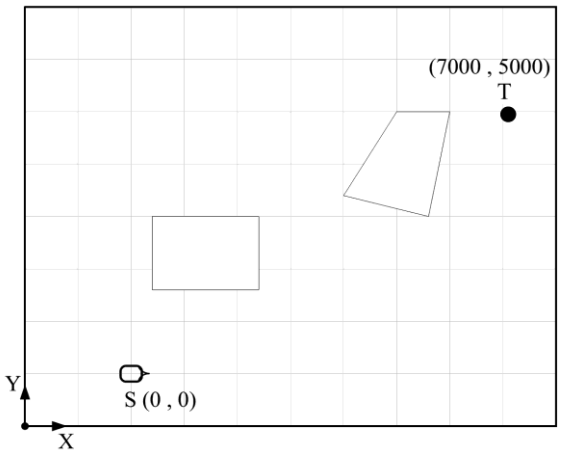

Fig. 5.1. Simulated environment in MobileSim Software to evaluate Bug 1, Bug 2 and DistBug algorithms.

During implementing the algorithms, the robot updates its positioning and navigation information, using acoustic sensors, detects borders (or walls) and by finding the corners of unknown obstacles moves towards the target.

In the simulation environment, the robot utilizes a distance meter to locate and update its information (including location and direction of travel). This is done to update instantaneously the position of robot to control the collisions with obstacles and find leaving points of obstacles. Also, it is important for the robot to have the ability to place itself on a line with an appropriate slope at any time of implementation of Bug 2 algorithm. It should be noted that although the position of the robot is clearly visible in a simulated environment, access to the full position in a real environment is difficult.

Detecting obstacles and following their walls using acoustic sensors is shown in Fig 5.2. The robot uses frontal sensors (labeled with numbers 2 through 7) to detect obstacles encountering it. It also uses sensors number 8 and 9, to follow the obstacle's border in a clockwise direction, and sensors numbers 1 and 16 in a counterclockwise direction. Sensors numbers 10 through 15 are related to backward movement of the robot.

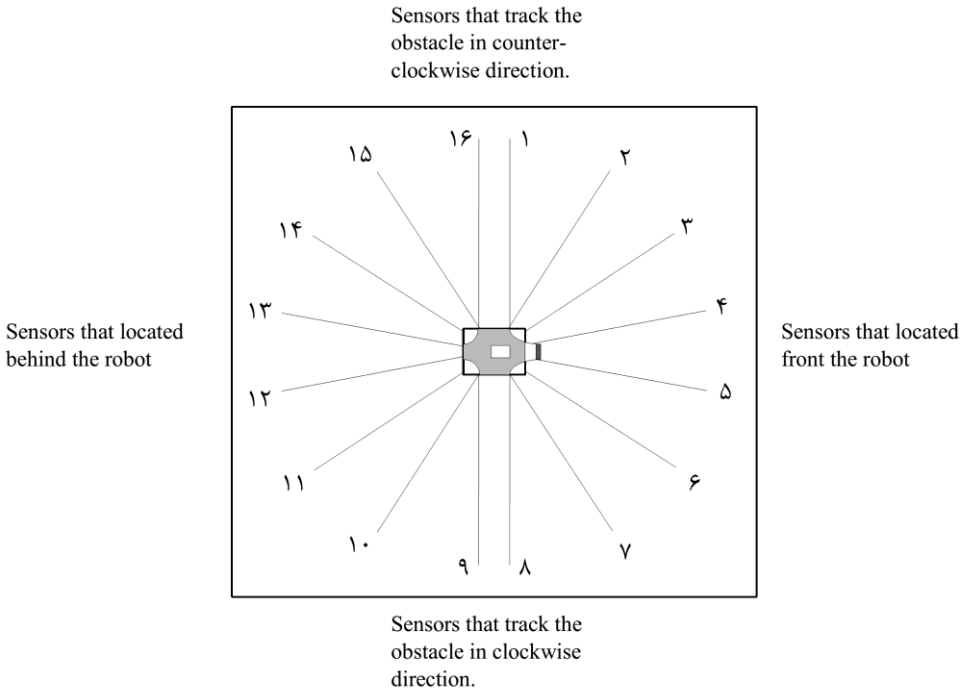

Fig. 5.2. Locating the robot sensors used in the testing of Bug 1, Bug 2 and DistBug algorithms.

5-2-2- *Tests and results*

The robot is located in a two-dimensional environment with coordinates of starting point (0,0) and target point (5000,7000). The length of shortest path between the starting points (*S*) and the target point (*T*) is 8,602 mm and the robot's speed is 100 millimeters per second (mm/s). The results of the implementation of Bug 1, Bug 2 and DistBug algorithms are shown in Fig. 5.3.

Fig. 5.4 also shows the graphs of traversed length by three algorithms of Bug 1, Bug 2 and DistBug along with path of environment-dominant bird (the best possible path). Improved results using Bug 1, Bug 2 and DistBug algorithms are clearly evident in this Figure.

As can be seen in Fig. 5.3a, in Bug 1 algorithm, while scanning itself the robot crosses from all the corners of the obstacles that it faces and compared to two other methods, has the slowest performance. However, this algorithm ensures reaching the target. The length of traversed path by the robot in this method is 29,022 mm.

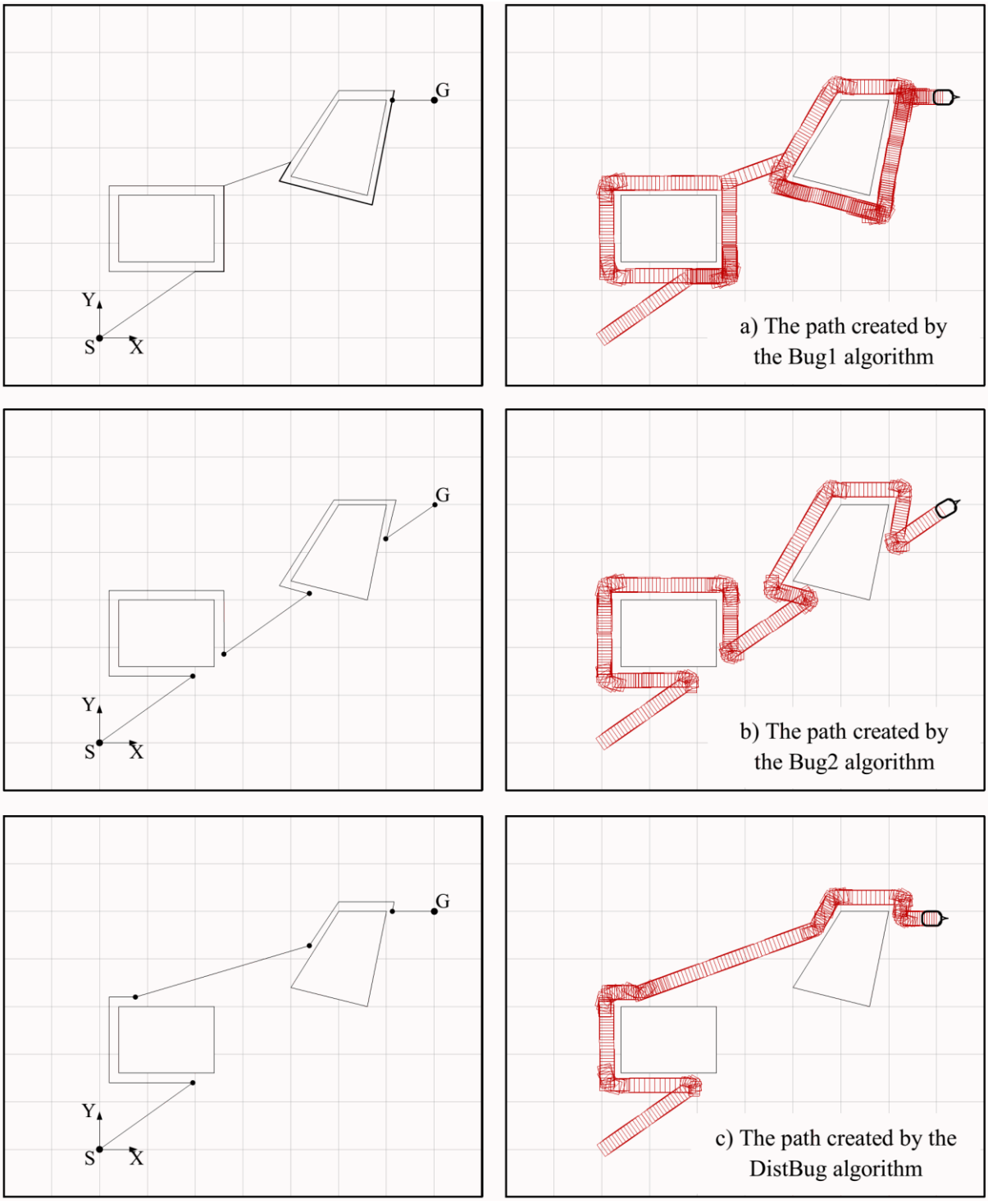

Fig. 5.3. Traversed paths created by Bug 1 (up), Bug2 (middle) and DistBug (down) algorithms.

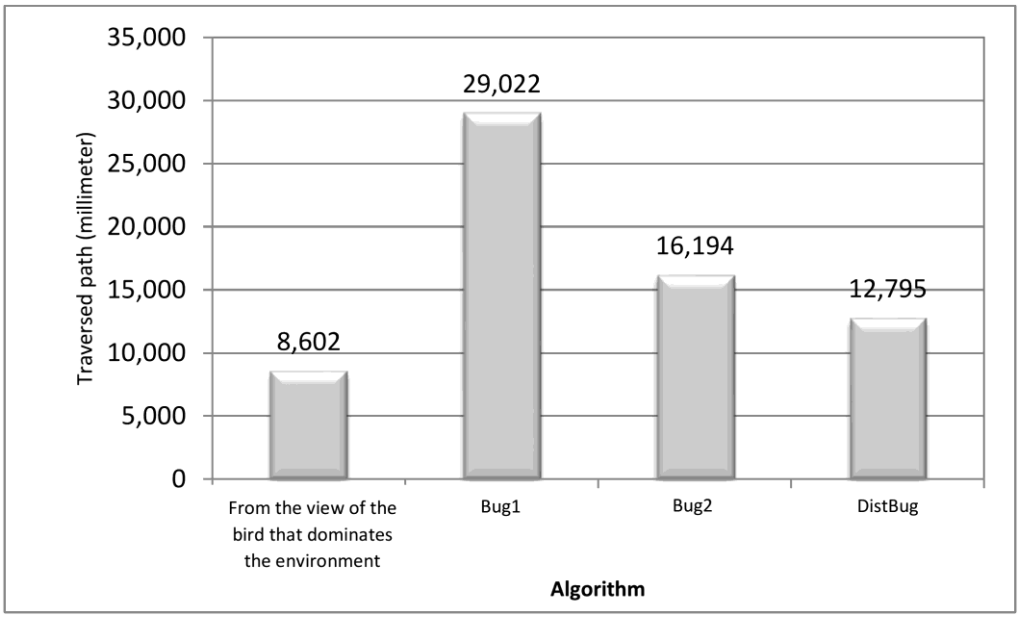

Fig. 5.4. Length comparison of the robot's traversed paths using different routing algorithms.

Using Bug 2 algorithm (Fig. 5.3b), the robot when facing the first obstacle and finding initial slope, passes by the obstacle from left side, until it again cuts the line connecting the starting point and target point, and from there on, continues the line on the same route. This process is also repeated for the next obstacle. As seen in the figure, the Bug 2 algorithm, unlike Bug 1 does not pass by the obstacle completely, which is why it is faster. However, in a winding path these two algorithms don't have significant advantages relative to one another. The length of traversed path in Bug algorithm 2 is 16,194 mm.

However, the traversed path in DistBug algorithm (Fig. 5.3c) has better conditions than Bug 1 and Bug 2. This algorithm allows using the capability of the sensors to find the shortest route to the greatest extent possible. Such that when looking for an obstacle's border, it constantly evaluates the direction of its current position to the target and at the first chance of seeing its free path towards it, leaves the obstacle. For this reason, the shortest traveled path among the three studied algorithms is DistBug. Also, DistBug has the ability to implement constraints discussed about simultaneous motion towards the target while following the obstacle's border. The traversed length of path by using this algorithm is 12,795 mm.

5-3- An analytical method to avoid collision of mobile robot with obstacles

In this section, first, modeling relations for seeking target at open space, including kinematic model, position control, rotation control and the way to stabilize during switching control systems are offered. Then, based on this modeling, a stable non-linear controller to avoid collision of robot with obstacles ahead during motion to the target is provided. Whenever the robot senses an object near itself, the rotation angle changes in terms of tangent of the angle between the robot and that object. Afterwards, by following that obstacle, the robot takes steps to search for a path to achieve the target. At the end, simulation and application results of using this method on a robot is provided.

5-3-1- Target searching at open spaces

With this method, the robot realizes its mission through the following two tasks:

First task: reducing the distance to the target in the absence of obstacle within a half-circle with a diameter of d_{obs} ahead of the robot. In this case, to avoid the collision of the robot to the obstacles, rotation of the robot is allowed.

Second task: After leaving the obstacle, the first task is repeated in order to steadily reduce the distance to the target. Consequently, by leaving behind all the obstacles, the robot reaches to the target point. Besides, if there is a need to rotate after reaching target, doing so is possible along with maintaining its location. The block diagram in Fig. 5.5 describes the process.

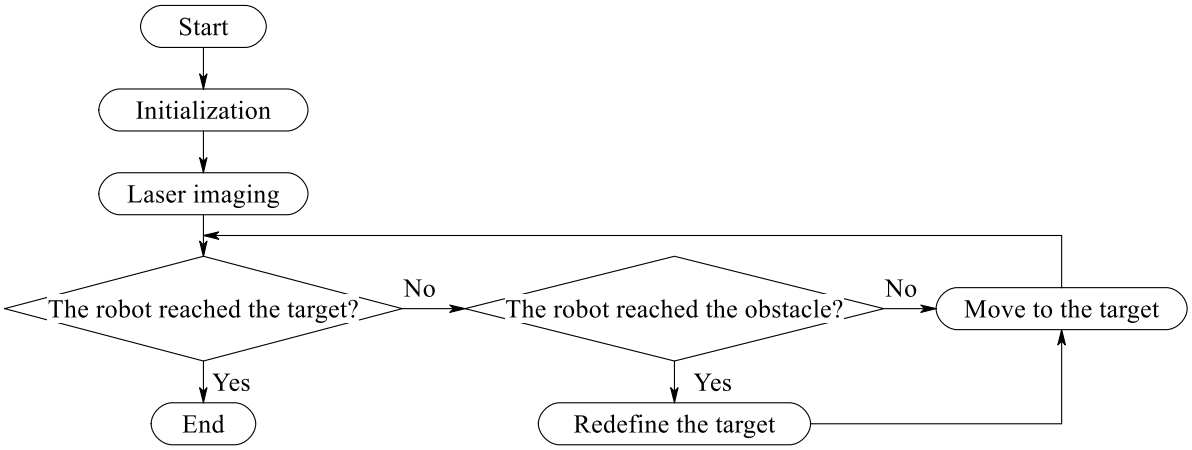

Fig. 5.5. Proposed process block diagram.calculatorca

5-3-2- Kinematic model of the robot

The differential equations dominating on the robot in the current test are as follows:

$$\begin{bmatrix} \dot{x} \\ \dot{y} \\ \dot{\psi} \end{bmatrix} = \begin{bmatrix} \cos\psi & -a\sin\psi \\ \sin\psi & a\cos\psi \\ 0 & 1 \end{bmatrix} \begin{bmatrix} u \\ \omega \end{bmatrix} \tag{5.1}$$

where, u and ω are linear and angular velocities respectively, x and y are current coordinates of the robot, ψ is deviation extent from world coordinate system $\langle O \rangle$ from axis x, and a is distance from the controllability point to the center axis connected to flywheel (Fig. 5.6).

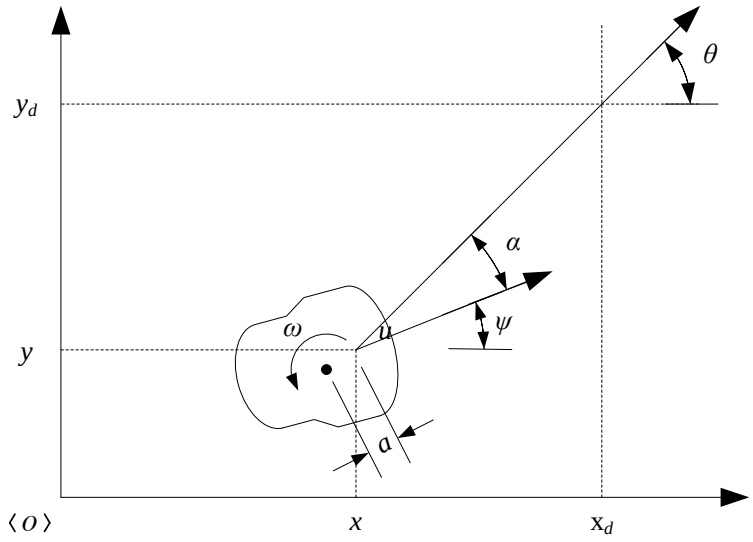

Fig. 5.6. Variables affecting the calculations of a robot moving towards the target.

The mathematical description of robot navigation towards the target in an environment with open obstacles in polar coordinates system, is presented (Secchi et al. 2001):

$$\dot{H} = \begin{bmatrix} \dot{\rho} \\ \dot{\alpha} \\ \dot{\theta} \end{bmatrix} = \begin{bmatrix} -\cos\alpha & -a\sin\alpha \\ \dfrac{\sin\alpha}{\rho} & -a\dfrac{\cos\alpha}{\rho} - 1 \\ \dfrac{\sin\alpha}{\rho} & -a\dfrac{\cos\alpha}{\rho} \end{bmatrix} \begin{bmatrix} u \\ \omega \end{bmatrix} + \begin{bmatrix} \dot{x}_d \cos\theta + \dot{y}_d \sin\theta \\ -\dot{x}_d \sin\theta + \dot{y}_d \cos\theta \\ -\dot{x}_d \sin\theta + \dot{y}_d \cos\theta \end{bmatrix} = \mathbf{Kv} \qquad (5.2)$$

where, ρ is the robot distance to the target. When the target is static (namely: $\dot{x}_d = \dot{y}_d = 0$) this relationship is summarized as:

$$\dot{H} = \mathbf{Kv} \qquad (5.3)$$

where, $\mathbf{K}$ is the first matrix in the equation (5.2), $\mathbf{v}$ is linear velocity vector, and angular velocity vector is $[u \quad \omega]^T$. It should be noted that ρ can't take zero value, because in this case, α and θ will be undefined. So with the approximation of $\rho \leq \delta$ we can assume that the robot is in the target position where it is assumed that δ*=30 mm*.

In Fig. 5.6, the target is shown with $\langle t \rangle$ and its coordinates in $< O >$ are specified by the user. The motion direction is always perpendicular to virtual axis of robot and makes angle α with position of the target. The angle α is defined as the rotation angle of the robot at the time of its placement in the target position and is obtained by the following equation:

$$\theta = \alpha + \psi \qquad (5.4)$$

5-3-3- *Position control in open space*

From Fig. 5.6 we can find out that with effective and appropriate control of values u and ω, the robot can be controlled. Control objectives in this part are $\rho \rightarrow 0$ and $\alpha \rightarrow 0$. Further, in this

section, the condition $\theta \rightarrow \theta_d$ is added to both above-mentioned conditions. So, here, the objective is making the position vector $\mathbf{H} = [\rho \quad \alpha]^T$ to approach to zero under arbitrary initial conditions. To design a controller that meets the above conditions, Lyapunov function is defined by the following equation:

$$V = \frac{1}{2}\mathbf{H}^T\mathbf{H} > 0 \tag{5.5}$$

For closed loop system stability $\mathbf{H} \rightarrow [0,0]^T$. It is necessary for the derivative of this function to be negative for all non-zero values H. By substituting equation (5.2) in the derivative of equation (5.5) we will have:

$$\dot{V} = \frac{1}{2}\dot{\mathbf{H}}^T\mathbf{K}\mathbf{v} > 0 \tag{5.6}$$

For all non-zero values **H**, it has a negative value. So the control rule will be as follows:

$$\mathbf{v} = \mathbf{K}^{-1}(\dot{\mathbf{H}}_d - \kappa \tanh \mathbf{H}) \tag{5.7}$$

Here κ is a given diagonal matrix. So with consideration of $\dot{\mathbf{H}}_d = 0$ (for static target) we have:

$$\dot{V} = -\mathbf{H}^T\kappa \tanh \mathbf{H} < 0 \tag{5.8}$$

when $\mathbf{H} \rightarrow 0$, it means that the reach of the robot to the target, in the case of absence of obstacles, is guaranteed. With arrival of the robot to the target, the values *u* and ω become zero, which means the robot remains static after reaching the target. After fulfilling the condition $\dot{\mathbf{H}}_d = 0$ in the equation (5.7), we have:

$$\begin{bmatrix} u \\ \omega \end{bmatrix} = \begin{bmatrix} u_{\max} & 0 \\ 0 & \omega_{\max} \end{bmatrix} \begin{bmatrix} \dfrac{\rho + a\cos\alpha}{a + \rho\cos\alpha} & \dfrac{a\rho\cos\alpha}{a + \rho\cos\alpha} \\ \dfrac{\sin\alpha}{a + \rho\cos\alpha} & 1 - \dfrac{a}{a + \rho\cos\alpha} \end{bmatrix} \begin{bmatrix} \tanh\rho \\ \tanh\alpha \end{bmatrix} \tag{5.9}$$

To fully assess the stability analysis, the angular behavior of θ at the time the robot reaches the target, must be investigated. With the knowledge that $\dot{\psi} = \omega$ and also, the system has asymptotic convergence, with reaching the robot to target, ω also tends to zero ($\omega \to 0$).On the other hand, when $\rho \to 0$ we will have: $tanh\,\rho / \rho \to 0$ which, subject to $t \to \infty$ it results in 0. So, $\theta = \psi$ converges to a certain amount, which indicates a good behavior of the robot to reach the target. Function tanh is used to maximize values u and ω. Amounts u_{max} and ω_{max} can be extracted from the robot's catalog.

The proposed control system for robot guidance towards obstacle-free environment is shown in Fig. 5.7. $X_d = [x_d \;\; y_d]^T$ is the target position and $X = [x \;\; y]^T$ is the current position of the robot that can be extracted from the traveled rout. Also we have:

$$\tilde{X} = [\tilde{x} \;\; \tilde{y}]^T = [(x_d - x) \;\; (y_d - y)]^T$$

where $\sqrt{\tilde{x}^2 + \tilde{y}^2} = \rho$ and $\tan^{-1}(\tilde{y} / \tilde{x}) = \theta$.

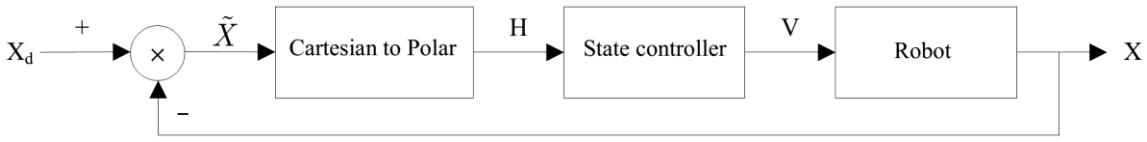

Fig. 5.7. Robot control system moving towards the target in an unobstructed environment.

5-3-4- *Rotation control at target*

Sometimes after reaching the target position, a rotation for the robot is necessary to be done. For this purpose, angle ψ should be controlled without any other action. To fulfill this mission,

an additional controller is designed in order to apply the appropriate angular velocity (ω) to the robot while its linear velocity (u) is still zero. For example, in Fig. 5 - 6, $\theta = \psi_d$. So, $\alpha = \psi_d - \psi = \tilde{\psi}$ is the final rotation error. So for a constant final rotation, we have $\dot{\alpha} = -\dot{\psi} = \dot{\tilde{\psi}}$ is constant. In such a case, Lyapunov function can be assumed as follows:

$$V(\alpha) = \frac{1}{2}\alpha^2 \tag{5.10}$$

where its first derivation in terms of time is as follows:

$$\dot{V}(\alpha) = \alpha\dot{\alpha} = \tilde{\psi}\left(-\omega + u\frac{\sin\tilde{\psi}}{\rho} - a\omega\frac{\cos\tilde{\psi}}{\rho}\right) \tag{5.11}$$

Assuming that:

$$\begin{cases} u = 0 \\ \omega = \omega_{\max}\tanh\tilde{\psi} \quad (\omega_{\max} > 0) \end{cases} \tag{5.12}$$

and recalling that we are at target position ($\rho \le \delta$) the following formula is obtained:

$$\dot{V}(\alpha) = -\omega_{\max}\tilde{\psi}\tanh\psi\left(1 + \frac{u}{\delta}\cos\tilde{\psi}\right) \tag{5.13}$$

This expression is definite negative with the condition $|\tilde{\psi}| < \pi/2$. Consequently, the rotation error ($\tilde{\psi}$) approaches asymptotically to zero, which means ψ tends to ψ_d.

5-3-5- Stability in switching control system

Afterwards, after reaching the target, the robot should place itself in a good final condition by rotating. So, switching from positional controller to situational controller is very necessary to reach to a suitable situation with regard to robot placement direction. In such a case, stability of control system must be assured during switching the controller. This can be done with Lyapunov's theorem expansion (Vidyasagar 2002). Since leading studies have suggested that Lyapunov's functions are the same, this condition is well established by itself and stability is guaranteed during switching from positional controller to situational controller.

5-3-6- Suggested method

In this section, a nonlinear controller with the objective to guide the robot without hitting the obstacles is introduced. A strategy has resulted in selection of a tangential direction on obstacles' border. This strategy is very similar to robot guidance in unknown environments.

The controller uses proposed methods in previous section to reduce the length of the robot path to the target. Before reaching the distance d_{obs} from the obstacle, the robot redefines the target position permanently and moves toward it. But, once the robot reaches the distance d_{obs} which is shown in Fig. 5.8, runs evasive maneuver.

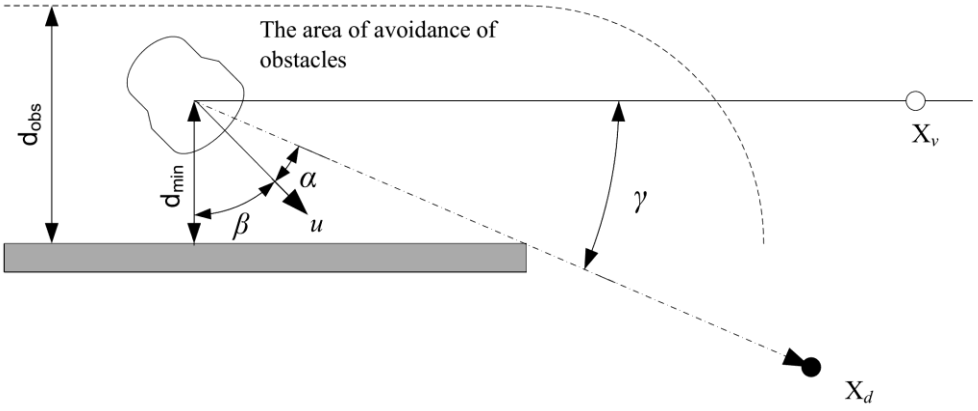

Fig. 5.8. Tangential escape strategy function near an obstacle.

As shown in Fig. 5.8, if the robot encounters an obstacle (in this case $d_{min} \le d_{obs}$) hypothetical target ($\mathbf{X}_v$) is obtained by applying a rotation matrix to actual position of the target ($\mathbf{X}_d$). It should be noted that the line connecting controlled points and virtual target is tangent on the perimeter.

Angle of rotation γ which identifies rotation matrix, can be quantified using a set of measurements of range-meter sensors. Recognizing β, which determines the location of the nearest obstacle, is necessary to define γ. After each time of calculating range, the proposed system specifies the distance d with the condition of $d \le d_{obs}$ and the angle β corresponding to it. These used range-meter sensors cover the range [0° 180°] with 1° steps. Also, we can cover interval [-90° +90°] with the range of 180°. Given this, if the obstacle is located on the right side of the robot, $\beta < 0$ and otherwise, $\beta > 0$. Given β, we have:

$$\gamma = \begin{cases} -90° + \beta - \alpha & \text{if } \beta \ge 0 \\ +90° + \beta - \alpha & \text{if } \beta < 0 \end{cases} \tag{5.14}$$

when $\alpha > 0$ it means the target is on the right side of robot axis movement. In Fig. 5.8 the angle γ has positive value and will result in the rotation of actual target towards the left side.

Given angle γ, hypothetical and real target positions can be related to each other as follows:

$$\mathbf{X}_v = \begin{bmatrix} \cos\gamma & -\sin\gamma \\ \sin\gamma & \cos\gamma \end{bmatrix} \mathbf{X}_d \tag{5.15}$$

where, $\mathbf{X}_d$ and $\mathbf{X}_v$ show the position of the virtual and real targets. Positional controller, having coordinates $\mathbf{X}_v$ follows the obstacle's border in tangential manner and guides the robot

towards the target. It is worth noting that in case of nonexistent obstacles, no change will be occurred in the actual target location ($\gamma = 0°$) and the robot steadily approaches the target.

The block diagram of proposed controller is shown in Fig. 5.9. By observing this diagram, we can find that the situational controller block is always active. This means that the robot does not stop to avoid obstacles. Based on this graph, and in order to stabilize situational controller asymptotically, after leaving behind all the obstacles, and in the case of accessing the target, the robot reaches to it. Later, I will proceed to discuss tangential escape strategy in dealing with different types of obstacles.

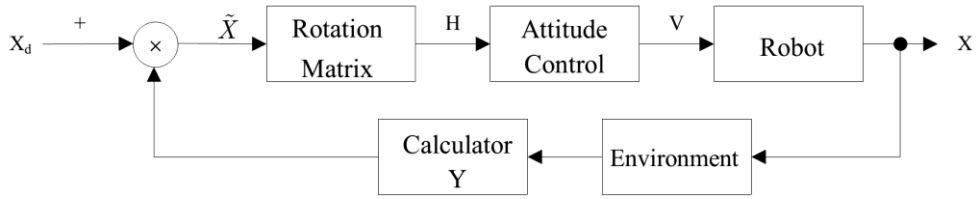

Fig. 5.9. Block diagram of a control system based on tangential scape strategy.

5-3-6-1- Facing corner-shaped obstacles

Sometimes the robot encounters with some situations, which requires more aggressive maneuvers to overcome obstacles. One of these situations is encountering obstacles *V*, *L* and *U*-Shaped. Fig. 5.10 shows a status in which the target is located under the horizontal part of an *L*-shaped obstacle.

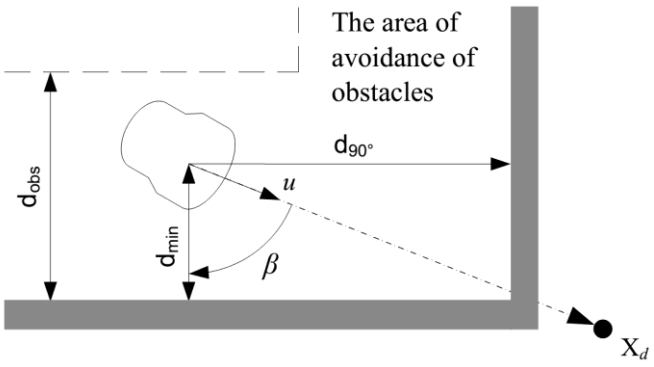

Fig. 10.5. Changing the tangential escape strategy due to confrontation with the corner-shaped obstacle (L).

In this case, the angle γ, which is defined in equation (5.14), does not provide the guarantees necessary to avoid the robot from obstacle. In fact, the robot is faced with vertical part of the obstacle and continues rotating around it. To speed up this operation, the amount γ when the distance d_{90} and d_{min} is less than d_{obs}, is corrected as follows:

$$\gamma = \begin{cases} -180° + \beta - \alpha & \text{if } \beta \geq 0 \\ +180° + \beta - \alpha & \text{if } \beta < 0 \end{cases} \tag{5.16}$$

In addition, the robot, at the same time as a massive maneuver, needs to change the definition of the virtual target to minimize the risk of collisions with obstacles during the escape maneuver. This goal is achieved by reducing the amount of *u*. A solution to reduce *u* is to reduce the amount $\rho = \|\mathbf{X}_v - \mathbf{X}\|^{1/2}$ in the escape operation. It is therefore suggested;

$$\mathbf{X}_v = \begin{bmatrix} \cos\gamma & -\sin\gamma \\ \sin\gamma & \cos\gamma \end{bmatrix} \begin{bmatrix} d_{\min}\cos\theta \\ d_{\min}\sin\theta \end{bmatrix} \tag{5.17}$$

In this way, the robot begins with a lower linear velocity, reducing the risk of collisions with obstacles during escape operations.

5-3-6-2- Facing concave obstacles

Another special situation requiring a special and separate review is when the rotation of the robot is inappropriate for the target. An appropriate example of this situation occurs when the robot has followed the side of the U-shaped obstacle (as shown in Fig. 5.11 with the darker field). The robot runs straight to the target from the front of the field and enters the U-shaped obstacle. By reaching the depth of the obstacle, the boundary is followed by the robot. By approaching the upper U-shaped obstacle, the robot reverses to the left, based on equations

(5.15) and (5.17), and goes to the darker position. In this situation, the rotation error of α represents the rotation fault of the robot relative to the target.

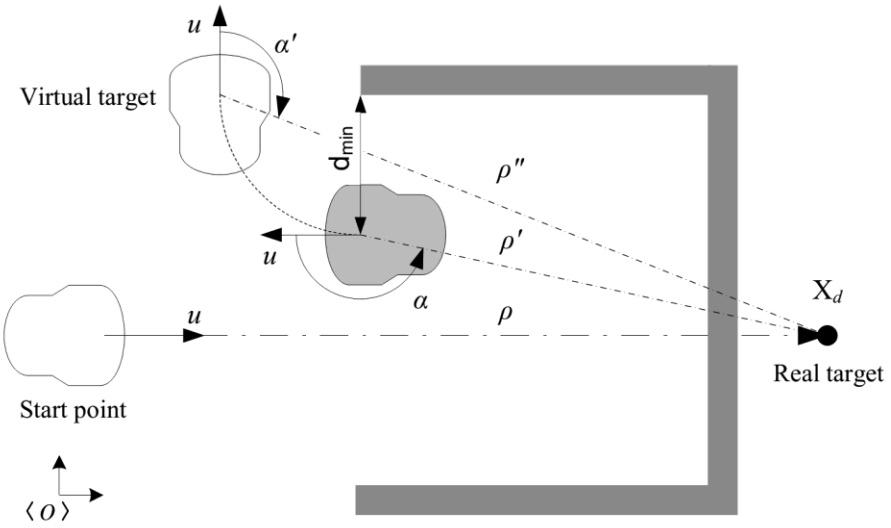

Fig. 5.11. 90-degree rotation of the robot for passing U-shaped obstacles.

After breaking the obstacle, the robot moves to the left to continue moving towards the real target, and gets stuck in the U-shaped obstacle, which is a local minimum. To get rid of these types of local minima, it is necessary to introduce a new sentence (P_{obs}). After a re-search, if there is at least one obstacle less than d_{obs}, the P_{obs} sentence will take one and otherwise it will be zeroed. By placing the robot in the position of tracking the obstacle boundary, there will be at least a distance of less than the d_{obs} to the end of the task. So, there is no change in the P_{obs} value until the end of the operation. After passing the obstacle and preventing getting stuck, the robot follows a path design algorithm in anonymous environments including the walls. After each change in the value of P_{obs}, the value $|\alpha|$ is also reviewed. If, as in Fig. 5.11, this parameter is greater than 90, the robot performs maneuvering for a path that is indicated by a dash- line in this figure. In this case, a virtual target is created and a tangential scape strategy is used to direct the robot towards the target. The new virtual purpose $[x_{tg} \quad y_{tg}]^T$ is defined by the following relationship:

$$\begin{bmatrix} x_{tg} \\ y_{tg} \end{bmatrix} = \begin{cases} \begin{bmatrix} x \\ y \end{bmatrix} + d_{\min} \begin{bmatrix} -\sin\psi & \cos\psi \\ \cos\psi & \sin\psi \end{bmatrix} \begin{bmatrix} 1 \\ 1 \end{bmatrix} & \text{if } \beta \geq 0 \\ \begin{bmatrix} x \\ y \end{bmatrix} + d_{\min} \begin{bmatrix} \sin\psi & \cos\psi \\ -\cos\psi & \sin\psi \end{bmatrix} \begin{bmatrix} 1 \\ 1 \end{bmatrix} & \text{if } \beta < 0 \end{cases} \tag{5.18}$$

In these relationships, $\mathbf{X} = [x \quad y]^{\mathrm{T}}$ refers to the current position of the robot in the null coordinate system, ψ to the current rotational orientation, $d_{\min}$ to the minimum distance from the robot to the precursor before resetting P_{obs}, and β to the corresponding angle with $d_{\min}$. After that, the robot uses the position control to search for the virtual target. If the obstacle appears in the pursuit of the virtual target, the virtual target is abandoned and the real purpose is taken into consideration. Otherwise, the angular position of the robot will be corrected by reaching the virtual target and will be in the bright gray position of Fig. 5.11. This is accomplished with the help of the attitude controller (described above). The optimal rotation angle is measured using the following relationship:

$$\psi_{tg} = \begin{cases} \psi - 90^{\circ} & \text{if } \beta \geq 0 \\ \psi + 90^{\circ} & \text{if } \beta < 0 \end{cases} \tag{5.19}$$

In this equation, ψ is the rotation of the robot just before resetting P_{obs}. After this rotation, the robot is placed in the virtual target location.

5-3-6-3- Using the stored information of the observed obstacles

Occasionally, the robot may find a situation in the workplace that it has already been trying to prevent while searching for the target. In this case, the obstacle will be checked for the second time by the robot, which means the robot enters an infinite loop and its inability to find the target.

The proposed controller utilizes an intermediate memory to store obstacle enclosures (that is, when the P_{obs} changes from zero to 1). In this regard, an arbitrary time interval (for example, 100 milliseconds) is selected as the reference time interval and places stored in memory, at the end of each interval, are compared to the current location of the robot. If no match is seen (or the memory is empty), the robot will continue to move continuously. In the case of a match, the robot rotates to find a path in the opposite direction of one and a half round (using the rotational controller), and then puts this point in its mid-term memory and re-moves. But if there are two matches, there is no way to reach the target.

5-3-6-4- Simulation and laboratory results

In order to validate the proposed method, several real experiments and simulations were carried out using the control system discussed, the results of which are presented in this section. The experiments were performed on a Pioneer 3D-DX robot (Fig. 5.12).

Fig. 5.12. Pioneer 3D-DX robot.

The robot is equipped with a Sick LMS100 laser search engine (installed by the manufacturer). At each turn, 181 distances (collectively, a semicircle) are measured by this search engine (Fig. 5.13). The laser scrolling angle is 1 degree and the sampling rate is 10 Hz (similar to other control systems of the lower level robots).

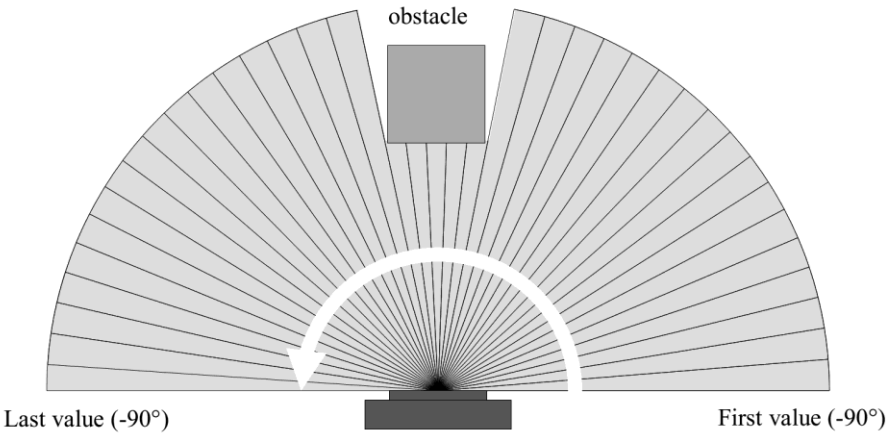

Fig. 5.13. How to record a range in the Sick LMS100 laser search engine in a semicircle.

In Fig. 5.14, a zigzag obstacle is tested and the robot path towards the target is shown. In this simulation, the robot examines six obstacles that are not scanned more than once.

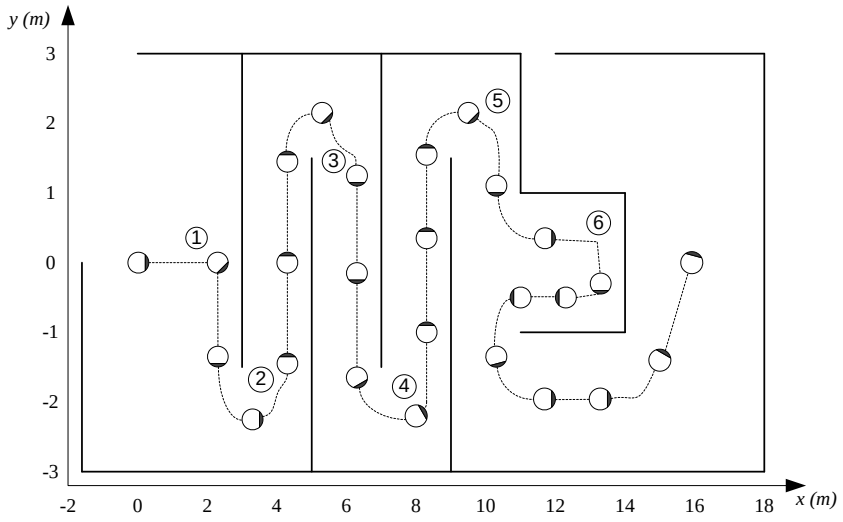

Fig. 5.14. The result of the implementation of a tangential escape algorithm in the zigzag environment.

In Figs. 5.15 and 5.16, black circles show positions that the robot has passed several times. By retrieving these points, the robot changes the direction of movement in the opposite direction by using the angular position controller. In the first figure, this maneuver is performed at two points with coordinates (2/5,2) and (5/5,2) (in the second, at a point with coordinates (1/5,0). It is clear that the proposed strategy can successfully bring the robot to its target.

In the following, four other tests are introduced. In the first test, reaching the target behind the U-shaped obstacle using the proposed algorithm is shown in Fig. 5.17. Position error, angular

position error, and rotation of the robot are shown in Fig. 5.18 to Fig. 5.20. The control signals u and ω are shown in Figs. 5. 21 and 5. 22.

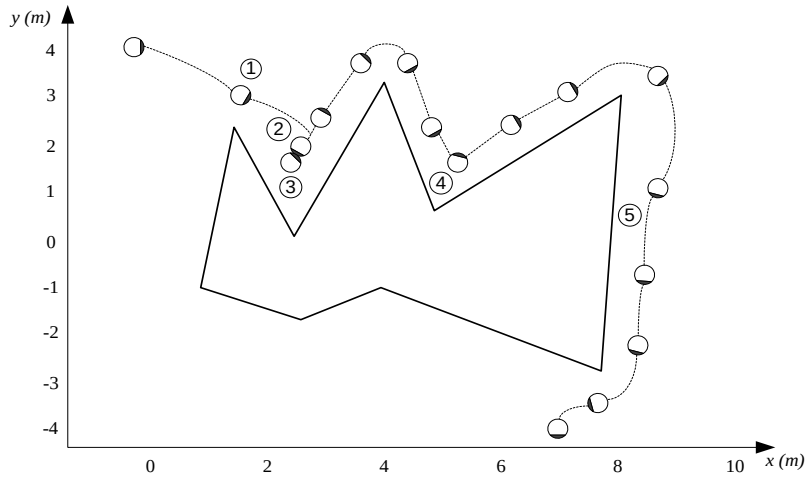

Fig. 5.15. The result of the implementation of a tangential escape algorithm in an environment with uneven convex and concave obstacles.

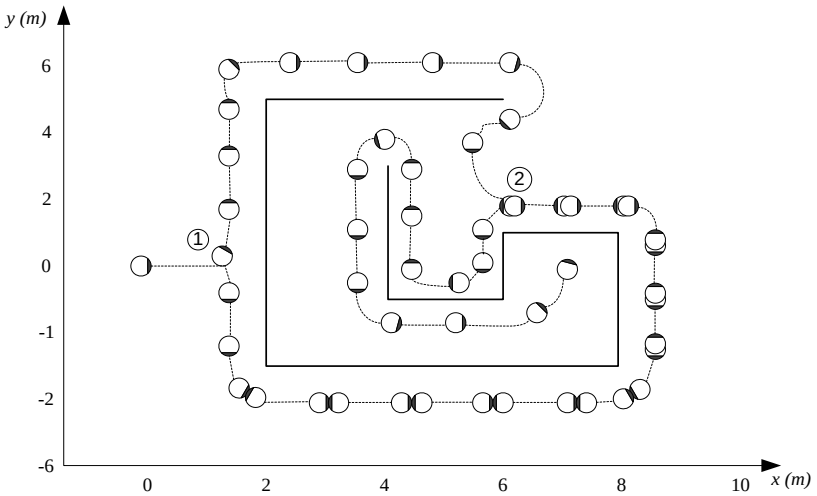

Fig. 5.16. The result of the implementation of the tangential escape algorithm in the sample environment.

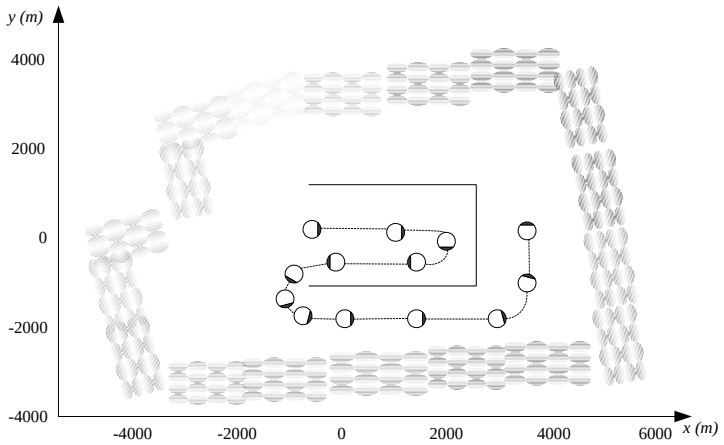

Fig. 5.17. The result of the implementation of a tangential escape algorithm in a U-shaped obstacle.

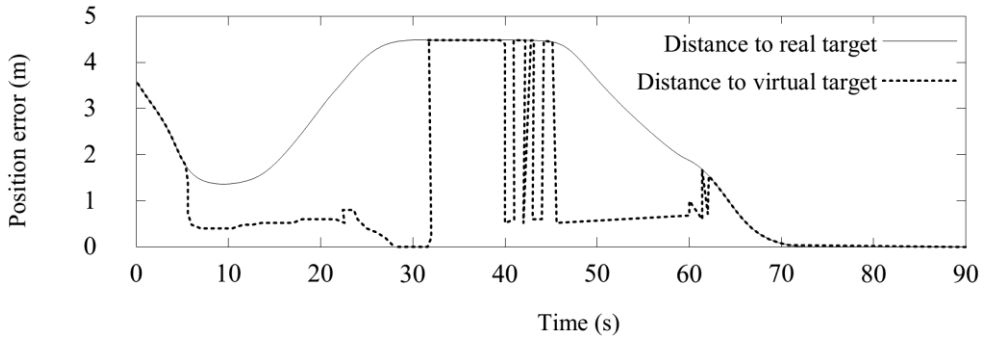

Fig. 5.18. Time position error for simulation in a U-shaped obstacle.

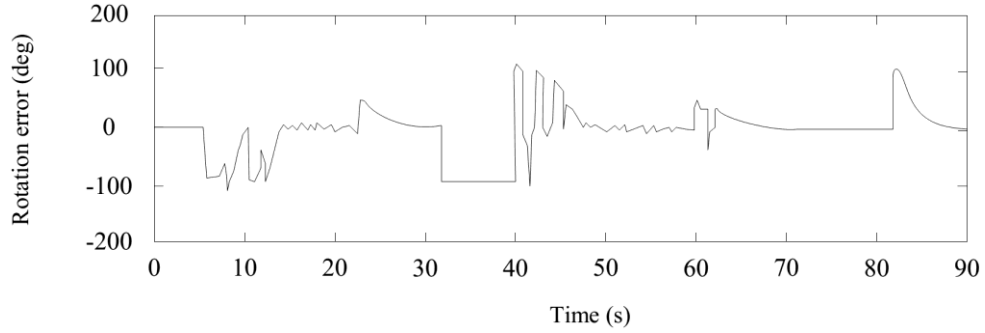

Fig. 5.19. Rotation error for simulation in a U-shaped obstacle.

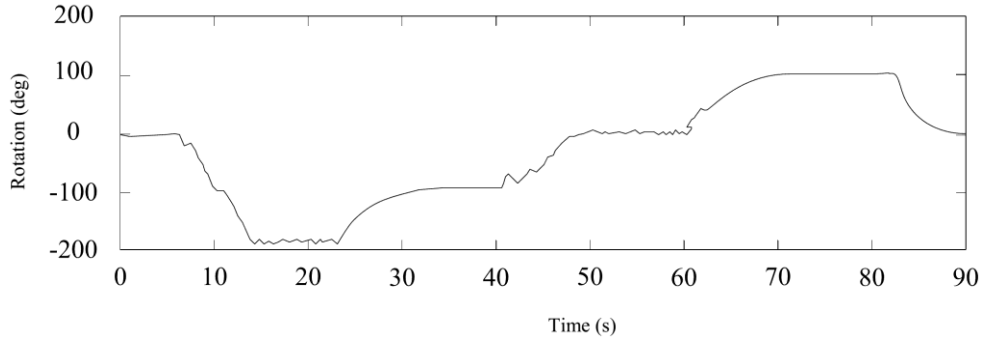

Fig. 5.20. Rotation angle in terms of time for simulation in a U-shaped obstacle.

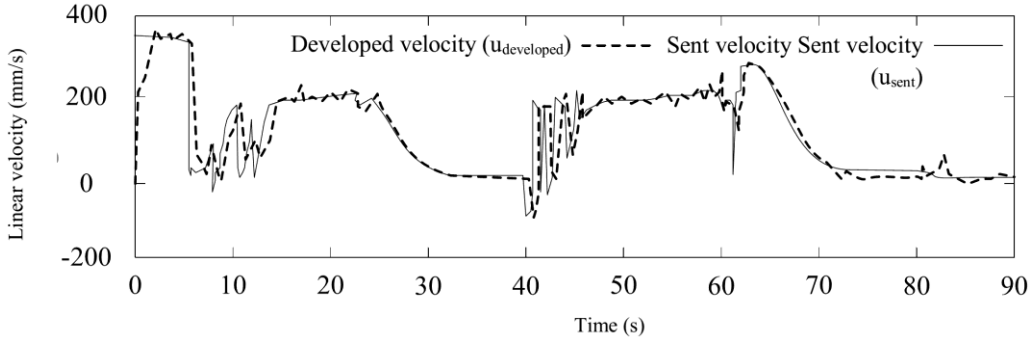

Fig. 5.21. Linear velocity in terms of time for simulation in a U-shaped obstacle.

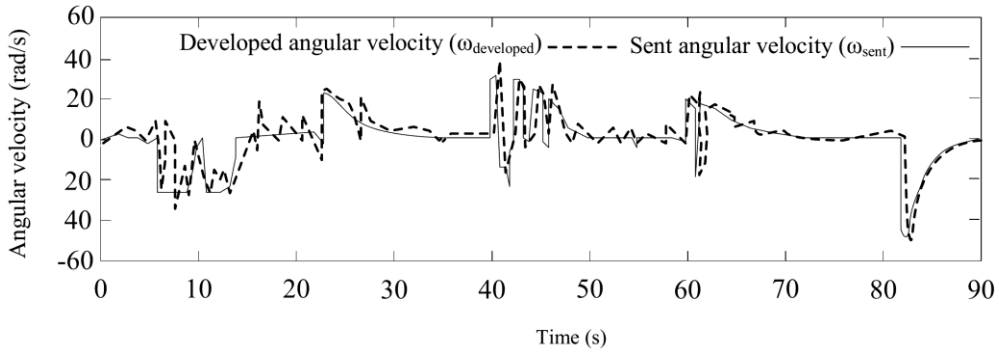

Fig. 5.22. angular velocity in terms of time for simulation in a U-shaped obstacle.

The routes traversed by the robot in the course of the three other experiments are shown in Fig. 5.23 to Fig. 5.25. The first case involves a Z-shaped obstacle, within which there are a number of other obstacles. The second and third experiments are related to obstacles with L and V shapes. The results indicate that the tangential escape route is efficient in directing the robot towards the target and avoiding the obstacles.

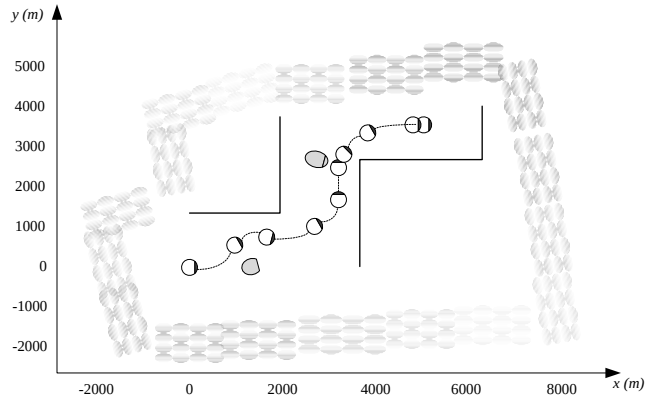

Fig. 5.23. Tangential escape algorithm implemented in an environment with a Z-shaped obstacle.

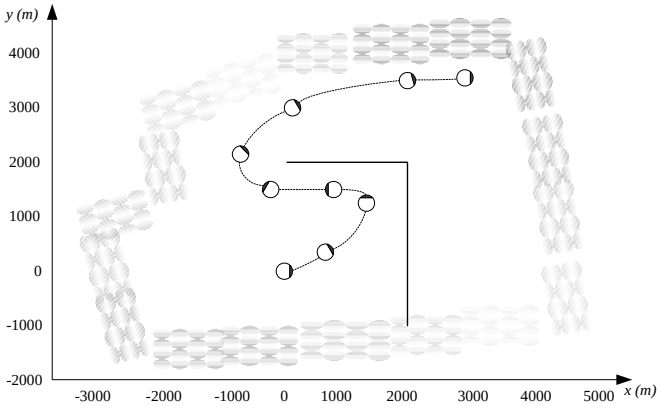

Fig. 5.24. Tangential escape algorithm implemented in an environment with a L-shaped obstacle.

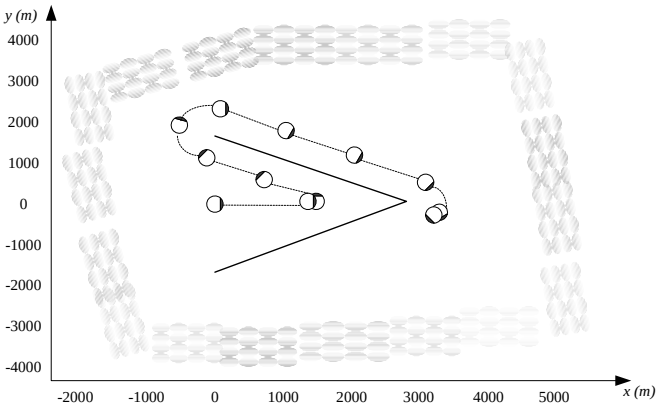

Fig. 5.25. Tangential escape algorithm implemented in an environment with a V-shaped obstacle.

5-4- Path planning regarding absence of danger space

This section discusses path-planning in a classic environment (including three types of spaces: e.g. obstacle, free and target) with four methods of:

- Synthetic potential field (Takagi-Sugeno)
- Linguistic method (Mamdani synthetic potential field)
- Markov decision-making processes
- Fuzzy Markov decision-making processes

These methods are described in follow.

5-4-1- Synthetic potential field (Takagi-Sugeno) method

5-4-1-1- Governing equations

A pair of electrical charges exert a force on each other as follows (Equation (5.20)) (Cheng 1989):

$$\vec{F} = k \frac{q_1 q_2}{|r|^2} \vec{e}_r \tag{5.20}$$

In this equation k is a constant, q_1 and q_2 are electrical charges, r is the distance between them, and $\vec{e}_r$ is the unit vector connecting the two. It is supposed that robot and obstacles carry

negative charges, while the target has a positive one. As the result, obstacles repulse and the target point attracts the robot. From electrostatic laws, it is concluded that one positive and N negatives charges exert a force to a negative charge calculated from (5.21):

$$\vec{F} = \vec{F}_a + \sum_{k=1}^{N} \vec{F}_d(k) \tag{5.21}$$

where, F_a and F_d are attraction and repulsion forces respectively, while k represents the number of obstacles. By confining each cell of meshed space to just a type of spaces, (5.21) is rewritten as (5.22).

$$\vec{F} = \vec{F}_a + \sum_{k=1}^{N} \vec{F}_d(i, j) \tag{5.22}$$

For that (i,j) outlines the position toward other cells; as $k = nj + i$ and n show the number of cells in a row. Forces F_a and F_d are calculable from vector decomposition along main axes of x and y as below:

$$\vec{F}_a = F_{ax}\mathbf{i} + F_{ay}\mathbf{j} \tag{5.23}$$

$$\vec{F}_d(i, j) = F_{dx}(i, j)\mathbf{i} + F_{dy}(i, j)\mathbf{j} \tag{5.24}$$

The respective components are as below:

$$F_{ax} = \vec{F}_a \cdot \frac{\vec{x}_{goal}}{|r_{goal}|} \tag{5.25}$$

$$F_{ay} = \vec{F}_a \cdot \frac{\vec{y}_{goal}}{|r_{goal}|} \tag{5.26}$$

$$F_{dx}(i, j) = \vec{F}_d(i, j) \cdot \frac{\vec{x}(i, j)}{|r(i, j)|} \tag{5.27}$$

$$F_{dy}(i, j) = \vec{F}_d(i, j) \cdot \frac{\vec{y}(i, j)}{|r(i, j)|} \tag{5.28}$$

By inserting (5.25) and (5.26) into (5.23), and (5.27), (5.28) into (5.25) we have:

$$\vec{F}_a = \vec{F}_a \cdot \frac{\vec{x}_{goal}}{\left|r_{goal}\right|}\mathbf{i} + \vec{F}_a \cdot \frac{\vec{y}_{goal}}{\left|r_{goal}\right|}\mathbf{j} \tag{5.29}$$

$$\vec{F}_d(i,j) = \vec{F}_d(i,j) \cdot \frac{\vec{x}_{goal}}{\left|r_{goal}\right|}\mathbf{i} + \vec{F}_d(i,j) \cdot \frac{\vec{y}_{goal}}{\left|r_{goal}\right|}\mathbf{j} \tag{5.30}$$

These two, change (5.21) into:

$$\vec{F} = \vec{F}_x + \vec{F}_y \tag{5.31}$$

where:

$$\begin{aligned} \vec{F}_x &= \left(\vec{F}_a \cdot \frac{\vec{x}_{goal}}{\left|r_{goal}\right|} + \sum_{k=1}^{N} \vec{F}_d(i,j) \cdot \frac{\vec{x}(i,j)}{\left|r(i,j)\right|} \right)\mathbf{i} \\ \vec{F}_y &= \left(\vec{F}_a \cdot \frac{\vec{y}_{goal}}{\left|r_{goal}\right|} + \sum_{k=1}^{N} \vec{F}_d(i,j) \cdot \frac{\vec{y}(i,j)}{\left|r(i,j)\right|} \right)\mathbf{j} \end{aligned} \tag{5.32}$$

As the obstacles are all the same (attributed as obstacle space), equation (5.20) can be rewritten for obstacles as:

$$\vec{F}_d(i,j) = -k_d \frac{1}{\left|r(i,j)\right|^2}\vec{e}_r \tag{5.33}$$

Considering the target point, it is possible to rewrite attraction formula as below:

$$\vec{F}_a = k_a \frac{1}{\left|r_{goal}\right|^2}\vec{e}_r \tag{5.34}$$

Inserting (5.33) and (5.34) into (5.32) yields:

$$\begin{aligned} \vec{F}_x &= \left(k_a \cdot \frac{\vec{x}_{goal}}{\left|r_{goal}\right|^3} - k_d \sum_{k=1}^{N} \frac{\vec{x}(i,j)}{\left|r(i,j)\right|^3} \right)\mathbf{i} \\ \vec{F}_y &= \left(k_a \cdot \frac{\vec{y}_{goal}}{\left|r_{goal}\right|^3} - k_d \sum_{k=1}^{N} \frac{\vec{y}(i,j)}{\left|r(i,j)\right|^3} \right)\mathbf{j} \end{aligned} \tag{5.35}$$

Each cell (except the target point) can share obstacle and free spaces beside some uncertainty. So, to fuzzify these relations, the magnitude of repulsive force is multiplied to membership function of obstacle space (μ). Thus, we have:

$$\vec{F}_x = \left(k_a \cdot \frac{\vec{x}_{goal}}{\left|r_{goal}\right|^3} - \mu k_d \sum_{k=1}^{N} \frac{\vec{x}(i,j)}{\left|r(i,j)\right|^3} \right) \mathbf{i}$$
$$\vec{F}_y = \left(k_a \cdot \frac{\vec{y}_{goal}}{\left|r_{goal}\right|^3} - \mu k_d \sum_{k=1}^{N} \frac{\vec{y}(i,j)}{\left|r(i,j)\right|^3} \right) \mathbf{j} \qquad (5.36)$$

To reach the target, the robot must adhere to the direction of force in the field. In other words, its angle must be:

$$\phi = \arctan 2(\vec{F}_y, \vec{F}_x) \qquad (5.37)$$

where, $\vec{F}_x$ and" defined as below:arctan2are from (5.36) and function " $\vec{F}_y$

$$\arctan 2(x,y) = \begin{cases} \arctan(y/x) & x > 0 \\ \arctan(y/x) + \pi & y \geq 0 \ ; \ x < 0 \\ \arctan(y/x) - \pi & y < 0 \ ; \ x < 0 \\ \pi/2 & y > 0 \ ; \ x = 0 \\ -\pi/2 & y < 0 \ ; \ x = 0 \\ \text{undefined} & y = 0 \ ; \ x = 0 \end{cases} \qquad (5.38)$$

5-4-1-2- The rectifier

In close proximity of target point, denominator of fractions in (5.36) tend to zero and accordingly, attraction takes large magnitudes. This phenomenon results in ineffectiveness of repulsive force from obstacles. To overcome this liability, it is proposed to add integer 1 to the denominator of relevant fraction.

$$\phi = \tan^{-1} 2\left(\begin{array}{l} k_a \cdot \dfrac{\vec{y}_{goal}}{\left|r_{goal}\right|^3 + 1} - \mu k_d \sum_{k=1}^{N} \dfrac{\vec{y}(i,j)}{\left|r(i,j)\right|^3}, \\ k_a \cdot \dfrac{\vec{x}_{goal}}{\left|r_{goal}\right|^3 + 1} - \mu k_d \sum_{k=1}^{N} \dfrac{\vec{x}(i,j)}{\left|r(i,j)\right|^3} \end{array} \right) \tag{5.39}$$

Figure 5.26 shows effect of this change.

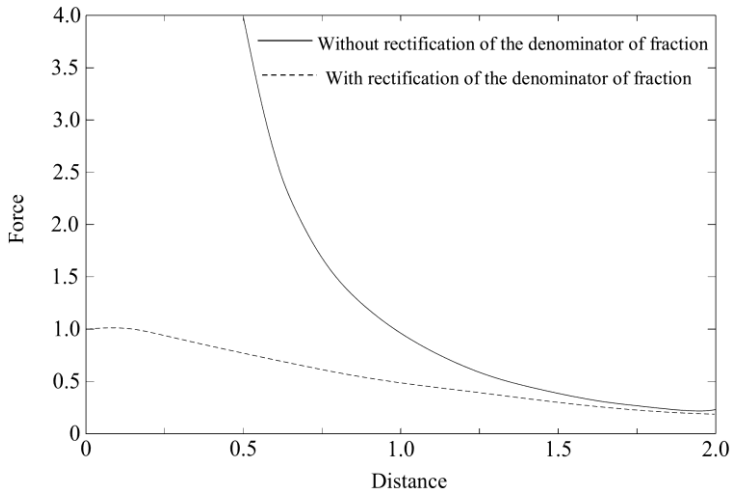

Fig. 5.26. Attraction force with and without rectifier.

5-4-1-3- Implementation

To test and evaluate the proposed method, a NAO humanoid robot from French company of Aldebaran is used (Robotics 2012). The results are presented in Fig. 5.27.

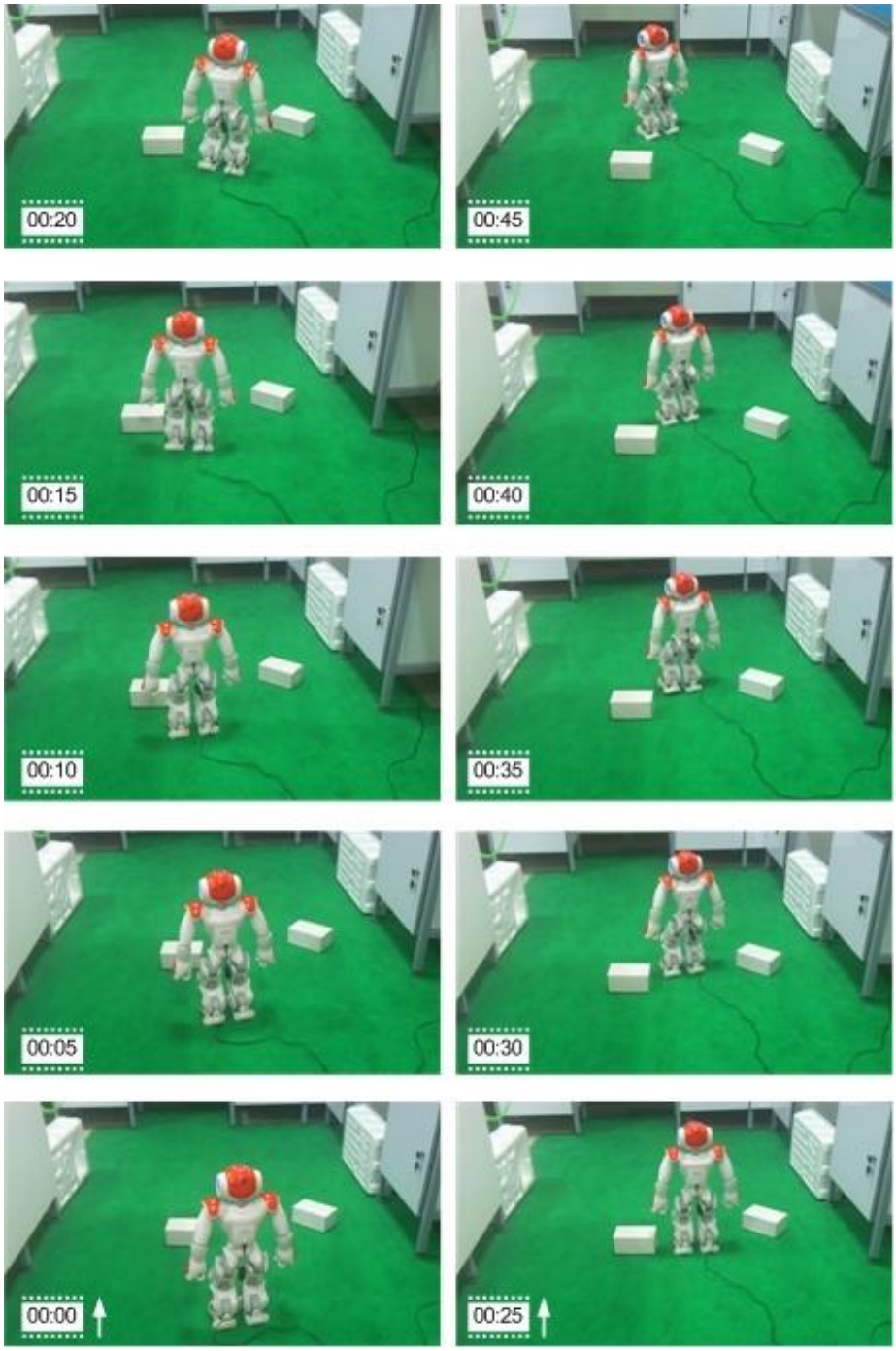

Fig. 5.27. Path surveyed by NAO humanoid robot using fuzzy synthetic potential field (Takagi-Sugeno).

5-4-2- Linguistic method (Mamdani synthetic potential field)

While linguistic method has a root in natural potential field, it tries to compute the field by language rules, instead of deterministic relations.

5-4-2-1- Fuzzy rules

The intensity of natural potential force is proportional with distance square. Also, the intensity of synthetic potential field must be a descending function of distance. Regarding dimensions of NAO and the height of its camera, its image is divided into 25 cells. Tables 5.1 and 5.2 summarize rules for calculating forces from obstacles and the target point. The variables are positive (P), zero (Z), very (V), medium (M) and Big (B).

Table 5.1. Mamdani rules for the force from obstacles in axes of *x* and *y*.

	Axis *x*					**Axis** *y*				
j \ *i*	1	2	3	4	5	1	2	3	4	5
1	VSN	VSN	Z	VSP	VSP	VSP	VSP	VSN	VSN	VSN
2	VSN	VSN	Z	VSP	VSP	VSN	SN	SN	SN	VSN
3	SP	SN	Z	SP	SP	SN	MN	MN	MN	SN
4	MN	MN	Z	MP	MP	MN	BN	VBN	BN	MN
5	BN	VBN	Z	VBP	BP	MN	VBN	VBN	VBN	MN

Table 5.2. Mamdani rules for the force from target point in axes of *x* and *y*.

	Axis *x*					**Axis** *y*				
j \ *i*	1	2	3	4	5	1	2	3	4	5
1	VSP	VSP	Z	VSN	VSN	VSP	VSP	VSP	VSP	VSP
2	VSP	VSP	Z	VSN	VSN	VSP	SP	SP	SP	VSP
3	SP	SP	Z	SN	SN	SP	MP	MP	MP	SP
4	MP	MP	Z	MN	MN	MP	BP	VBP	BP	MP
5	BP	VBP	Z	VBN	BN	MP	VBP	VBP	VBP	BP

5-4-2-2- Sub-target

When the target is seen by the robot, a (real or limit) non-zero magnitude is assigned (through membership function fuzzification) to cells containing the target point. This obviously attracts robot to the target. On the other hand, if robot fails to view the target, it receives a virtual repulsive force and gives up to approach the target. To overcome this problem, a virtual target is assumed to be there in nearest cell to the main target (5.28).

5-4-2-3- Defuzzification

Regarding *n* and *m*, there are totally 4*nm* fuzzy rules (here, 100) that determine the level of output. In natural potential field, the force exerted on a charged body is the sum of every single force issued by other charged bodies (superposition principle). As a guide, it can be repeated for synthetic potential field, too. In this method, superposition is equivalent to weighted average defuzzification that is defined as below:

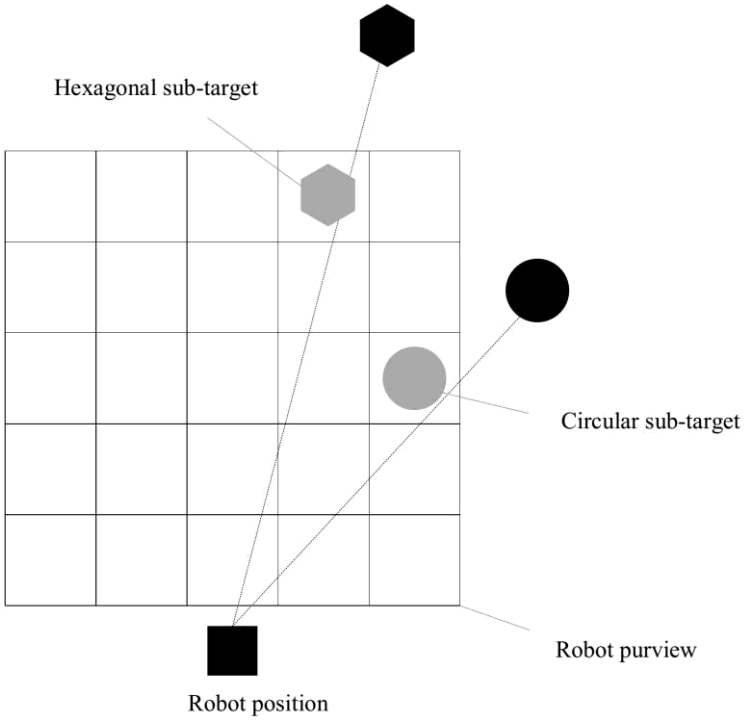

Fig. 5.28. Positions of robot and sub-targets in purview of robot.

$$f_x = \frac{\sum_{i=1}^{N} P_{\text{obstacle}}^{i} \hat{f}_{rx}^{i} + P_{\text{target}}^{i} \hat{f}_{ax}^{i}}{\sum_{i=1}^{N} P_{\text{obstacle}}^{i} + P_{\text{target}}^{i}} \tag{40.5}$$

$$f_y = \frac{\sum_{i=1}^{N} P_{\text{obstacle}}^{i} \hat{f}_{ry}^{i} + P_{\text{target}}^{i} \hat{f}_{ay}^{i}}{\sum_{i=1}^{N} P_{\text{obstacle}}^{i} + P_{\text{target}}^{i}} \tag{41.5}$$

where, P_{obstacle}^{i} is the probability of obstacle presence, P_{target}^{i} is the probability of target presence, and f_x and f_y are respectively force components along *x* and *y* axes.

5-4-2-4- Simplification

In the proposed method, robot moves in the direction of field and therefore, knowing a mere direction suffices. As in (5.40) and (5.41) denominators of fractions are the same, it is possible to multiply both equations into the common denominator to simplify them without changing directions of forces.

$$f'_x = \sum_{i=1}^{N} P^i_{\text{obstacle}} \hat{f}^i_{rx} + P^i_{\text{target}} \hat{f}^i_{ax} \tag{5.42}$$

$$f'_y = \sum_{i=1}^{N} P^i_{\text{obstacle}} \hat{f}^i_{ry} + P^i_{\text{target}} \hat{f}^i_{ay} \tag{5.43}$$

It is possible to determine direction of force with the following formula:

$$\phi = \arctan 2(f'_y, f'_x) \tag{5.44}$$

in which function “arctan2” is the same as (5.38). Figure 5.29 shows the results of testing this method.

Fig. 5.29. Path surveyed by NAO humanoid robot with linguistic method (Mamdani synthetic potential field).

5-4-3- Markov decision-making processes

Andrey Markov presented a mathematical framework for decision-making modeling in situations that the outcomes are to some extend random and out of control. Markov decision-making processes are generalized forms of Markov chains which choices and rewards are added to. In other words, Markov decision-making processes are discrete-time stochastic

control processes. Thus, in each time-step process has the state s and the decision-maker chooses form possible actions. The process then, randomly moves to the next state s' and reward *R* is given to the decision-maker. Therefore, the probability of which a process goes to a certain state is a function of the chosen action. This means that state s' depends on state *s* and action of the decision-maker a, while a and s are independent from all former actions and states. In other words, moving from a state to another in Markov decision-making processes has Markov property (Hu and Yue 2007; Kolobov 2012; Puterman 2014; Sheskin 2016).

The main problem in Markov decision-making processes is finding a policy for. Policy is the function with output of action π done by the decision-maker in state s. The goal is to find the policy which by the cumulative magnitude (discrete) rewards is maximum.

Value function represents the magnitude of expected rewards which a system receives by working from state *s* and following the policy. Therefore, each policy leads to a value function. Thus:

$$V^{\pi}(s_0) = E\left[R(s_0) + \gamma R(s_1) + \gamma^2 R(s_2) + \cdots | \pi \right] = E\left[\sum_{t=0}^{N} \gamma^t R(s_t) | \pi \right] \tag{5.45}$$

The equation can be rewritten as below:

$$V^{\pi}(s_0) = E\left[R(s_0) + \gamma \left(R(s_1) + \gamma R(s_2) + \cdots \right) | \pi \right] \tag{5.46}$$

Equation (5.46) is named after Bellman and is abbreviated to:

$$V^{\pi}(s) = E\left[R(s) + \gamma \sum_{s'} P(s,a,s') V^{\pi}(s') \right] \tag{5.47}$$

By showing optimum policy and optimum value function with π^* and V^*, respectively, we have:

$$V^*(s) = R(s) + \max_a \gamma \sum_{s'} P(s,a,s') V^*(s') \tag{5.48}$$

$$\pi^*(s) = \arg\max_a \sum_{s'} P(s,a,s')V^*(s') \tag{5.49}$$

By assuming *n* states, there will be *n* equations and *n* unknown, which constitute a solvable system of equations (in the case 25 equations are solved).

5-4-3-1- Routing

It is possible to use Markov decision-making processes in determining movement direction of robot in each step. To do so, bumping into obstacles is accompanied by a negative reward, while reaching the target point embodies a positive one. As the result, the robot may prefer to remain motionless in some situations (e.g. proximity of an obstacle to the target) in order to avoid negative reward. To overcome this problem, a small negative reward is assigned to free space (compared to the big negative reward of obstacles). In short, the reward is calculated as below:

$$R(i,j) = P_{goal}(i,j) - w_1 P_{freespace}(i,j) - w_2 P_{obstacle}(i,j) \tag{5.50}$$

In some occasions (e.g. Fig. 5.30), the target is out of robot's field of view. Thus, a sub-target is utilized (instead of target, itself) to make the robot approaches the target. Fig. 5.31 shows the probable movement function of robot assumed by it to be displaced forward.

Bellman equation is nonlinear and hard to solve. Regarding various states which the robot is encountered to in each step, solving all these equations is impossible. On contrivance, is numerical calculations; for example, in this research magnitude repetition method is used. Below, the algorithm is brought:

```
Input: Reward function R(s)
Output: Value function V(s)
 begin
     ∀s  V(s) → 0
     repeat
          for all the s do
               R(s) + max_a γ ∑ P(s, a, s′)V(s′) → B(s)
          end
          B(s) → V(s)
         until V(s) converges;
end
```

Markov decision-making processes, always, propose the optimum path based on the current state which means the history of movement has no effectiveness. The optimum path is not always the best option, because, the robot has not a full view from its environment. For example, a robot moving along a wall has problems in seeing the end of it (is beside the wall but cannot see it) and whether tries to approach the target directly, may severely collide to the wall. A rectifier can unravel the problem by informing the robot from lateral obstacles and preventing collision in the next steps. Figures 5.32 and 5.33 show results of an experiment including the rectifier in a base environment with different obstacles and target arrangements.

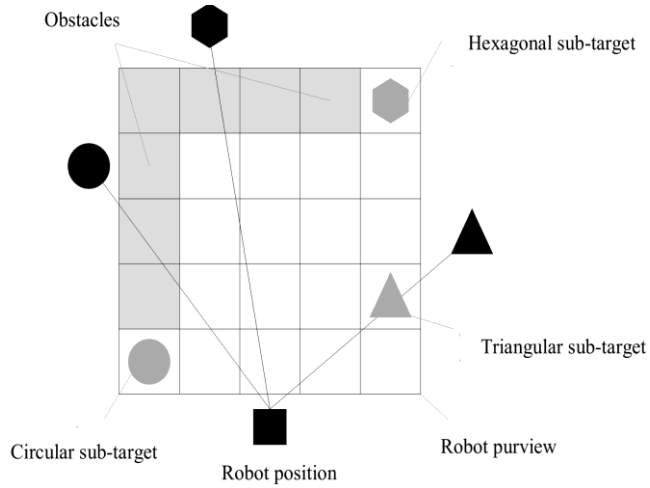

Fig. 5.30. The procedure for assigning sub-targets for the main target.

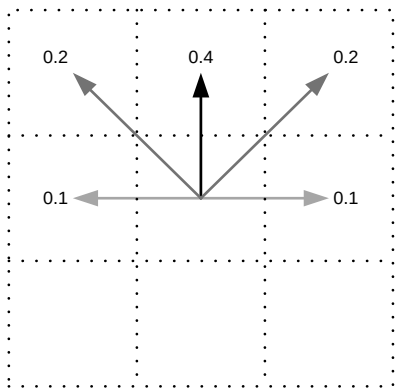

Fig. 5.31. Probability of moving to other states based on selecting forward movement.

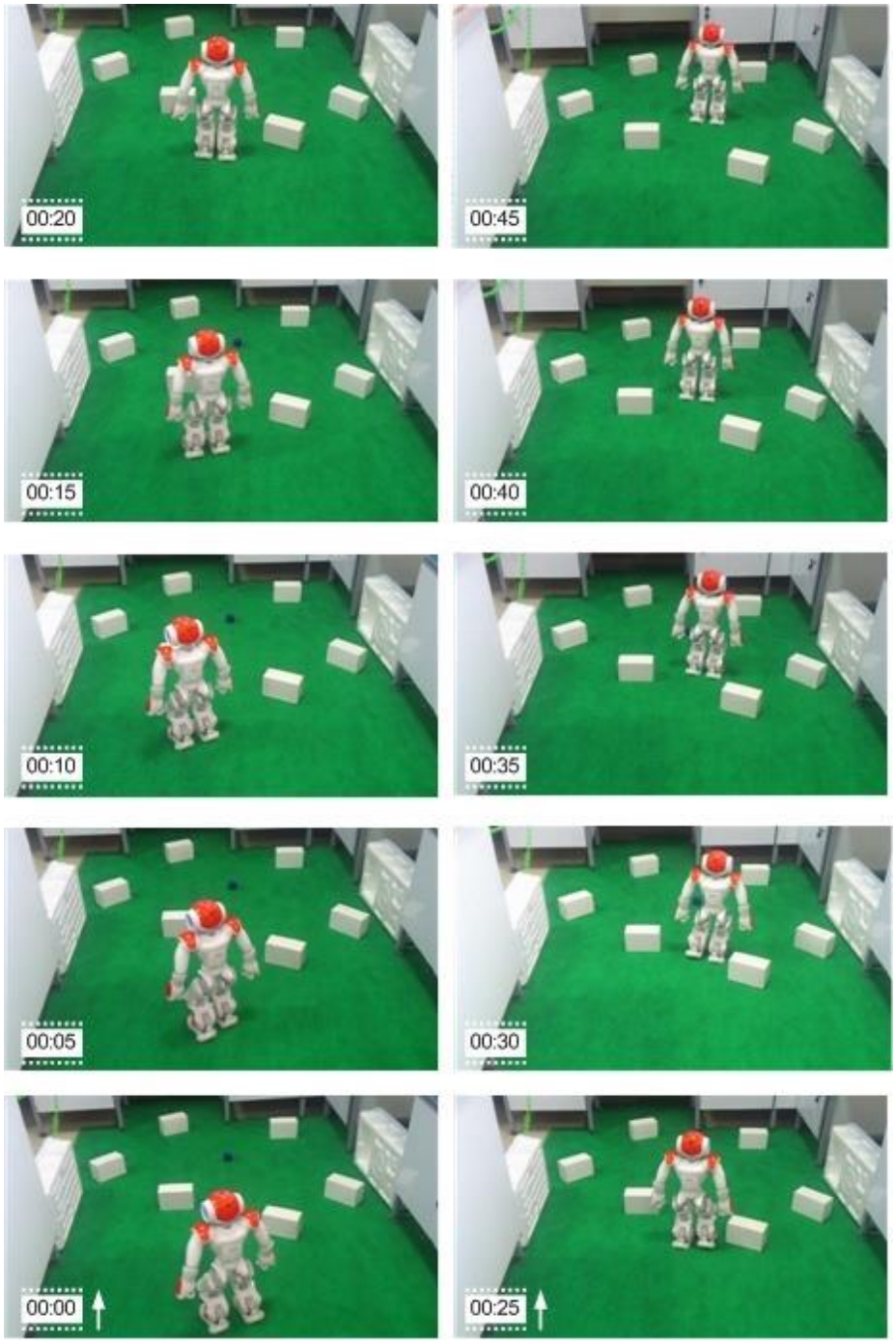

Fig. 5.32. Path surveyed by NAO humanoid robot with Markov decision-making processes method-the first sample environment.

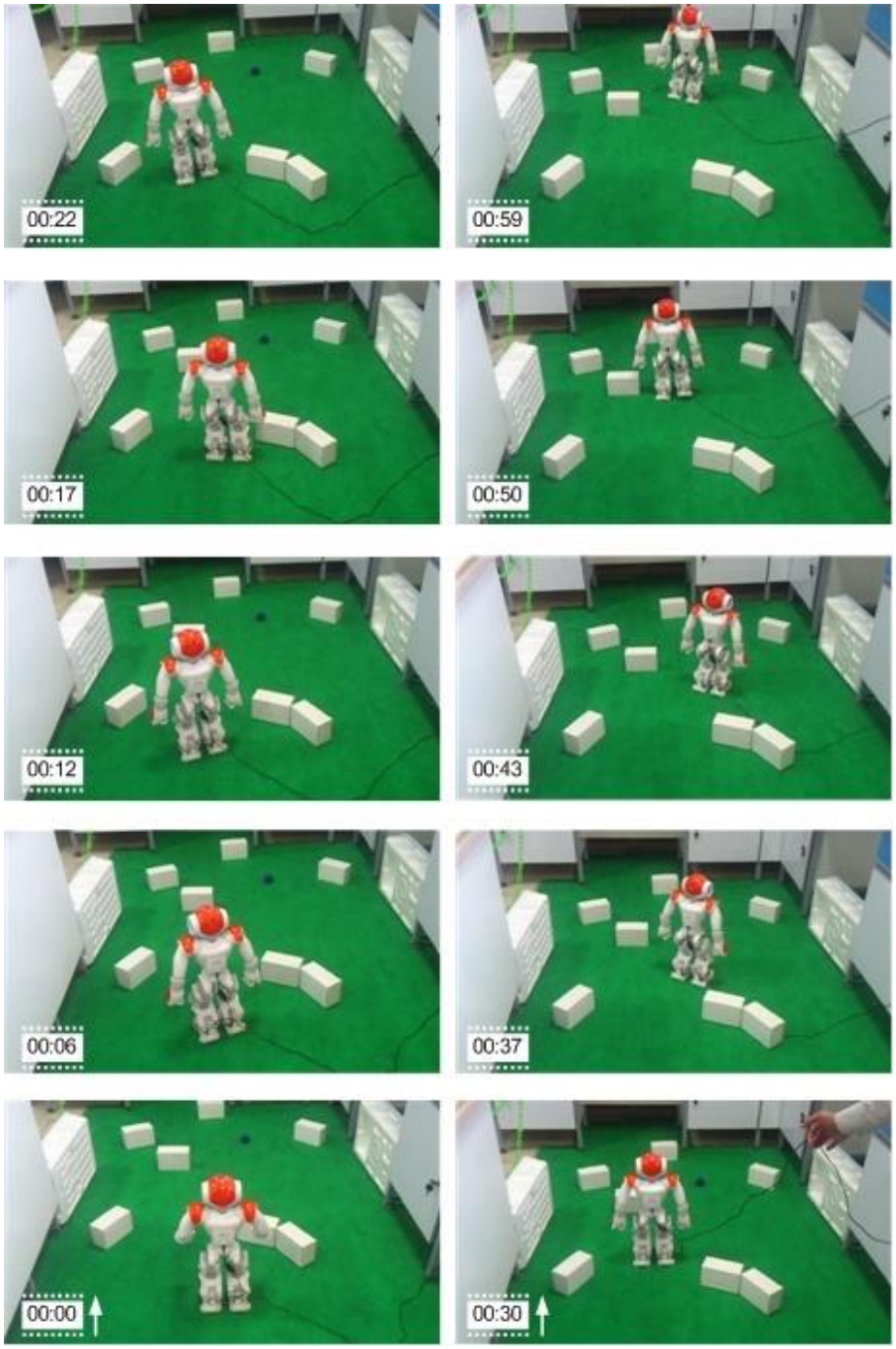

Fig. 5.33. Path surveyed by NAO humanoid robot with Markov decision-making processes method-the second sample environment.

5-4-4- *Fuzzy Markov decision-making processes*

As mentioned before, policy in Markov decision-making processes, chooses the (discrete) action which yields in the most (discrete) reward. Here, I had tried to correct classic decision-making framework. To do so, the first step is to evaluate value function. Then, a fuzzy system

determines the action (here, direction of robot's motion) based on the function which is discussed as follows.

According to reward, value function takes different intervals in different steps. This is while, fuzzy inference engine inputs are fuzzy sums of values 0 to 1. Hence, the cost function must be normalized in the first step. Thus:

$$V^{new}(i,j)=\frac{V^{*}(i,j)-b}{a-b} \quad , \quad a=\max_{(i,j)}V^{*}(i,j) \quad , \quad b=\min_{(i,j)}V^{*}(i,j) \tag{5.51}$$

where, $V^{new}(i,j)$ is the normalized value function, $V^{*}(i,j)$ is the value function in each step, and *a* and *b* are the maximum and minimum of $V^{*}(i,j)$, respectively.

In essence, inputs of inference engine are a neighborhood of robot's position. While, only the nearest neighborhoods are chosen as optimal in the classic (without inference), this method expands the radius of neighborhood. Table 5.3 summarizes the square of Euclidean distance between each cell and robot's position. This is amended by Fig. 5.34 in which four neighborhoods with different radii are represented.

Table 5.3 Square of distance between each cell and robot's position.

	1	**2**	**3**	**4**	**5**
1	29	26	25	26	29
2	20	17	14	17	20
3	14	10	9	10	14
4	8	5	4	5	8
5	5	2	1	2	5
			Robot		

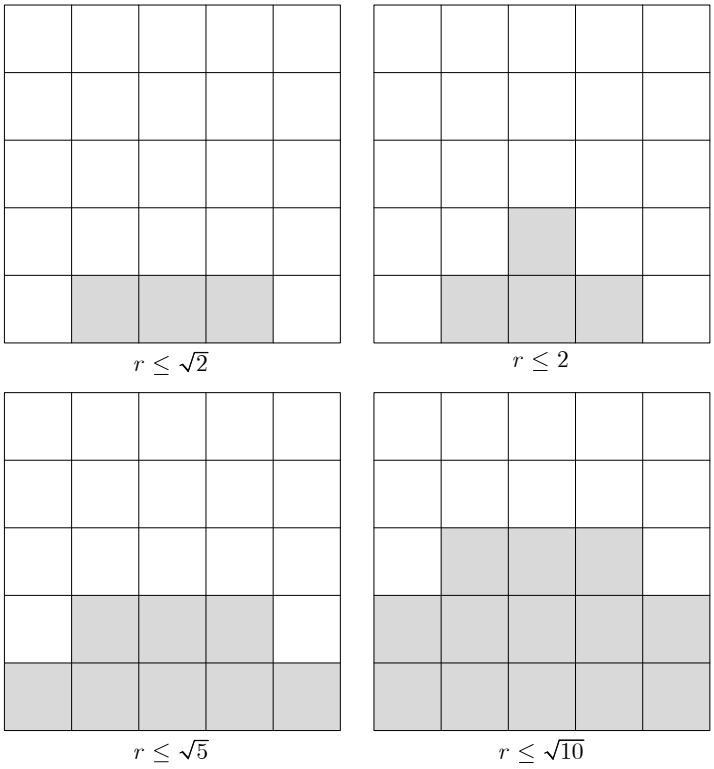

Fig. 5.34. Four different neighborhoods of robot in its frontal view.

Here, I have chosen neighborhood radius to be $\sqrt{10}$ and inputs of fuzzy inference engine are produced by (Table 5.4).

Table 5.4 Inputs of fuzzy inference method with neighborhood radius of $\sqrt{10}$ for a robot with 25 cells of view.

	1	**2**	**3**	**4**	**5**
1					
2					
3		X_1	X_2	X_3	
4	X_4	X_5	X_6	X_7	X_8
5	X_9	X_{10}	X_{11}	X_{12}	X_{13}
			Robot		

To continue, the new value function is fuzzified. One option is regarding the value function, itself, as the membership function. This may result in over-fuzzification of path which is undesired. To overcome this liability, other fuzzification functions (e.g. exponential) may be uses. For example, it is possible to compute membership function as below:

$$\mu(A_i) = x_i^n \tag{5.52}$$

where, x_i is the probability of x in cell i and n is an integer (e.g. 1, 2, 3 …). Choosing the right integer needs experience and depends on environment and robot camera.

Each cell is dominated by a rule. The rule calculates angle ϕ, which determines the direction of robot movement. Right-hand angles are defined positive, left-hands are negative while the head-on direction coincides to zero.

1- If A_1=1, then ϕ is a very small positive angle.
2- If A_2=1, then ϕ is zero.
3- If A_3=1, then ϕ is a very small negative angle.
4- If A_4=1, then ϕ is a medium positive angle.
5- If A_5=1, then ϕ is a small positive angle.
6- If A_6=1, then ϕ is a zero angle.
7- If A_7=1, then ϕ is a small negative angle.
8- If A_8=1, then ϕ is a medium negative angle.
9- If A_9=1, then ϕ is a big positive angle.
10- If A_{10}=1, then ϕ is a medium positive angle.
11- If A_{11}=1, then ϕ is a zero angle.
12- If A_{12}=1, then ϕ is a medium negative angle.
13- If A_{13}=1, then ϕ is a big negative angle.

From different existing defuzzification methods, weighted average is chosen and used as follows:

$$\phi = \frac{\sum \mu(A_i)\hat{\phi}_i}{\sum \mu(A_i)} \tag{5.53}$$

where, f is the defuzzified angle of movement direction, $\mu(A_i)$ is the membership function and $\hat{\phi}_i$ is the angle of movement direction. The results are brought in Fig. 5.35.

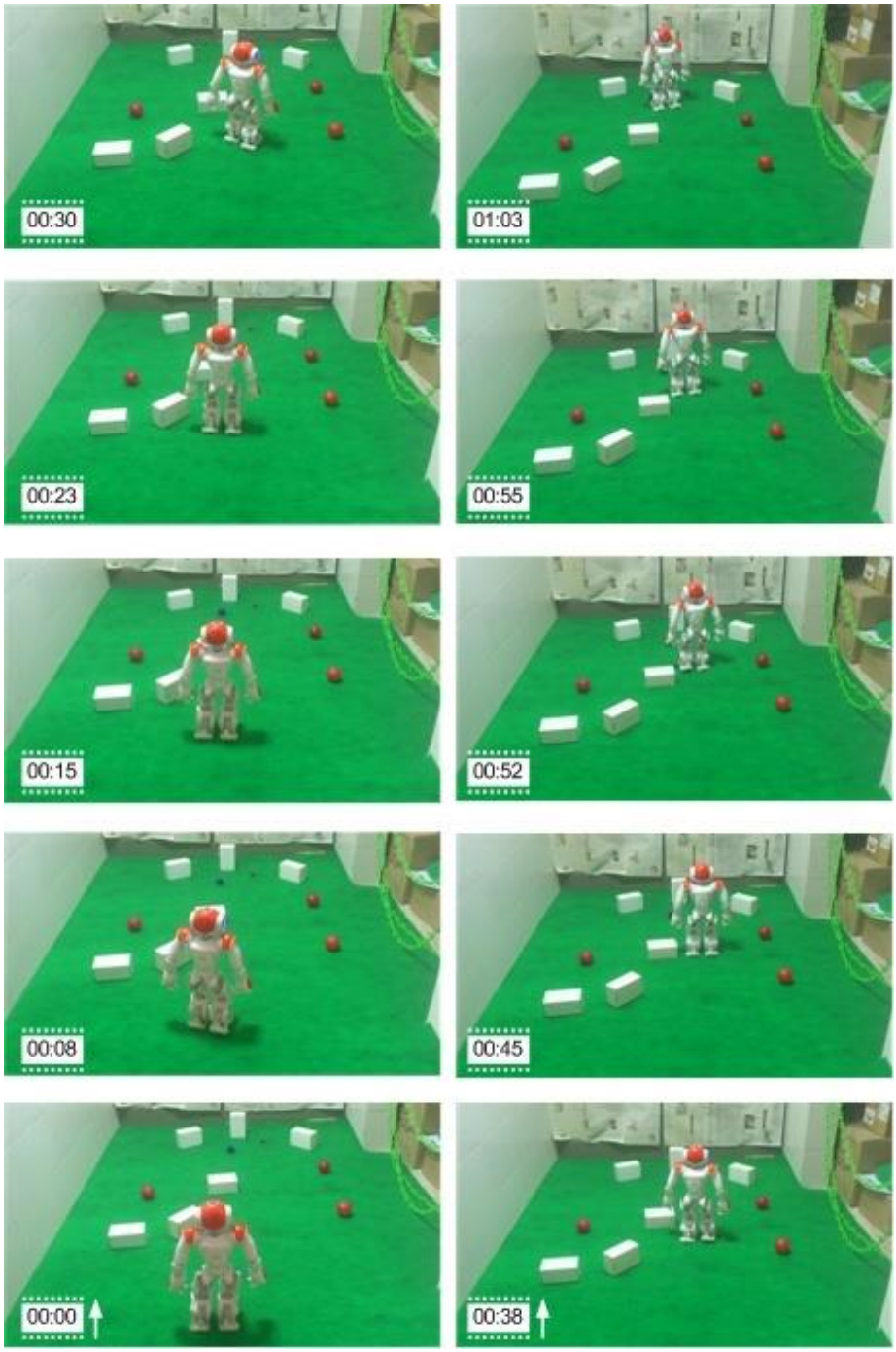

Fig. 5.35. Path surveyed by NAO humanoid robot with fuzzy Markov decision-making processes method.

5-5- Path-Planning in the presence of Danger space

In the previous section, four methods were proposed for path-planning of humanoid robots in an environment formed from, free, obstacle and target spaces. This is while some humanoid robots are not confined to these three types of spaces. For example, trees may be regarded as

obstacles in a wooded area; but mud pits are not preventing and the robot is able to cross. Meanwhile, it is not wise to choose a muddy path in the presence of dry ground. In this case, mud pits should not be regarded as free spaces (as dry ground) nor obstacles (as trees). To solve this problem, a new space named “danger space” is introduced and added to the traditional threesome. Danger space is extendible to other cases like greasy floor in a factory, areas in sight and range of enemy in a battleground, or the playground in a downtown park (which robot presence is considered disturbance).

5-5-1- *Disadvantages of reward calculation by linear relations*

In the previous section, equation (5.50) was proposed for reward in cells free of danger space. By assuming linear relations, it is possible to extend it for danger space as below:

$$R(i,j) = P_{target}(i,j) - w_1 P_{freespace}(i,j) - w_2 P_{danger}(i,j) - w_3 P_{obstacle}(i,j) \tag{5.54}$$

Although, this relation looks sound, but its linear nature makes trouble. For example, with the coefficient of danger space close to the one for free space, the path crossing danger spaces is preferred over the path which only includes free space cells, which is obviously, undesired. Also, if the coefficients of danger and obstacle spaces have not a meaningful difference, in the case which the path only is conceivable through danger space, the robot may choose to traverse an obstacle. By choosing an average magnitude for the coefficient of danger space, both of aforementioned problems may arise. Therefore, an intelligent arrangement for determining reward seems necessary.

As the first option, synthetic neural network was chosen an implemented which failed to show satisfying results. The second option is fuzzy inference method for reward calculation which is discussed in the follow section.

5-5-2- Reward calculation by fuzzy inference system

5-5-2-1- Fuzzification

Gaussian method is chosen for fuzzification. As seen in Fig. 5.36, the space surrounded in each cell is a member of fuzzy set including: zero, small, medium, big, very big. The figure shows these members using a Gaussian function from left to right.

5-5-2-2- Fuzzy inference engine

Here, Takegi-Sugeno method is used to calculate reward as rules Table 5.5 suggest and multiplication is chosen for fuzzy intersection.

Table 5.5. Fuzzy inference rule for reward.

Rule	Obstacle	Danger	Free	Target	Reward
1	Zero	Zero	Zero	Huge	Target
2	Zero	Zero	Huge	Zero	Free
3	Zero	Huge	Zero	Zero	Danger
4	Huge	Zero	Zero	Zero	Obstacle
5	Big	Zero	Zero	Small	0.1Target
6	Big	Zero	Small	Zero	0.8Obstacle
7	Big	Small	Zero	Zero	Obstacle
8	Medium	Zero	Zero	Medium	0.1Target
9	Medium	Zero	Medium	Zero	0.8Obstacle
10	Medium	Medium	Zero	Zero	Obstacle
11	Medium	Zero	Small	Small	0.1Target
12	Medium	Small	Zero	Small	0.1Target
13	Medium	Small	Small	Zero	0.6 Obstacle
14	Small	Big	Zero	Zero	0.4 Obstacle
15	Small	Medium	Small	Zero	0.4 Obstacle
16	Small	Medium	Zero	Small	0.1Target
17	Small	Small	Medium	Zero	0.4 Obstacle
18	Small	Small	Zero	Medium	0.2Target
19	Small	Zero	Big	Zero	Danger
20	Small	Zero	Medium	Small	0.1Target
21	Small	Zero	Small	Medium	0.2Target
22	Small	Zero	Zero	Big	0.25Target
23	Zero	Big	Small	Zero	Danger
24	Zero	Big	Zero	Small	0.333Target
25	Zero	Medium	Medium	Zero	0.5 Danger
26	Zero	Medium	Zero	Medium	0.75Target
27	Zero	Medium	Small	Small	0.5Target
28	Zero	Small	Big	Zero	0.25 Danger
29	Zero	Small	Zero	Big	Target
30	Zero	Small	Medium	Small	0.667Target
31	Zero	Small	Small	Medium	0.75Target
32	Zero	Zero	Big	Small	0.75Target
33	Zero	Zero	Medium	Medium	Target
34	Zero	Zero	Small	Big	Target

5-5-2-3- Defuzzification

Here, weighted average method is used for defuzzification of reward as:

$$\text{Reward} = \frac{\sum \mu_i \hat{R}_i}{\sum \mu_i} \tag{5.55}$$

in which "Reward" is defuzzified of reward, μ_i is the membership function, and $\hat{R}_i$ is reward of each fuzzy rule.

Decision-making in path-planning: This remainder of this method is similar to fuzzy Markov decision-making processes, mentioned before. To show applicability, the method is tested in an environment with two different arrangement of obstacles and the target point (Figs. 5.37 and 5.38).

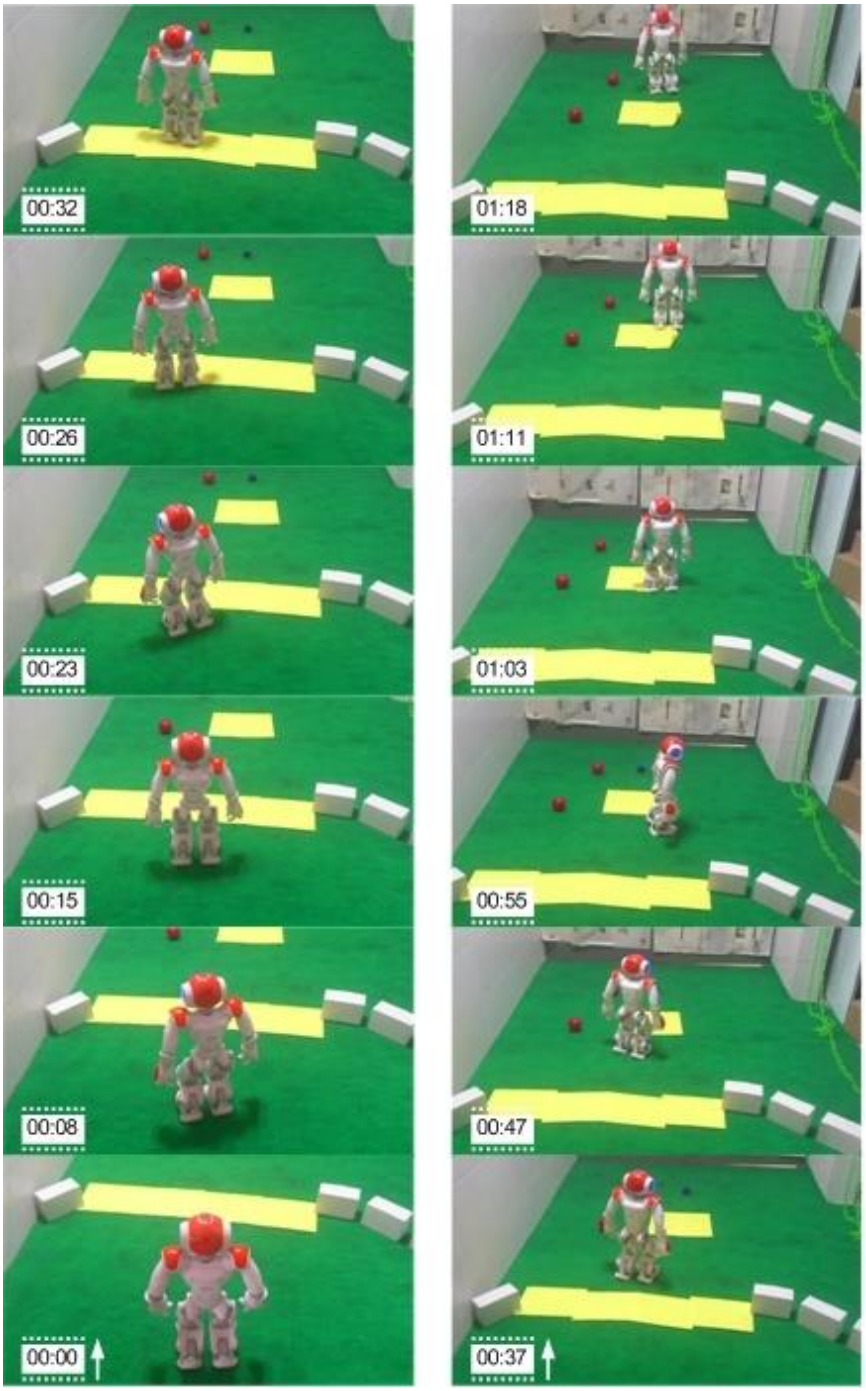

Fig. 5.37. Path surveyed by NAO humanoid robot in presence of danger space – the first sample environment.

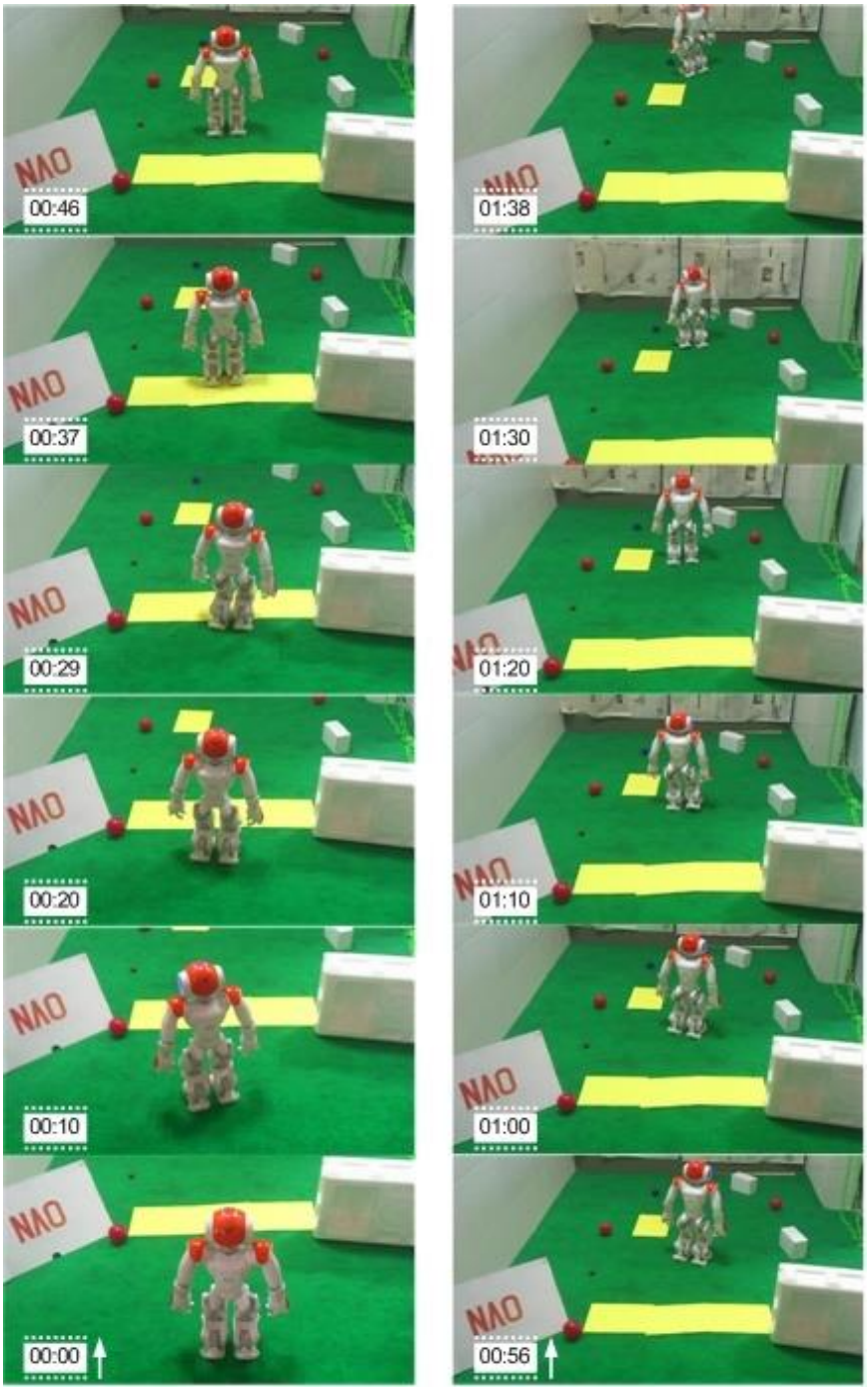

Fig. 5.38. Path surveyed by NAO humanoid robot in presence of danger space – the second sample environment.

References

Abelson H, DiSessa AA (1986) Turtle geometry: The computer as a medium for exploring mathematics. MIT press

Alpaslan Y, Osman P (2009) Performance Comparison of Bug Algorithms for Mobile Robots. In: 5th International Advanced Technologies Symposium (IATS'09).

Barraquand J, Latombe J-C (1991) Robot motion planning: A distributed representation approach. Int J Rob Res 10:628–649.

Bianco G, Cassinis R (1996) Multi-strategic approach for robot path planning. In: Advanced Mobile Robot, 1996., Proceedings of the First Euromicro Workshop on. IEEE, pp 108–115

Borenstein J, Koren Y (1991) The vector field histogram-fast obstacle avoidance for mobile robots. IEEE Trans Robot Autom 7:278–288.

Brandão AS, Sarcinelli-Filho M, Carelli R (2013) An analytical approach to avoid obstacles in mobile robot navigation. Int J Adv Robot Syst 10:278.

Bräunl T (2008) Embedded robotics: mobile robot design and applications with embedded systems. Springer Science & Business Media

Cheng DK (1989) Field and wave electromagnetics. Pearson Education India

Choset HM (2005) Principles of robot motion: theory, algorithms, and implementation. MIT press

Donald BR (1987) A search algorithm for motion planning with six degrees of freedom. Artif Intell 31:295–353.

Dorst L, Trovato K (1989) Optimal path planning by cost wave propagation in metric configuration space. In: 1988 Robotics Conferences. International Society for Optics and Photonics, pp 186–197

Foux G, Heymann M, Bruckstein A (1993) Two-dimensional robot navigation among unknown stationary polygonal obstacles. IEEE Trans Robot Autom 9:96–102.

Geraerts R, Overmars MH (2004) A comparative study of probabilistic roadmap planners. In: Algorithmic Foundations of Robotics V. Springer, pp 43–57

Horiuchi Y, Noborio H (2001) Evaluation of path length made in sensor-based path-planning with the alternative following. In: Robotics and Automation, 2001. Proceedings 2001 ICRA. IEEE International Conference on. IEEE, pp 1728–1735

Hu Q, Yue W (2007) Markov decision processes with their applications. Springer Science & Business Media

Huang Y, Cao Z, Hall E (1986) Region filling operations for mobile robot using computer graphics. In: Robotics and Automation. Proceedings. 1986 IEEE International Conference on. IEEE, pp 1607–1614

Jarvis RA (1985) Collision-free trajectory planning using distance transforms. Trans Inst Eng Aust Mech Eng 10:187–191.

Kamon I, Rimon E, Rivlin E (1998) Tangentbug: A range-sensor-based navigation algorithm. Int J Rob Res 17:934–953.

Kamon I, Rimon E, Rivlin E (1999) Range-sensor based navigation in three dimensions. In: Robotics and Automation, 1999. Proceedings. 1999 IEEE International Conference on. IEEE, pp 163–169

Kamon I, Rivlin E (1997) Sensory-based motion planning with global proofs. IEEE Trans Robot Autom 13:814–822.

Kavraki LE, Svestka P, Latombe J-C, Overmars MH (1996) Probabilistic roadmaps for path planning in high-dimensional configuration spaces. IEEE Trans Robot Autom 12:566–580.

Khatib O (1986) Real-time obstacle avoidance for manipulators and mobile robots. Int J Rob Res 5:90–98.

Khatib O, Le Maitre JF (1978) DYNAMIC CONTROLOF MANIPULATORS OPERATING IN A COMPLEX ENVIRONMENT. In: On Theory and Practice of Robots and Manipulators, 3rd CISM-IFToMM Symp.

Kim S-K, Russell JS, Koo K-J (2003) Construction robot path-planning for earthwork operations. J Comput Civ Eng 17:97–104.

Ko WS, Senevieatne LD, Earles SWE (1993) Space representation and map building-A triangulation model to path planning with obstacle avoidance. In: Intelligent Robots and Systems' 93, IROS'93. Proceedings of the 1993 IEEE/RSJ International Conference on. IEEE, pp 2222–2227

Koditschek D (1987) Exact robot navigation by means of potential functions: Some topological considerations. In: Robotics and Automation. Proceedings. 1987 IEEE International Conference on. IEEE, pp 1–6

Kolobov A (2012) Planning with Markov decision processes: An AI perspective. Synth Lect Artif Intell Mach Learn 6:1–210.

Kriechbaum KL (2006) Tools and algorithms for mobile robot navigation with uncertain localization.

Land S, Choset H (1998) Coverage path planning for landmine location. In: Third International Symposium on Technology and the Mine Problem.

Langer RA, Coelho LS, Oliveira GHC (2007) K-Bug, a new bug approach for mobile robot's path planning. In: Control Applications, 2007. CCA 2007. IEEE International Conference on. IEEE, pp 403–408

Latombe J-C (2012) Robot motion planning. Springer Science & Business Media

Laubach SL, Burdick JW (1999) An autonomous sensor-based path-planner for planetary microrovers. In: Robotics and Automation, 1999. Proceedings. 1999 IEEE International Conference on. IEEE, pp 347–354

LaValle SM (2006) Planning algorithms. Cambridge university press

Lengyel J, Reichert M, Donald BR, Greenberg DP (1990) Real-time robot motion planning using rasterizing computer graphics hardware. ACM

Lozano-Perez T (1983) Spatial planning: A configuration space approach. IEEE Trans Comput 108–120.

Lozano-Perez T (1987) A simple motion-planning algorithm for general robot manipulators. IEEE J Robot Autom 3:224–238.

Lozano-Pérez T, Wesley MA (1979) An algorithm for planning collision-free paths among polyhedral obstacles. Commun ACM 22:560–570.

Lucas C, Lumelsky V, Stepanov A (1988) Comments on" Dynamic path planning for a mobile automation with limited information on the environment"[with reply]. IEEE Trans Automat Contr 33:511–512.

Lumelsky V (1986a) Continuous motion planning in unknown environment for a 3D cartesian robot arm. In: Robotics and Automation. Proceedings. 1986 IEEE International Conference on. IEEE, pp 1050–1055

Lumelsky V (1987a) Algorithmic issues of sensor-based robot motion planning. In: Decision and Control, 1987. 26th IEEE Conference on. IEEE, pp 1796–1801

Lumelsky V (1989) On the connection between maze-searching and robot planning algorithms. In: Proc. of the 28th IEEE Conf. on Decision and Control.

Lumelsky V (1987b) Effect of kinematics on motion planning for planar robot arms moving amidst unknown obstacles. IEEE J Robot Autom 3:207–223.

Lumelsky V, Skewis T (1988) A paradigm for incorporating vision in the robot navigation function. In: Robotics and Automation, 1988. Proceedings., 1988 IEEE International Conference on. IEEE, pp 734–739

Lumelsky V, Stepanov A (1986) Dynamic path planning for a mobile automaton with limited information on the environment. IEEE Trans Automat Contr 31:1058–1063.

Lumelsky V, Sun K (1987) Gross motion planning for a simple 3D articulated robot arm moving amidst unknown arbitrarily shaped obstacles. In: Robotics and Automation. Proceedings. 1987 IEEE International Conference on. IEEE, pp 1929–1934

Lumelsky V, Tiwari S (1994) An algorithm for maze searching with azimuth input. In: Robotics and Automation, 1994. Proceedings., 1994 IEEE International Conference on. IEEE, pp 111–116

Lumelsky VJ (1988) On the connection between maze-searching and robot motion planning algorithms. In: Decision and Control, 1988., Proceedings of the 27th IEEE Conference on. IEEE, pp 2270–2275

Lumelsky VJ (1985) Effect of robot kinematics on motion planning in unknown environment. In: Decision and Control, 1985 24th IEEE Conference on. IEEE, pp 338–343

Lumelsky VJ (1986b) Continuous robot motion planning in unknown environment. In: Adaptive and Learning Systems. Springer, pp 339–358

Lumelsky VJ (1991) A comparative study on the path length performance of maze-searching and robot motion planning algorithms. IEEE Trans Robot Autom 7:57–66.

Lumelsky VJ (1987c) Dynamic path planning for a planar articulated robot arm moving amidst unknown obstacles. Automatica 23:551–570.

Lumelsky VJ, Skewis T (1990) Incorporating range sensing in the robot navigation function. IEEE Trans Syst Man Cybern 20:1058–1069.

Lumelsky VJ, Stepanov AA (1984) Effect of uncertainty on continuous path planning for an autonomous vehicle. In: Decision and Control, 1984. The 23rd IEEE Conference on. IEEE, pp 1616–1621

Lumelsky VJ, Stepanov AA (1987) Path-planning strategies for a point mobile automaton moving amidst unknown obstacles of arbitrary shape. Algorithmica 2:403–430.

Magid E, Rivlin E (2004) CAUTIOUSBUG: A competitive algorithm for sensory-based robot navigation. In: Intelligent Robots and Systems, 2004.(IROS 2004). Proceedings. 2004 IEEE/RSJ International Conference on. IEEE, pp 2757–2762

Masoud SA, Masoud AA (2002) Motion planning in the presence of directional and regional

avoidance constraints using nonlinear, anisotropic, harmonic potential fields: a physical metaphor. IEEE Trans Syst Man, Cybern A Syst Humans 32:705–723.

Miskon MF, Russell AR (2009) Close Range Inspection Using Novelty Detection Results. In: International Conference on Intelligent Robotics and Applications. Springer, pp 947–956

Ng JS (2010) An analysis of mobile robot navigation algorithms in unknown environments.

Nilsson NJ (1969) A mobile automaton: An application of artificial intelligence techniques. SRI INTERNATIONAL MENLO PARK CA ARTIFICIAL INTELLIGENCE CENTER

Ollis M, Stentz A (1996) First results in vision-based crop line tracking. In: Robotics and Automation, 1996. Proceedings., 1996 IEEE International Conference on. IEEE, pp 951–956

Ore O, Ore Y (1962) Theory of graphs. American Mathematical Society Providence, RI

Pavlidis T (1981) Contour filling in raster graphics. ACM

Pearl J (1984) Heuristics: intelligent search strategies for computer problem solving.

Puterman ML (2014) Markov decision processes: discrete stochastic dynamic programming. John Wiley & Sons

Robotics A (2012) NAO Next gen H25 datasheet.

Sankaranarayanan A, Vidyasagar M (1990) A new path planning algorithm for moving a point object amidst unknown obstacles in a plane. In: Robotics and Automation, 1990. Proceedings., 1990 IEEE International Conference on. IEEE, pp 1930–1936

Schwartz JT, Sharir M (1983) On the "piano movers'" problem I. The case of a two-dimensional rigid polygonal body moving amidst polygonal barriers. Commun pure Appl Math 36:345–398.

Sciavicco L, Siciliano B (2012) Modelling and control of robot manipulators. Springer Science & Business Media

Secchi H, Carelli R, Mut V (2001) Discrete stable control of mobile robots with obstacles avoidance. In: International conference on advanced robotics, ICAR. pp 405–411

Sheskin TJ (2016) Markov chains and decision processes for engineers and managers. CRC Press

Skewis T, Lumelsky V (1994) Experiments with a mobile robot operating in a cluttered unknown environment. J F Robot 11:281–300.

Spandl H (1992) Das HALMOR System. In: Maschinelles Lernen. Springer, pp 63–97

Sun K, Lumelsky V (1987) Computer simulation of sensor-based robot collision avoidance in an unknown environment. Robotica 5:291–302.

Trevisan M, Idiart MAP, Prestes E, Engel PM (2006) Exploratory navigation based on dynamical boundary value problems. J Intell Robot Syst 45:101–114.

Udupa SM (1977) Collision detection and avoidance in computer controlled manipulators.

Vidyasagar M (2002) Nonlinear systems analysis. SIAM

Yap CK (1987) Algorithmic Motion Planning. Advances in Robotics, vol. 1: Algorithmic and Geometric Aspects,(JT Schwartz and C. Yap, Eds.).